The Chick Embryo; A new drug delivery model for neuroblastoma

Thesis submitted in accordance with the requirements of the University of Liverpool for the degree of Master in Philosophy by:

Grace Borrill Mather

August 2014

Acknowledgments

There are many people whom I must thank for their support and assistance with this project. I began this year with no previous experience in laboratory based work, and it is largely through the excellent teaching and patience of Dr Sokratis Theocharatos that I have become confident in conducting lab work independently.

Others in the lab including Megan Palmer, Kejhal Khursheed, Zu Jing Jing and Anne Herman must also be thanked for enabling such a pleasant working environment, and always being ready to offer advice and feedback. Their regular contributions to lab meetings have helped to inspire new ideas and expand my knowledge base considerably.

A special thanks must go to my supervisors Dr Diana Moss and Professor Paul Losty. Dr Moss has been an incredibly approachable and supportive supervisor throughout this project. She has provided me with excellent supervision, advice and support through the year, without which none of this work would have been possible. I would also like to thank Professor Losty whose excellent enthusiasm for this interesting topic inspired mine and who has provided crucial advice and support in the transition from the hospital to lab based working environment. He has been especially helpful in offering advice and feedback on throughout this work.

I must also thank all those at Alder Hey children's hospital that have provided me with this incredibly valuable and interesting opportunity.

Finally to all of my family and friends, a final thanks for their unwavering support and assistance.

Abstract

Neuroblastoma (NB) commonly presents as high risk disease which despite intensive multimodal therapies is often fatal. Preclinical models are required to aid the development of novel therapeutics for this challenging childhood malignancy, however current systems are complex and inherently costly. We aimed to explore the ability of the chick embryo to act as a new tool for NB therapeutic research.

"High risk"- MYCN amplified human neuroblastoma cells were xenografted on to the surface of the chick embryo chorioallantoic membrane (CAM) and tumours allowed to form over a 7 day period. qPCR was used to detect the effects of a differentiation agent, retinoic acid (RA), firstly on NB cells in culture, and then on NB tumours in the chick embryo model.

Tumours formed in the chick embryo model 4 days after the introduction of NB cells on to the CAM. After 7 days, analysis of fully formed tumours demonstrated active proliferation and vascular recruitment from the surrounding CAM. In culture, RA induced morphological changes consistent with the differentiation of NB cells. RT-qPCR identified reproducible changes in gene expression in response to RA. Increased expression of differentiation markers ROBO2 and STMN4 and decreased expression of the stem cell marker KLF4 was observed in cell culture. Similar changes in the expression of these genes were also seen during *in vivo* chick embryo experiments. Against expectations, levels of the MYCN transcription factor did not fall significantly following 3 days of RA treatment during *in vitro* or *in vivo* experimentation. These results suggest that other targets may also be involved in the RA induced differentiation of these cells.

We have observed the ability of the chick embryo to act as an in vivo model system for NB therapeutic research. Reproducible changes in gene expression induced by the administration of retinoic acid have been detected using this model.

Abbreviations

ALK - anaplastic lymphoma kinase

APMA - 4-aminophenyl mercuric acetate

arrayCGH - array comparative genomic hybridization

ATRX - alpha thalassemia/mental retardation syndrome X-linked

BLAST - Basic local alignment search tool

BMP - bone morphogenetic proteins

BSA - bovine serum albumin

CAF - cancer associated fibroblast

CAM - chorioallantoic membrane

CCHS - congenital central hypoventilation syndrome

cDNA - complementary deoxyribonucleic acid

DM - double minute

DMEM - - dulbecco's modified eagle medium

DMSO - Dimethyl sulfoxide

EdU - 5-ethynyl-2'-deoxyuridine

EFS - event free survival

FCS - fetal calf serum

GAP43 - growth associated protein 43

GAPDH - glyceraldehyde-3-phosphate dehydrogenase

GEMM - genetically engineered murine models

GFP - green fluorescent protein.

H&E - hematoxylin and eosin

HIF-1α - hypoxia inducible factor 1α

HLH/LZ - helix-loop-helix/leucine zipper

HPRT1 - hypoxanthine phosphoribosyltransferase 1

HSR - homogeneously staining region

HuD - the human homolog of *Drosophila* embryonic lethal abnormal vision protein

IDRF - Imaging defined risk factor

INPC - International Neuroblastoma Pathology Classification

INRGSS - The International Neuroblastoma Risk Group Staging System

KLF4 - Kruppel-like factor 4

LOH - Loss of heterozygosity

mIBG - metaiodobenzylguanidine

miRNA - microRNA

MIZ-1 - Myc-interacting zinc-finger protein-1

MMP - matrix metalloproteinases

mRNA - messanger RNA

MYCN - Neuroblastoma-derived v-myc avian myelocytomatosis viral related oncogene

NB - Neuroblastoma

NCI - national cancer institute

NF70 - Neurofilament 70

NF-L - neurofilament protein L

NRQ - normalised relative quantification

NRT - No-reverse transcriptase

NSE - Neurone specific enolase

NT - no-template

PCR - polymerase chain reaction

PHOX2a - paired-like homeobox 2a

PHOX2b - paired-like homeobox 2b

PPTP - Paediatric Preclinical Testing Program

PS - penicillin streptomycin

qPCR - quantitative PCR

RA - retinoic acid

RAR - retinoic acid receptor

RARE - retinoic acid response elements

ROBO2 - roundabout, axon guidance receptor, homolog 2

RXR - retinoid X receptor

SD - Standard deviation

SEM - standard error of the mean

SP-1 - specific protein 1

STMN4 - stathmin-like 4

TGF-β - transforming growth factor-β

UBC - ubiquitin C

Contents

1.Introduction;

1.1.Neuroblastoma

Neuroblastoma (NB) is a malignancy found almost exclusively in children. It is thought to originate from primordial neural crest cells that normally give rise to the adrenal medulla and sympathetic neural ganglia (Park, Bagatell et al. 2013). Neuroblastoma is an interesting and heterogeneous disease which remains a significant cause of childhood mortality.

1.1.1.Epidemiology

In the UK, the annual incidence of neuroblastoma is between 6 and 8 per million children under the age of 15 (Hildebrandt and Traunecker 2005, Fisher and Tweddle 2012). Neuroblastomas are the most common malignancies in children under 1 year, and account of 14% of all cancers in children under 5 years (Izbicki, Mazur et al. 2003, Heck, Ritz et al. 2009). In the context of all paediatric cancers it is the fourth most frequent malignancy, following leukaemia, tumours of the central nervous system and the lymphomas (Izbicki, Mazur et al. 2003, Heck, Ritz et al. 2009).

Age at diagnosis represents a key prognostic factor in neuroblastoma, with the oldest patients experiencing the worst mortality statistics (Park, Bagatell et al. 2013). A North American review of 3059 neuroblastoma cases, found that 40% of patients were diagnosed in infancy, 89% by age 5 and 98% by age 10 (Heck, Ritz et al. 2009). 19 months represents the median age at diagnosis for children with neuroblastoma. Despite this, patients from a broad spectrum of age ranges have been diagnosed with the disease and both neonatal and adult cases have been reported (Izbicki, Mazur et al. 2003, Fisher and Tweddle 2012).

The National Registry of Childhood Tumours found that between 1991 and 2000, 22.6% of neonatal cancer cases registered in Great Britain were neuroblastomas and “foetal neuroblastomas” have been identified on ultrasound scans as early as 23 weeks (Fisher and

Tweddle 2012). Neonatal cases tend to display favourable tumour biology and generally have an excellent prognosis. Many cases undergo spontaneous regression under only supportive therapy (Fisher and Tweddle 2012).

Adult neuroblastoma is extremely rare, and often lacks features such as MYCN amplification, elevated urinary catecholamimes, and MIBG avidity found paediatric cases (Esiashvili, Goodman et al. 2007). In medical literature there are several small reports on cases of neuroblastoma diagnosed among adults (Miranda Soares, Quirino Filho et al. 2010, Ohtaki, Ishii et al. 2011, Bayrak, Seckiner et al. 2012). Outcomes, though highly variable, are generally significantly worse in this population (Smith, Minter et al. 2013).

Evidence from international cancer registries suggests that neuroblastoma is more common in Caucasian patients, however it is unclear as to whether this is primarily due to increased disease surveillance in this population (Heck, Ritz et al. 2009). In terms of gender, it is generally thought to affect both sexes equally although a slight predisposition in males has been identified in some studies (Izbicki, Mazur et al. 2003, Heck, Ritz et al. 2009).

Neuroblastoma, like retinoblastoma and Wilms' tumour, is an embryonal malignancy that is notable for having both sporadic and hereditary forms (D'Orazio 2010). Familial neuroblastomas account for less than 5% of all cases, with the majority being due to germ line mutations in ALK and PHOX2B (Heck, Ritz et al. 2009). Analysis of pedigree structures has indicated an autosomal dominant mode of inheritance with incomplete penetrance, similar to that seen in other paediatric malignancies (Maris and Matthay 1999). Familial cases have traditionally been thought to occur in those that are younger, and have multiple lesions at diagnosis, however some more recent evidence has disputed this claim (Claviez, Lakomek et al. 2004, Heck, Ritz et al. 2009).

1.1.2.Aetiology

In contrast to adult cancers, very few causative factors have been identified in paediatric malignancies. Studies have examined links between several lifestyle, familial and environmental factors and neuroblastoma. However due to the rarity of the condition, such

studies are often subject to biases and have small sample sizes. Despite limitations, consistencies between certain studies have implicated several aetiological factors which appear to warrant further investigation. Maternal alcohol consumption, paternal occupational exposure to hydrocarbons, dusts and solders, the use of diuretics, pain medications and low birth weight have all been implicated with increased risk. In contrast, vitamin supplementation and asthma seem to be protective (Heck, Ritz et al. 2009). However in both cases stronger evidence is required to verify these findings.

1.1.3.Neural Crest

The neural crest is an embryonic cell type unique to vertebrates. It was first identified in the developing chick embryo by Wilhelm His in 1868 (Bronner and LeDouarin 2012). It can be defined as a cell population which: arises at the neural plate border (figure 1); expresses a combination of neural crest markers; and migrates away from the neural tube along defined pathways, to form multiple derivatives (figure 2) (Bronner and LeDouarin 2012). Neural crest derived cell lineages are diverse and include melanocytes, sympathetic ganglia, enteric ganglion cells, Schwann cells and sensory neurons.

Some neural crest cells differentiate to sympathoadrenal lineage (Figure 2). These cells first migrate towards the dorsal aorta. At the dorsal aorta, the migrating neural crest progenitor cells committed to the sympathoadrenal lineage initiate their differentiation programme. From that point, the cells commit to either becoming adrenal chromaffin cells or sympathetic ganglia. At this stage of differentiation enzymes involved in catecholamine biosynthesis are up regulated (Cheung and Dyer 2013). The anatomical locations in which neuroblastomas are found, as well as the cellular and neurochemical features of the disease, have led to the assertion that it arises from neural crest derived elements of the sympathetic nervous system.

This text box is where the unabridged thesis included the following third party copyrighted material:

Gammill, L. S. and M. Bronner-Fraser (2003). "Neural crest specification: migrating into genomics." Nat Rev Neurosci 4(10): 795-805.

Figure 2 - Neurulation

The neural crest is first induced at the region of the neural plate boarder (green). After neural tube closure, the neural crest delaminates from the region between the dorsal neural tube and overlying ectoderm and migrates out towards the periphery. Adapted from **(Gammill and Bronner-Fraser 2003)**

This text box is where the unabridged thesis included the following third party copyrighted material:

Cheung, N. K. V. and M. A. Dyer (2013). "Neuroblastoma: Developmental biology, cancer genomics and immunotherapy." Nature Reviews Cancer 13(6): 397-411.

Figure 1 - - Development of the sympathoadrenal lineage of the neural crest

This diagram describes the path of the subset of neural crest cells giving rise to the adrenal gland and sympathetic ganglia as they migrate and undergo differentiation. BMP; bone morphogenetic protein, CXCR4; CXC chemokine receptor 4, DBH; dopamine β-hydroxylase, EMT epithelial–mesenchymal transition, HAND2; heart and neural crest derivatives-expressed protein 2, INSM1; insulinoma-associated protein , PHOX; paired-like homeobox, SOX; sex-determining region Y-box, TH; tyrosine hydroxylase. Adapted from (Cheung and Dyer 2013)

The first signals believed to initiate neural crest cell differentiation are the bone morphogenetic proteins (BMPs) (Huber, Combs et al. 2002). Other key transcription factors coordinating the direction of differentiation into sympathetic neurons include; mammalian achaete scute homolog-1 (MASH1), Neuroblastoma-derived v-myc avian myelocytomatosis viral related oncogene (MYCN), hypoxia inducible factor 1α (HIF1α), HuD - the human homolog of *Drosophila* embryonic lethal abnormal vision protein, paired-like homeobox 2a and 2b (PHOX2a, PHOX2b), and p73 (a member of the p53 family) (Figure 2) (Nakagawara 2004). Further downstream, terminal differentiation of sympathetic neurons is strongly regulated by the signalling of neurotrophin family members and their receptors (Nakagawara 2001, Nakagawara 2004). The regulation of such genes is essential to normal differentiation of these cells. Neuroblastoma is thought to be an aberration of normal development in which differentiation has not occurred. It is not therefore surprising that defects in these pathways have been identified in many patients with the disease, blocking differentiation and apoptosis.

1.1.4.Genetics

The basis of genetic predisposition to neuroblastoma is emerging via genome-wide association and whole-genome sequencing analyses (Molenaar, Koster et al. 2012). However, in contrast to adult cancers, there is a general scarcity of recurrent somatic mutations in neuroblastoma (Molenaar, Koster et al. 2012). Major efforts over the years have been focused on discovering somatic mutations in human tumours. Numerous studies have demonstrated that genomic and transcriptomic profiles can be predictive of clinical disease course, so that a combination of messenger RNA (mRNA), microRNA (miRNA) and array comparative genomic hybridization (arrayCGH) are now being used to better define prognostic characteristics and provide insight into the molecular basis of clinical heterogeneity (Asgharzadeh, Pique-Regi et al. 2006, Vermeulen, De Preter et al. 2009, De Preter, Vermeulen et al. 2010, Domingo-Fernandez, Watters et al. 2013).

Many believe that target based therapy tailored towards tumour-specific mutations holds the key to precision therapy, and ultimately to eradicating cancer (Morgenstern, Baruchel et

al. 2013). Investigations into the genetics of neuroblastoma have identified a wide variety of genetic abnormalities. Interestingly different genetic aberrations are often observed in age dependent manor (Vandesompele, Baudis et al. 2005).

Abnormalities involving the amplification or mutation of genes such as MYCN, paired PHOX2B, anaplastic lymphoma receptor tyrosine kinase (ALK) and the Aurora kinases have been identified in neuroblastoma (Sridhar, Al-Moallem et al. 2013).

PHOX2B was the first gene found to possess inherited mutations in familial cases of neuroblastoma (Trochet, Bourdeaut et al. 2004). PHOX2B is a homeobox transcription factor and plays a critical role in the normal development of neural crest cell derived structures. It consists of three exons encoding a highly conserved 314–amino-acid protein with two polyalanine repeats. In most instances, individuals affected by constitutional PHOX2B mutations also have phenotypic characteristics of other neural crest-derived disorders, mainly congenital central hypoventilation syndrome (CCHS) and/or Hirschsprung disease (Mosse, Laudenslager et al. 2004, Bourdeaut, Trochet et al. 2005, Sridhar, Al-Moallem et al. 2013). In neuroblastoma germline *PHOX2B* mutations tend to be either missense alterations in highly conserved regions or mutations that result in a frameshift, giving rise to an altered or truncated protein lacking the second polyalanine motif (Pei, Luther et al. 2013). Mutated Phox2b protein has been shown increase proliferation and block differentiation of neuronal cells in culture. However the exact mechanism which leads a *Phox2b* mutation to result in neuroblastoma remains unknown (Thorner 2014).

Similarly, mutations of anaplastic lymphoma kinase are the leading cause of hereditary neuroblastoma as well as being present in around 8 – 12% of sporadic cases (George, Sanda et al. 2008, Kumar, Zhong et al. , Carpenter and Mossé 2012). Anaplastic lymphoma kinase was first described in 1994 as the nucleophosmin-ALK fusion protein that is expressed in the majority of anaplastic large-cell lymphomas (Kumar, Zhong et al. , Kruczynski, Delsol et al. 2012). It is a member of the insulin receptor protein-tyrosine kinase superfamily, most closely related to leukocyte tyrosine kinase (Ltk) (Mossé, Wood et al. 2009, Kruczynski, Delsol et al. 2012, Roskoski Jr 2013).

ALK is expressed transiently in specific regions of the central and peripheral nervous system, mostly in neuronal cells. It is essential for normal development. ALK expression persists at a

lower level in the adult brain but not in other tissues (Kruczynski, Delsol et al. 2012). However, ALK activity has been found in an expanding number of tumour types including, lymphomas, inflammatory myofibroblastic tumour, small cell lung cancer and neuroblastoma (Kruczynski, Delsol et al. 2012). It is one of the few oncogenes activated in both hematopoietic and non-hematopoietic malignancies.

The most frequent ALK aberration neuroblastoma is the R1275Q mutation in which there is a substitution at position 1275 in ALK, from an arginine (R) to a glutamine (Q). It occurs in the germline of patients with hereditary predisposition, and is detected in almost 50% of tumours with ALK mutation. The other most common ALK mutations in sporadic cases of neuroblastoma are found at positions F1174, and F1245. All of these mutations activate ALK, are located in key regulatory regions of the receptor thyrosine kinase domain. Each has been demonstrated to have transformation capabilities *in vitro* and *in vivo*. Furthermore, a comparison of the ALK mutation frequency in relation to genomic subtype has revealed that F1174L mutants are observed in a higher frequency of MYCN-amplified tumours, correlating with a poor clinical outcome (Schönherr, Ruuth et al. 2012).

The most widely researched gene associated with neuroblastoma is MYCN. Approximately 25% of neuroblastomas are characterized by amplification and consequent over expression of the MYCN transcription factor. MYCN amplification is considered one of the most robust independent prognostic factors for unfavourable outcome in this disease (Brodeur, Seeger et al. 1984).

MYCN was first discovered in 1983 by Schwab et al as a paralog of c-Myc. The Myc family of transcription factors is composed by three elements: c-MYC, L-MYC, and MYCN. MYC, MYCN, and MYCL are helix-loop-helix/leucine zipper (HLH/LZ) proteins that form a heterodimer complex with MAX causing transcriptional activation of target genes (Kamijo and Nakagawara 2012, Gherardi, Valli et al. 2013). MYCN can also repress gene expression by binding to other transcription factors such as Myc-interacting zinc-finger protein-1 (MIZ-1) and specific protein 1 (SP-1) and thereby inhibiting transcription of their down-stream targets (Westermark, Wilhelm et al. 2011). In neuroblastoma MYCN amplification occurs as part of a segmental chromosomal imbalance in which a variable portion of chromosome 2, always containing the MYCN gene, is amplified. Amplified copies of MYCN can be present

either extra-chromosomally as double minutes (DMs) or intrachromosomally as homogeneously staining regions (HSRs). HSRs are generally located on different chromosomes, not at the resident site, 2p24, of MYCN (Corvi, Amler et al. 1994, Kamijo and Nakagawara 2012) .

The Aurora kinases are a family of serine/threonine kinases that are integral to the regulation of mitosis and cytokinesis. There are three known members of the Aurora family expressed in mammalian cells: Aurora A, B, and C. The first Aurora kinase discovered, Aurora A, derived its name from a mutant form of the protein found in *Drosophila melanogaster* that caused the formation of monopolar spindles reminiscent of the aurora borealis due to failure of centrosome separation (Kelly, Ecsedy et al. 2011). Amplification of Aurora kinase A (AURKA) has been reported in breast (Kallioniemi, Kallioniemi et al. 1994), and colon (Schlegel, Stumm et al. 1995) cancers, as well as in neuroblastoma cell lines (Zhou, Kuang et al. 1998). In neuroblastoma, AURKA overexpression is associated with highrisk group of tumors, MYCN amplification, disease-relapse and decreased progression free survival (Shang, Burlingame et al. 2009). Furthermore, AURKA has been shown to stabilize MYCN protein levels in neuroblastoma (Otto, Horn et al. 2009) making it an exciting therapeutic target in this disease and consequently several compounds are currently under development which aim to act on this target (Kelly, Ecsedy et al. 2011, Health 2014).

In addition, numerous recurrent large scale genomic imbalances have been observed in neuroblastoma. Loss of heterozygosity (LOH) of chromosome regions 1p, 3p, and 11q, along with gain of chromosome 1q and 17q material, are associated with poor patient survival (Sridhar, Al-Moallem et al. 2013). It is also notable that the presence of any segmental chromosomal imbalance, is its self, indicative of poor patient survival (Janoueix-Lerosey, Schleiermacher et al. 2009). In contrast, tumours with hyperdiploid or near-triploid chromosome complements, with whole-chromosome gains and losses and few, segmental imbalances, have favourable clinical outcomes (Vandesompele, Baudis et al. 2005).

1.1.5.Histopathology

Neuroblastomas are one of several tumours arising from the neural crest. Such neural crest derived tumours display various stages of neuronal differentiation. Of these tumours, ganglioneuromas are the most differentiated and consist of mature neurons which form clusters, surrounded by a dense stroma of Schwann cells. Ganglioneuroblastomas are characterized by a mixture of mature and maturing ganglion cells as well as undifferentiated neuroblasts. Neuroblastomas represent the most undifferentiated and aggressive of neural crest derived tumours. They consist of small round blue cells with hyperchromatic nuclei and scant cytoplasm. Pseudorosettes surrounding eosinophilic material in the interstitial space are a common finding (Alexander 2000, Carachi 2002, Hildebrandt and Traunecker 2005, Kim and Chung 2006).

Neuroblastic tumors consist of two cell populations: neuroblastic/ganglionic cells and Schwann cells. Based on the maturation sequence of the neuroblastic cells and the volume of the Schwannian stroma, these tumors have been morphologically classified(Du, Hozumi et al. 2008). The International Neuroblastoma Pathology Committee Classification was originally proposed in 1988, and revised in 1993. It ranks neuroblastoma histology as favourable or unfavourable according to several key features. The classification system builds on the Shimada classification, a system which considers patient age along with histological features such as degree of schwannian stroma (Figure 3), cellular differentiation, and the mitosis-karyorrhexis index (Joshi 2000, Ikeda, Iehara et al. 2002). Cells may be divided into three histological subtypes depending on the different grades of neuroblastic differentiation observed; undifferentiated, poorely differentiated and differentiating. Unfavourable histology has been shown to confer a worse prognosis in patients with the disease. The ability to stratify patients according to risk is vital in all cancers however, this ability undoubtedly holds greater importance in diseases such as neuroblastoma, where outcomes are so highly variable, and intense multimodal therapies often hold serious consequences.

This text box is where the unabridged thesis included the following third party copyrighted material:

Gurcan, M. "Neuroblastoma." Retrieved 23rd April, 2014, from http://bmi.osu.edu/~gurcan/neuroblastoma.php

Figure 3– Neuroblastoma pathological classification.

Diagram displaying the 3 grades of neuroblastoma differentiation observed and the two levels of stromal development. Undifferentiated neuroblastoma is characterised by small / medium cells with thin rim of cytoplasm, indistinct cell borders, round / oval nuclei with salt and pepper (coarsely granular) chromatin and indistinct nucleoli; no neuropil; 5% or less of tumour has features of differentiation towards ganglion cells; no / minimal ganglioneuromatous stroma. Poorly differentiated neuroblastoma has the same appearance as undifferentiated neuroblastoma but with neuropil. **Differentiating neuroblastoma:** 6-49% of tumour cells show ganglionic differentiation (abundant eosinophilic or amphophilic cytoplasm, large eccentric nuclei with vesicular chromatin and single prominent nucleoli), often at periphery of tumor; if 50% or more, call ganglioneuroblastoma, intermixed; usually abundant neuropil. The degree of differentiation and stromal development in used in the International pathological classification system for neuroblastoma and has prognostic significance. Undifferentiated neuroblastoma which is stroma poor has the worst prognosis. Adapted from (Gurcan)

1.1.6.Clinical Features

Neuroblastoma may arise from any neural crest element of the sympathetic nervous system (Sridhar, Al-Moallem et al. 2013). The clinical features of the disease reflect both the anatomical location of the tumour, as well as the extent of the disease (Young, Toretsky et al. 2000). The diverse range of neural crest derived sympathetoadrenal structures means that the location of the primary tumour can be anywhere along the sympathetic chain from the neck to the groin (Maris, Hogarty et al. 2007). This variation in location, as well as the varying degree of histopathological differentiation, results in an array of enigmatic tumours demonstrating diverse clinical and biological characteristics.

Neuroblastomas most commonly present in the adrenals (32%) or the (extra-adrenal) abdomen (28.4%) followed by the thorax (15%), pelvis (5.6%) and neck (2%) (Mazur 2010). The first symptoms can often be vague and nonspecific; loss of appetite or fatigue is common. Intra-abdominal neuroblastoma often presents as an asymptomatic mass that is detected incidentally by parents or a paediatrician during a routine clinic visit (Kim and Chung 2006). Symptoms are often due to the mass effect of tumours and give varying complaints depending on their anatomic location. Abdominal masses may compress the renal vessels, activate the renin-angiotensin axis, and cause hypertension. Rarely, hypertension is from the direct effect of catecholamine-secreting tumours (Davenport, Blanco et al. 2012).

When neuroblastoma is located paraspinally with intraforaminal invasion, children may develop peripheral neurologic deficits, including paralysis and urinary or faecal incontinence (Sandberg, Bilsky et al. 2003). Horner's syndrome and superior vena cava syndrome are described in patients with high mediastinal lesions (Alejandro Cruz 2013). These tumours, when extending into the neck, could also cause airway compression (Davenport, Blanco et al. 2012). Opsoclonus-myoclonus syndrome is manifested as ataxia and random eye movements, or "dancing eyes". It is a rare immune phenomenon with cross reactivity of neuroblastoma antibodies with cerebella or brain stem neuronal tissue (Davenport, Blanco et al. 2012).

Metastasis is present in 50% of neuroblastoma patients at the time of diagnosis. Frequent spread to bone marrow (70%), bone (55%), lymph nodes (30%), liver (30%), and brain (18%) is observed (DuBois, Kalika et al. 1999, Maris, Hogarty et al. 2007). Metastasis is often manifested by hepatomegaly, subcutaneous nodules ("blueberry muffin baby"), and bone pain. The characteristic bilateral periorbital ecchymosis, which is a sign of metastatic disease, is typically caused by intraorbital masses (Davenport, Blanco et al. 2012). In infants with stage 4S neuroblastoma abdominal distension resulting from massive liver infiltration and subcutaneous nodules are often features. In some cases the massive hepatomegaly can lead to respiratory distress, and kidney or bowel function can be impaired due to obstruction by the tumour. Their medical condition of such patients can rapidly deteriorate within hours or days.

1.1.7.Screening and Diagnosis

Attempts at screening for neuroblastoma have been trialled in countries such as Germany, Japan and Canada using elevated urinary catecholmines as the method of detection (Schilling, Spix et al. 2002, Woods, Gao et al. 2002). The studies were successful in identifying previously unrecognised patients, with the incidence of neuroblastoma increasing in these areas. However despite an increase in incidence of the disease, changes in the mortality associated with neuroblastoma did not follow (Tsubono and Hisamichi 2004). Screening is therefore believed to only identify a greater number of patients with favourable tumour biology who would undergo spontaneous regression and therefore did not require medical intervention (Yamamoto, Hanada et al. 1998). It has been subsequently abandoned in these areas.

Tools such as metaiodobenzylguanidine (mIBG) scanning, tumour imaging modalities, biopsies and urinary catecholamine metabolite detection aid both the diagnosis and staging of neuroblastoma (NCI). However, ultimately an unequivocal pathologic diagnosis of neuroblastoma must be made from tumour tissue by light microscopy (with or without immunohistology, electron microscopy, increased urine, or serum catecholamine metabolites), or bone marrow aspirate or trephine biopsy contain unequivocal tumour cells

(e.g., syncytia or immunocytologically positive clumps of cells) and increased urine or serum catecholamine metabolites (Brodeur, Pritchard et al. 1994).

1.1.8.Staging

Given the diversity of neuroblastoma as a disease, accurate staging and risk stratification is vital to ensuring the appropriate management of patients. Over time there have been many systems developed for staging neuroblastoma. The International Neuroblastoma Staging System was developed in 1988 and represented the first step in developing consistent staging worldwide (Schönherr, Ruuth et al.). It is a postoperative system using the extent of surgical resection to categorise patients (see Table **1**)and much of the published literature refers to this system.

The International Neuroblastoma Risk Group Staging System (INRGSS) is a preoperative staging system. Here staging is determined by the presence or absence of image-defined risk factors (IDRFs) and/or metastatic tumour at the time of diagnosis (see Table 2). IDRFs are surgical risk factors, detected by imaging, that increase the risk or difficulty of complete tumour excision (Monclair, Brodeur et al. 2009).

Table 1 - The International Neuroblastoma Staging System

Stage	Description
1	Localised tumour with complete gross excision, with or without microscopic residual disease; representative ipsilateral lymph nodes negative for tumour microscopically.
2A	Localised tumour with incomplete gross excision; representative ipsilateral non-adherent lymph nodes negative for tumour microscopically[1].
2B	Localised tumour with or without complete gross excision, with ipsilateral non-adherent lymph nodes positive for tumour. Enlarged contralateral lymph nodes must be negative microscopically
3	Unresectable unilateral tumour infiltrating across the midline, with or without regional lymph node involvement; or localised unilateral tumour with contralateral regional lymph node involvement; or midline tumour with bilateral extension by infiltration (unresectable) or by lymph node involvement.[2]
4	Any primary tumour with dissemination to distant lymph nodes, bone, bone marrow, liver, skin, and/or other organs, except as defined for stage 4S.
4S	(By definition patients must be <1 year of age). Localized primary tumour, as defined for stage 1, 2A, or 2B, with dissemination limited to skin, liver, and/or bone marrow[3].

[1] lymph nodes attached to and removed with the primary tumour may be positive
[2] The midline is defined as the vertebral column. Tumors originating on one side and crossing the midline must infiltrate to or beyond the opposite side of the vertebral column.
[3]Marrow involvement should involve <10% of total nucleated cells identified as malignant by bone biopsy or by bone marrow aspirate. More extensive bone marrow involvement would be considered stage 4 disease. The results of the mIBG scan, if performed, should be negative for disease in the bone marrow.
Adapted from (Institute 2014)

Table 2: International Neuroblastoma Risk Group Staging System

Stage	Description
L1	Localised tumour not involving vital structures as defined by the list of image-defined risk factors and confined to one body compartment.
L2	Locoregional tumour with presence of one or more image-defined risk factors.
M	Distant metastatic disease (except stage MS)
MS	Metastatic disease in children younger than 18 months with metastases confined to skin, liver, and/or bone marrow.

The International Neuroblastoma Risk Group Staging System - based on image defined risk factors L1 and L2 refer to localized disease where as M and MS refer to those with metastatic spread. Adapted from (Monclair, Brodeur et al. 2009)

Table 3- International Neuroblastoma Risk Group classification

INRG Stage	Age (months)	Histologic Category	Grade of Tumor Differentiation	*MYCN*	11q Aberration	Ploidy	Pretreatment Risk Group
L1/L2		GN maturing; GNB intermixed					A Very low
L1		Any, except GN maturing or GNB intermixed		NA			B Very low
				Amp			K High
L2	< 18	Any, except GN maturing or GNB intermixed		NA	No		D Low
					Yes		G Intermediate
	≥ 18	GNB nodular; neuroblastoma	Differentiating	NA	No		E Low
					Yes		H Intermediate
			Poorly differentiated or undifferentiated	NA			
				Amp			N High
M	< 18			NA		Hyperdiploid	F Low
	< 12			NA		Diploid	I Intermediate
	12 to < 18			NA		Diploid	J Intermediate
	< 18			Amp			O High
	≥ 18						P High
MS	< 18			NA	No		C Very low
					Yes		Q High
				Amp			R High

International Neuroblastoma Risk Group classification - a system designed to provide overall risk stratification based on a wide variety of patient derived and disease based features. Adapted from (Monclair, Brodeur et al. 2009)

Overall risk stratification is achieved by the International Neuroblastoma Risk Group classification (Table 3) (Monclair, Brodeur et al.). This system combines information regarding patient age at diagnosis, International Neuroblastoma Staging System clinical stage, MYCN status, DNA index, and the International Neuroblastoma Pathology Classification (INPC) category (Schönherr, Ruuth et al.). The output is categorization into very low, low, intermediate or high risk. It is on the bases of this classification that most treatment protocols are directed.

1.1.9.Management

Management of patients with neuroblastoma is clearly defined according to stage-based protocols. This enigmatic disease with a diverse range of clinical behaviours has a correspondingly diverse range of management options. Treatment ranges from watchful waiting to surgical resection with radiotherapy, myloablative chemotherapy with analogous

stem cell transplant, differentiation therapy and immunotherapy (Mullassery, Dominici et al. 2009).

Surgery

Surgical resection of the primary tumour is standard treatment for all but the lowest risk tumours; patients under 6 months old that have adrenal masses under 3 cm may not require it. In other low-risk patients surgery may not need to be complete for treatment to be successful. In intermediate and high risk patients surgical resection represents a corner stone of treatment (Mullassery, Dominici et al. 2009).

Lower-stage neuroblastoma is often encapsulated and can be surgically excised. However higher-stage disease often infiltrates adjacent organs, surround critical nerves and vessels, and may therefore be largely unresectable at the time of diagnosis (Mullassery, Dominici et al. 2009). Many forms of treatment have consequently evolved to aid in the management of these difficult patients.

Chemotherapy

Chemotheraputic agents often employed in the treatment of intermediate risk neuroblastoma include carboplatin, cyclophosphamide, doxorubicin, and etoposide. Patients usually receive 4-8 cycles depending on the biology of the tumour (Mullassery, Dominici et al. 2009).

In high risk disease, high dose chemotherapy is commonly employed. Induction therapy may include dose-intensive cycles of cisplatin and etoposide alternating with vincristine, cyclophosphamide, and doxorubicin prior to surgery. These regimes are used to try and reduce the tumour burden and facilitate surgery. Post-surgical high-dose myeloablative chemotherapy is often employed with peripheral blood stem cell support (Castel, Segura et al. 2013). Agents include carboplatin/etoposide/melphalan or busulfan/melphalan.

Radiation therapy

In high risk patients radiotherapy may be used where complete excision of the primary tumour was not achieved. Some patients may also receive radiotherapy to metastatic sites.

Differentiation therapies

Differentiation status is a key prognostic factor in neuroblastoma with the least differentiated phenotypes displaying the worst prognosis for patients. In fact many view neuroblastoma its self as an aberration of normal development and 4S tumours may spontaneously regress to leave more differentiated benign ganglioneuromas (Park, Bagatell et al. 2013). It therefore follows that any drug which may drive differentiation may also offer therapeutic potential in neuroblastoma.

Retinoic acid is a retinoid compound known to cause differentiation. Retinoic acid induces neurite outgrowth and differentiation of human neuroblastoma cells in vitro and in vivo, and is part of standard therapy for high risk neuroblastomas (Reynolds, Kane et al. 1991, Matthay, Villablanca et al. 1999, Shimada, Ambros et al. 1999, Matthay, Reynolds et al. 2009). High risk patients commonly receive 6 months of treatment with oral isotretinoin.

Immunotherapy

GD2 is a disialoganglioside found on the surface of the majority of neuroblastoma cells. It has limited distribution in other human tissues making anti-GD2 monoclonal antibodies suitable for immunotherapy (Castel, Segura et al. 2013). After binding to neuroblastoma cells the antibody induces complement-dependent and antibody-dependent cytotoxic lysis of tumour cells (Cheung and Dyer 2013). Anti-GD2 antibodies are given in cases of high risk neuroblastoma alongside differentiation therapies.

Overview of high risk treatment protocol:

1.INDUCTION

Rapid COJEC chemotherapy (cisplatin, vincristine, carboplatin, etoposide, and cyclophosphamide)

Response criteria positive?

YES - move to 2.

NO - TVD (topotecan, vincristine, doxorubicin) rescue strategy

2.SURGERY

Aim; gross total resection

3. MYELOABLATIVE CHEMOTHERAPY

Peripheral blood stem cells harvested and returned to the patient after myeloablative therapy is completed using busulphan and melphalan

4. RANDOMISATION FOR IMMUNOTHERAPY

Patients either receive:

a – GD2 antibody or

b – GD2 antibody + IL2

5. 13-CIS ISORETINOIC ACID

Patients from both 4a and 4b receive 13-cis retinoic acid treatment

*Information derived from (Mullassery, Dominici et al. 2009)

1.1.10.Prognosis

Based on the International Neuroblastoma Risk Group classification very low risk patients have a 5-year event free survival (EFS) of over 85%; low risk 5-year EFS > 75% to ≤ 85%; intermediate risk 5-year EFS ≥ 50% to ≤ 75%. Over 50% of patients with neuroblastoma are categorised as high risk at the time of diagnosis. In high risk patients, despite the aggressive multimodal therapy employed in their treatment, 5-year EFS remains less than 50% (Monclair, Brodeur et al. 2009).

More than half of the children diagnosed with high-risk neuroblastoma either do not respond to conventional therapies, or relapse after treatment. Furthermore, current therapies such as intensive chemo-radiotherapy are associated with substantial acute and late toxicities. These facts coupled with the lack of clear aetiological factors and failure of screening programmes means the need to identify treatments which are more effective and have fewer adverse effects is great (Laverdiere, Liu et al. 2009, London, Castel et al. 2011).

1.2.Drug Discovery and Model Systems

The process of drug discovery is both lengthy and costly. Potential targets must first be identified and validated before compounds interacting with these targets are designed. From here a lead compound must demonstrate significant reproducible effects on their intended target, first in cell culture and later in preclinical models. Compounds must be deemed safe, effective and have a suitable a therapeutic window before reaching human subjects in phase I, II and III clinical trials (Hughes, Rees et al. 2011). As our understanding of human biology and disease processes is increasing, the number of potential therapeutic targets is rising exponentially (Kurosawa, Akahori et al. 2008, Yang, Adelstein et al. 2012). However for every 5,000-10,000 compounds that enter the research and development pipeline only 1, on average, is ultimately licensed for patient use (Azmi 2014). It is not surprising therefore that pharmaceutical companies report the costs of launching a new medicine as approaching several billion dollars and that the process may take up to 15 years to complete (Paul, Mytelka et al. 2010, Hughes, Rees et al. 2011, Jorge Mestre-Ferrandiz 2012). The process of evaluating these compounds and recognising the 1 in 10,000 leads which has the potential to be successful in clinical trials requires cost-efficient, pharmacologically relevant preclinical animal models.

This text box is where the unabridged thesis included the following third party copyrighted material:

Fishman, M. C. and J. A. Porter (2005). "Pharmaceuticals: a new grammar for drug discovery." Nature 437(7058): 491-493.

Figure 4– timeline for drug development
This diagram highlights the lengthy process of drug development in particular the vast amount of time and work that occurs prior to the implementation of clinical trials. Image adapted from (Fishman and Porter 2005)

In recent years a major effort to uncover new therapeutic strategies for all childhood cancers has begun. Legislative changes both in the US and Europe, as well as initiatives such as Europe's Innovative Therapies for Children with Cancer consortium and the USA's the Paediatric Preclinical Testing Program (PPTP), have driven this effort (EMA , ITCC , OLPA , Houghton, Morton et al. 2007, Zwaan, Kearns et al. 2010). A shift in methodology utilizing hypothesis-driven biologically targeted approaches, as well as major energies into establishing effective pre-clinical models have been key focuses of these projects (Kearns and Morland 2014).

Animal models are critical to the development of novel anti-cancer agents. They are even more vital in the field of paediatric cancer, where low numbers of patients may significantly hinder clinical trials (Moreno, Chesler et al. 2011, Kumar, Mokhtari et al. 2012). Previous decisions to implement clinical trials in paediatric patients have been based on the therapeutic effects observed in adult cancer patients (Moreno, Chesler et al. 2011, Kumar, Mokhtari et al. 2012). There are multiple examples throughout childhood malignancies that this approach does not produce valuable results. Paediatric cancers, even those of the same type as adult cancers, represent an entirely separate disease entity and therefore must be modelled as such (Sultan, Qaddoumi et al. 2009, Korshunov, Remke et al. 2010, Paugh, Qu et al. 2010, Faria and Almeida 2012).

Over time the animal models used in therapeutic research have evolved and are now capable of providing far more than insight into the dose limiting toxicity, distribution and metabolism of drugs. Our understanding of many areas of cancer medicine and therapeutics has increased, and so has knowledge of those organisms used in research. It is now possible not only to observe, but to manipulate the complex disease processes involved in malignancy in a manner that would be impossible in patients. Animal models involving various species, genetic aberrations, cell lines and exposures are used in the development of potential therapeutic compounds (Khleif SN 2000, Kelland 2004, Richmond and Su 2008, Moreno, Chesler et al. 2011). However each model, as an approximation of reality, has inherent limitations, and with greater complexity often comes increased time, and cost as well as other hindrances (Khleif SN 2000).

1.2.1.Mouse Models

Of the species used in therapeutic research, the mouse is undoubtedly the most common. Several factors including the small size, propensity to breed in captivity, lifespan, extensive physiological and molecular similarities to humans, as well as an entirely sequenced genome have made the mouse an attractive organism for use in laboratory research (Frese and Tuveson 2007). Laboratory experiments involving mice date back to as early at 1664 and mice models have been used for over a century (NCI). Some models such as those employing inbreeding techniques have remained relatively consistent over time. However others involving manipulation of the genome are constantly evolving with current knowledge and techniques (NCI).

Inbred mice allow genetic homogeneity to be established and certain characteristics to be selectively bred in or out. They are produced using at least 20 consecutive generations of sister-brother or parent-offspring matings, or are traceable to a single ancestral pair in the 20th or subsequent generation (TJL). Inbred mouse strains are homogeneous at almost all gene loci and each strain has a unique set of characteristics setting it apart from others (TJL). Several inbred strains have undergone whole genome sequencing and sources such as the mouse phenome database provide a vast amount of valuable data regarding each strain(TJL).

Similarly, the mouse genome is manipulated for research purposes in genetically engineered murine models (GEMM). In 1981 researchers discovered that the mouse germline could be changed to accept the delivery and consistent expression of foreign genes (Gordon and Ruddle 1981). These techniques were used to the explore oncogenes and their role in tumourigenesis. Later the role of tumour suppressor genes was also explored using "knock out" studies (Capecchi 1989). The genetic profile of these mice is altered so that one or several genes believed to be involved in transformation or malignancy are mutated, deleted or over expressed. The effect of altering these genes is then studied over time and the therapeutic responses of these tumours may be followed in vivo (Richmond and Su 2008).

The appropriate DNA segment is first prepared, then injected or introduced into suitable recipient eggs or embryos (NCI). The resultant animals may be characterised and used for further experimentation. The gene of interest may be newly added giving "knock-in" mice; be artificially silenced giving "knock-out" mice; or be subject to conditional transgenics, in which the altered components are under the control of some kind of regulatory switch to turn on or off the gene with various chemical, developmental stage, or tissue-specific mechanisms(Chesler and Weiss 2011). Regardless of the type of mouse produced the same basic method of DNA preparation, introduction and characterisation is always employed (NCI).

Improvements in many technological aspects relating to GEMM have led to a significant increase in the use of these models over the past 20 years(8). Furthermore the degree of manipulation in terms of the timing and location of gene expression is ever evolving and complex. New models that utilize latent, conditional and inducible alleles are able mimic the *in vivo* setting in which sporadic human cancers occur in an increasingly realistic fashion.

In neuroblastoma the well-characterized TH-*MYCN* GEMM is used for a variety of molecular-genetic, developmental and pre-clinical therapeutics applications (Chesler, Goldenberg et al. 2007, Hogarty, Norris et al. 2008, Rounbehler, Li et al. 2009). As the single best predictor of poor outcome in those with neuroblastoma MYCN provides an attractive target for use in the GEMM setting. The TH-MYCN mouse created in 1997 acts as a model for high risk, MYCN amplified neuroblastoma (Chesler and Weiss 2011).

TH-*MYCN* mice are constructed using a first-generation transgenic approach. Exogenous DNA is introduced into the nucleus of fertilized murine oocytes resulting in random integration of the transgenic construct into genomic DNA. The construct used incorporates the cDNA of the human MYCN, ligated downstream of the rat tyrosine hydroxylase promotor. The rabbit b-globin enhancer enhances expression, and a herpes simplex virus thymidine kinase gene sequence is used as a transcription terminator (Weiss, Aldape et al. 1997).The use of rat tyrosine hydroxylase targets expression of the MYCN gene to the neural crest - the cells from which neuroblastoma is derived. The model has been subsequently used in a wide variety of research disciplines involving molecular genetics, developmental biology, imaging technology, gene interactions and therapeutics (Chesler and Weiss 2011). Examples include the angiogenesis inhibitor HPMA copolymer-TNP-470 conjugate (caplostatin) and ornithine decaroboxylase inhibitor adifluoromethylornithine (Chesler, Goldenberg et al. 2008, Rounbehler, Li et al. 2009, Teitz, Stanke et al. 2011).

More recently a mouse model over expressing ALK^{F1174L} in the neural crest has also been generated. The ALK^{F1174L} mutation is associated with intrinsic and acquired resistance to ALK targeted therapies such as crizotinib, and co-segregates with *MYCN* in neuroblastoma (Sasaki, Okuda et al. 2010). Patients with the ALK^{F1174L} mutation and MYCN amplification represent a subgroup of extremely high risk neuroblastoma patients (Azarova, Gautam et al. 2011). Compared to ALK^{F1174L} and *MYCN* alone, co-expression of these two oncogenes led to the development of neuroblastoma at onset, higher penetrance, and with enhanced lethality in this model. Although these ALK mutations only affect a small proportion of neuroblastoma patients, this model may still provide valuable in testing therapies aimed to target such high risk patients (Berry, Luther et al. 2012).

GEMM have many strengths. Tumours arise spontaneously, in an immunocompetent host and in an appropriate tissue and microenvironment (Chesler and Weiss 2011). Our understanding of the interactions between tumour and host has expanded massively in recent years, and is now well recognised as an important aspect of tumour biology (Gadea, Joyce et al. 2006). GEMM may therefore give better representation of normal cancer biology and therefore provide meaningful therapeutic research which better translates into patient benefit in a clinical setting.

Despite these strengths there are many criticisms of the GEMM. It is difficult to reproduce the heterogeneity of gene mutations and expression patterns seen throughout primary tumours in this model (Ruggeri, Camp et al. 2014). Although work is being undertaken to reproduce these patterns it still remains a key shortcoming. This difference may account for the increased sensitivity to certain therapeutic agents designed to act on a gene of interest which have observed in compounds tested in these models (Tuveson and Jacks 2002).

Another problem associated with these models is that they often fail to recapitulate the metastatic patterns observed in patients. Neuroblastoma is a highly metastatic paediatric malignancy with metastases located in the bone morrow in around 70% of cases. However the TH-MYCN model fails to reproduce this pattern and exhibits only a very limited capacity for metastasis to the bone marrow (<5% incidence) (Teitz, Inoue et al. 2013). This presents a significant limitation, and the extent to which therapeutic effects can be modelled successfully using the TH-MYCN mouse. Whether this represents an artefact of murine physiology or a definitive difference between TH-MYCN tumourigenesis and human counterparts is as yet unclear. However more recently cross-breeding between TH-MYCN mice and strains deficient in caspase-8 have been shown to give rise to a significantly higher degree of bone metastases suggesting other candidate genes may enhance metastasis (Teitz, Inoue et al. 2013).

In addition, as a therapeutic model GEMM may also have other limitations. Several practical issues such as cost, patents, long latencies to tumour development, low tumour penetrance as well as the difficulty in monitoring tumour development and therapeutic response limit the use of these models in routine pre-clinical drug screening (Chesler and Weiss 2011). Furthermore, many feel strongly that conducting therapeutic research on mouse cells is unlikely to provide valuable results.

1.2.2.Transplantation models

Transplantation models are another commonly used cancer research tool. Here various systems and techniques are used to propagate tumour tissues in different hosts, allowing controlled studies *in vivo*. Allograft mouse tumour models involve the transplantation of tissues derived from the same species as the host. Similar to GEMM, the tumours generated by these mice are not human, which may limit the value of results obtained from their study. In contrast, Xenograft models involve the transplantation of human tissues into mouse models and are widely used in therapeutic research.

Xenograft tumour models have been explored since the mid 1960s, however only became frequently used after the identification of the athymic nude mutant mouse which were deficient in T cells (Peterson and Houghton 2004). Due to the exogenic nature of the tissue transplanted into xenograft models, host immune rejection of the tissue represents a major barrier and hosts must therefore be immune-deficient. The more recent discovery of other immune-deficient mouse strains such as (SCID) mice has further expanded the options for host transplantation in these models (Zhou, Facciponte et al. 2014).

Xenografts are most commonly subcutaneous, where cells are injected beneath the hosts skin, or orthotopic, whereby the tissue is transplanted into the tissue from which it would have originated. Subcutaneous xenografts permit the monitoring of tumour growth and drug response without requiring sophisticated techniques (Kumar, Mokhtari et al. 2012). However othotopic models are thought to better recapitulate the intricacies and cell-cell interactions of the local microenvironment in which a primary tumour grows, invades and disseminates (Ruggeri, Camp et al. 2014). Orthotopic models of neuroblastoma commonly involve the injection of cells into the adrenal gland of mice (Teitz, Stanke et al. 2011). Such models require precise implantation skill, are time consuming, and do not allow direct visual monitoring of tumour. With improvements in non-invasive imaging techniques, lack of direct tumour visualisation can be overcome, though still adds additional complexity and cost to the model (Albanese, Rodriguez et al. 2013).

Experimental metastases models have also been developed. Here tumour cells are injected directly into the host's blood stream. Such models allow modelling of therapies designed to target disseminated disease. In neuroblastoma the injection of cancer cells into the aorta of mice has been shown to produce large adrenal tumours with micrometastases observed in the liver and femur - a pattern closely reflecting that seen in patients with the disease (Engler, Thiel et al. 2001). Neuroblastoma cells injected into the tail vein of mice have been observed to produce smaller adrenal tumours with far fewer micrometastses indicating the site of injection may be of importance (Engler, Thiel et al. 2001).

In all xenograft models transplanted cells may originate from established human cancer cell lines or primary tumour samples. The use of cancer cell lines is convenient but means that the resultant tumours fail to recapitulate the many of the features of primary tumours and display limited clinical predictability in the therapeutic setting. With increasing passage number cells are predisposed to genetic drift and loss of heterogeneity. The transplantation of freshly excised human tumour tissue preserves the genetic, histological and phenotypic features of the tumour providing a more realistic model system. It is however, labour intensive and costly (Ruggeri, Camp et al. 2014).

A large number of studies have been conducted using xenograft models to evaluate potential compounds for the treatment of neuroblastoma (Chanthery, Gustafson et al. 2012). The NCI's paediatric preclinical testing programme has led to better characterisation of these models and a more systematic approach to therapeutic screening in general. Neuroblastoma is routinely used here as part of a panel of xenograft tumour models used to screen new compounds for significant antitumour activity (NCI). These models have identified multiple compounds which have gone on for further trials. For example MLN8237, a small molecule inhibitor of Aurora Kinase A was first identified in this way and is currently under Phase I/II Study in Combination with Irinotecan and Temozolomide for Patients with Relapsed or Refractory Neuroblastoma (Health 2014).

The main disadvantage of xenograft models is the need for immune compromise. Immune cells have a significant effect on therapeutic response and therefore it is difficult to reliably predict a novel agents therapeutic effect from these models (Schreiber, Old et al. 2011).

Although mice are the most commonly utilized organism, several others have been used in cancer research. Rats and dogs are among the other organisms more commonly employed, the larger size of these organisms can makes them amiable for exploring metastases(Kumar, Mokhtari et al. 2012).

All of the models discussed here have both strengths and limitations to their use in therapeutic research (Table 4). It is evident that no one model can answer all of the questions posed in the search for novel compounds, but the correct use of carefully selected models is most appropriate. One factor common to all of these models is the growing complexity and cost associated with their use. In the context of the rapidly increasing number of potential targets new models are required which can help to discern which drugs should be used in these more complex systems.

Table 4 - A comparison of xenograft and GEMM

Model type	Use in NB	Advantages	Disadvantages	References
GEMM	TH-MYCN mouse TH-MYCN;Casp8 *ALK*^{F1174L} mouse	Tumours arise spontaneously Immunocompetant host Correct microenvironment Genetic changes can be targeted to specific cells, and at specific times	Lack of heterogeneity of tumours Mouse tumour cells, not human Failure to reproduce metastatic patterns Expensive	(Weiss, Aldape et al. 1997, Berry, Luther et al. 2012, Teitz, Inoue et al. 2013)
Xenograft (subcutaneous)	PPTP	Tumour growth can be monitored easily Tumours grow rapidly and uniformly so less animals are needed Human cells are used	Tumours do not form in a native microenviroment - lack of tumour-host interation Immune compromise	(Houghton, Morton et al. 2007)
Xenograft (orthotopic)		Reproduce the organ microenviroment Human cells are used	Required precise implantation skill More difficult to monitor tumour growth Immune compromise	(Khanna, Jaboin et al. 2002)

PPTP - pediatric preclinical testing program

1.3.The Chick Embryo Model

Both the chicken and the egg have remained of great interest throughout human history. Aristotle conducted the first recorded experiments with chicken eggs as early as 330BC (Mason 2008). The subsequent centuries of experimentation using chick embryos has resulted in a wealth of information regarding the development of this species, as well as informing us on diverse aspects of development and disease in humans. Avian embryos such as the chicks have been instrumental not only to the field of developmental biology, but have also made significant contributions to research in cancer biology, virology, immunology, cell biology and neuroscience (Kain, Miller et al. 2014). The discovery of NGF by Rita Levi-Montalcini is just one example of several Nobel Prize winning discoveries made using the chick embryo model (Vergara and Canto-Soler 2012).

In 1889 the first attempts at a comprehensive morphological atlas of chick development were produced. These first works provided the bases for Viktor Hamburger and Howard Hamilton's later published 46 stages of development which provide consistency between various disciplines utilising the chick embryo (Hamburger and Hamilton 1951). At the point the egg is laid the chick embryo is at the blastula stage. In 2 to 3 days it undergoes gastrulation, neurulation and histogenesis, completing its entire development by the time of hatching in just 21 days (Vergara and Canto-Soler 2012). The early work of those such as Hamburger and Hamilton has been further built upon making the chick embryo a well characterised model with a fully sequenced genome (Vergara and Canto-Soler 2012).

Figure 5 - **The stages of chick development**
Image displaying the 46 Hamburger and Hamilton (HH) stages of chick development, and how they relate to the length of incubation (E). Adapted from Kristin et al (Kain, Miller et al. 2014)

Several key characteristics of the chick embryo have been crucial in establishing its role within various research modalities. The significant similarity of the chick to the human embryo at the molecular, cellular and anatomical levels; its rapid development; the accessibility of the developing embryo for visualization and experimental manipulation; and its comparatively large size and planar structure during early developmental stages represent several of this models key advantages (Vergara and Canto-Soler 2012).

There are also many practical and economical advantages of the this model which should not be overlooked. Current UK regulations do not require researchers to possess a home office licence when working with chick embryos up to 14 days of incubation. Eggs are available year round almost anywhere in the world. They can be purchased in specific quantities and may be stored easily for several days prior to incubation, allowing researchers to easily obtain embryos at the specific developmental stage that suits their need. Furthermore in the context of the increasingly costly model systems available in modern research the low cost of the eggs and their housing is extremely relevant and makes their use feasible in a wide range of laboratories (Vergara and Canto-Soler 2012).

Ethical considerations relating to animal research are also important to consider. The 3 r's: replace; reduce; refine pertaining to this field highlight the need to consider other means of conducting research wherever possible. Work with chick embryos may offer the ability to reduce the number of animals used in various research fields.

While much of the research involving the chick has involved the embryo its self, studies have also been conducted on the extra-embryonic membranes surrounding the developing embryo.

1.3.1.The Chorioallantoic membrane

The chick has three extra-embryonic membranes surrounding it during development. The chorioallantoic membrane (CAM) is one such membrane serving multiple functions. The CAM is involved in the exchange of respiratory gases, calcium transport from the eggshell,

acid-base homeostasis in the embryo, and ion and water reabsorption from the allantoic fluid (Gabrielli and Accili 2010).

The CAM is formed by the fusion of the allantoic membrane and the chorion around days 5 to 6 of incubation. It develops, progressively adhering to the acellular inner membrane just inside the eggs shell and surrounds the embryo by days 11 and 12. By day 10 of incubation, the CAM comprises the fully developed capillary plexus, an extensive capillary network which gradually comes to lie in a plane on the outer surface of the chorion (Ribatti, Nico et al. 2001, Gabrielli and Accili 2010).

Structurally, the CAM consists of three layers derived from distinct embryonic tissues; the ectodermal chorionic epithelium; an intermediate mesoderm; and the endodermal allantoic epithelium (Ribatti, Nico et al. 2001, Gabrielli and Accili 2010).

This text box is where the unabridged thesis included the following third party copyrighted material:

Mccartney, A. (2013). "From Amphibians to Amniotes." Retrieved 19th October, 2014, from http://annmccartneyblog.com/2013/01/23/from-amphibians-to-amniotes/.

Figure 6 - Diagram of the chick embryo highlighting the extraembryonic membranes. The chorion and allantosis (labelled in grey) fuse to form the chorioallantoic membrane at day 5-6 of embryonic development. Adapted from (Mccartney 2013)

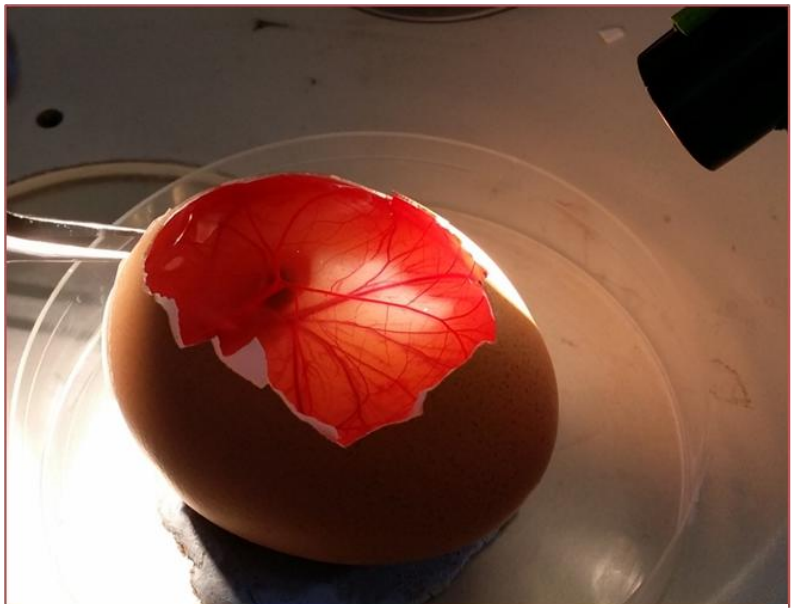

Figure 8 - The chick chorioallantoic membrane (CAM) - this image, taken 8 days after incubation (E8) demonstrates the highly vascular CAM

This text box is where the unabridged thesis included the following third party copyrighted material:

Gabrielli, M. G. and D. Accili (2010). "The chick chorioallantoic membrane: a model of molecular, structural, and functional adaptation to transepithelial ion transport and barrier function during embryonic development." J Biomed Biotechnol 2010:

Figure 7 - A section through the CAM demonstrating the three tissue layers (B-D). A: shell membrane. B:chorionic epithelium. C: mesoderm layer. D allantoic epithelium E: allantoic cavity. Adapted from Gabrielli *et al*

The CAM is most widely known for its role in angiogenesis research however it has also been used in cancer research for decades (Sommers, Sullivan et al. 1952). The work of James Murphy in 1916 demonstrated the natural immunodeficiency of the chick embryo until around 2 weeks into its development making it amenable to tumour xenografting (Murphy 1916). In 1982 Armstrong *et al* published a paper describing the ability of several different types of tumour cells to invade the CAMs epithelial layer. The authors demonstrated that following light trauma to the CAMs surface, tumour cells readily invade the superficial epithelial layer and form tumours beneath it (Armstrong, Quigley et al. 1982).

Within this field, growing recognition of the chick embryo models advantages means interest in the CAM is increasing rapidly, and consequently it is being used to explore the invasive and metastatic properties of an expanding number of malignancies. To date, works describing the use of the CAM model in relation to Burkitt lymphoma, osteosarcoma, ovarian cancer, colon cancer, prostate cancer, glioma, melanoma, breast cancer, anaplastic thyroid cancer and leukaemia have been published (Kobayashi, Koshida et al. 1998, Carrodeguas, Rodolosse et al. 2005, Hagedorn, Javerzat et al. 2005, Taizi, Deutsch et al. 2006, Balciuniene, Tamasauskas et al. 2009, Subauste, Kupriyanova et al. 2009, Strojnik, Kavalar et al. 2010, Palmer, Lewis et al. 2011, Klingenberg 2014, Yang 2014). Studies have generally used these techniques as a means of describing and quantifying the invasive/metastatic capabilities of these malignancies, however others have sectioned and characterised the tumours that they formed. These studies found the morphology and expression of cell markers to be similar to that of primary samples (Klingenberg 2014, Yang 2014).

There have been a limited number of studies utilizing the chick xenograft model for therapeutic research. Due to the highly vascular nature of the CAM the majority of these have been related to angiogenesis (Lin, Chen et al. 2013, Ozcetin, Aigner et al. 2013). Similarly in the context of neuroblastoma research, work with the CAM has been limited and published works largely relate to angiogenesis and its inhibition (Marimpietri, Brignole et al. 2007, Mangieri, Nico et al. 2009, Azar, Azar et al. 2011). Here we aim to demonstrate that CAM xenograft model represents a high through-put, economically viable yet highly informative model system in the context of neuroblastoma drug discovery.

2.Project Aims

Given the growing number of malignancies shown to successfully form tumours on the chick CAM we hypothesised that neuroblastoma cells would also demonstrate this ability. Furthermore, as others have also suggested we hypothesised that cells growing in this system would provide an highly practical means of preclinical therapeutic testing.

In order to explore the ability of the chick embryo to act as a new pre-clinical therapeutic model system for neuroblastoma, this project aimed to:

- Establish and optimise a protocol for the xenografting of different neuroblastoma cells on to the surface of the CAM, focusing on "high risk" MYCN amplified cell lines.

- Determine a suitable mode of drug delivery to tumours forming beneath the CAMs surface.

- Determine a suitable time window during which drugs may be delivered to tumours and allowed to exert their effects.

- Establish a suitable means of measuring the effects exerted by therapeutic compounds on neuroblastoma tumours formed in the model.

- Test therapeutic compounds within the chick embryo model focusing on elements of standard neuroblastoma therapy

3.Materials and Methods

3.1.Cell Culture

Several different neuroblastoma cell lines were cultured and introduced into the chick embryo environment during this project. Cell lines are established from samples of primary or metastatic tumours which are obtained from patients during surgical resection, bone marrow aspiration, and occasionally from peripheral blood. Each has different characteristics which can be seen here - Table 5.

Cell line	Fluorescent label	Culture medium	Source	Characteristics
SKNAS	GFP when used alone Red tomato when mixed with GFP labelled cells	FCS - 10% Pen Strep - 1% NEAA - 1% DMEM	Metastatic site: bone marrow	Single copy MYCN Chromosome 1p deletion
BE(2)-C	GFP	FCS - 10% Pen Strep - 1% NEAA - 1% DMEM	BE(2)-C is a clone of the SK-N-BE(2) neuroblastoma cell line that was established from a bone marrow biopsy taken from a child with disseminated neuroblastoma after repeated courses of chemotherapy and radiotherapy.	MYCN amplified Chromosome 1p deletion Chromosome 17 translocation; t(3;17)(p21;q21)
KELLY	GFP	FCS - 10% Pen Strep - 1% RPMI	Isolated from a metastatic brain lesion in a 1.1 year old boy	MYCN amplified ALK
IMR-32	GFP	FCS - 10% Pen Strep - 1% NEAA - 1% RPMI	Isolated from an abdominal NB in a 13-month-old boy	MYCN amplified 1p deletion 47 + XY karyotype

Table 5 - neuroblastoma cell lines
This table outlines the key features of the cell lines used in the project as well as the conditions in which they were cultured. DMEM - Dulbecco's modified eagle medium; FCS - fetal calf serum; GFP - green fluorescent protein; Pen Strep - *Penicillin Streptomycin.*

To aid the identification of NB cells used in the chick model cell lines were transduced with lentiviral particles containing eGFP or dTomato (carried out by Dr. Sokratis Theocharatos at the University of Liverpool). eGFP and dTomato provided these cells with a stable fluorescent label and therefore allowed visualisation of the cells under UV light. Where different cell lines were used together one GFP and one red Tomato cell line was used so that the distribution of differing cells could be identified.

Cells were cultured in T75cm² tissue culture flasks (Corning, UK) containing 10ml of appropriate culture media (see Table 5). Flasks were incubated in a humidified environment at 37°C, 5% CO_2.

In order to continually supply the NB cells with the nutrients they needed, media was removed every 2-3 days and replaced with 10mL of fresh, pre-warmed media. When culture dishes reached 80 – 90% confluence cells were passaged. During passaging old media was removed and cells were washed once with 5mL of PBS (Dulbecco's Phosphate Buffered Saline, Life Technologies). 1mL of 0.05%Trypsin EDTA 1x Solution (Sigma Aldrich) was added and cells were incubated for 1 minute at 37°C. Detached cells were transferred to a falcon tube and centrifuged (5min, 101×g). The pellet was resuspended in 1mL of culture medium and seeded at a density of 1-3x10^6.

3.1.1.Culturing NB cells with retinoic acid

9 - cis retinoic acid (RA) (Sigma) was diluted in DMSO to make 0.16mM aliquots and stored at -80˚C. A final 10µM concentration of RA was obtained by diluting the stock solution with the appropriate cell culture medium (see Table 5).

Cells were seeded at a density of 2x10^6 and left to settle for 24hours. After 24hours old medium was discarded and 10µL of the appropriate medium containing retinoic acid was used to replace it. Controls were cultured with medium supplemented with DMSO at the same concentration. Every 48 hours the medium was again replaced with fresh RA or DMSO containing medium. Cells were incubated with RA for a either 3 or 6 days prior to RNA extraction.

3.1.2.Culturing NB cells with MLN8237

MLN8237 powder (Sigma) was reconstituted in DMSO to make 0.1M aliquots and then stored at -80˚C according to the manufacturer's instructions. Final concentrations of MLN8237 were reached using the appropriate cell medium.

Cells were seeded as for RA experiments and again left to settle for 24 hours. After 24 hours cell culture medium was discarded and replaced with 1µM, 4µM and 10µM concentrations of MLN8237 containing medium. Medium was changed every 48 hours and cells were cultured for a total of 3 or 6 days.

3.1.3.Culturing chick embryonic heart fibroblasts

Eggs were incubated under physiological conditions until E8. At E8 embryonic hearts were dissected and shredded into approximately 10 pieces per heart. The shredded tissue was then transferred into a cell culture Petri dish and 5mL of L15 medium (Sigma) was added. Hearts were incubated for 3 days at 37°C, 5% CO2.

3.2.Incubation and fenestration of chick embryos

Chick embryo experiments were carefully performed in accordance with the current UK Home Office guidance.

Fertilised white leghorn chicken eggs were obtained from Lees Lane Poultry, Wirral, UK. The eggs were placed into an incubator (Multihatch Mark II) and maintained at approximately 37˚C and 40% relative humidity. Eggs were not rolled as they would be in normal physiological settings, in order to ensure easy access to the embryo at later stages in development.

To prevent the extraembryonic membranes from fusing to the inner surface of the shell, albumin was removed from the egg. 48-72 hours after incubation the eggs were removed from the incubator and gently cleaned using 70% ethanol. A pin was used to gently puncture the base of the egg allowing access. 3 - 4mL of albumin was then removed by inserting a (19G Terumo) needle connected to (5mL Terumo) syringe into the puncture site. The puncture was then sealed using a small square of adhesive tape to prevent any further leakage from the site.

Following the removal of albumin from the egg, a small window was cut into the shell allowing access to the underlying embryo and membranes. A 1cm² window was carefully cut into the shell using a hand held circular drill. The window was then resealed using adhesive tape. Eggs were again incubated under the same conditions until E7.

3.2.1.Implanting NB cells on to the CAM

At E7 windowed eggs were removed from the incubator and assessed for survival. In the surviving eggs, cells were implanted topically on to the newly developed CAM.

The appropriate NB cell line was selected. Flasks containing the cells had their medium removed and cells were washed once with DPBS (Dulbecco's Phosphate Buffered Saline, Life Technologies), and then trypsinised and pelleted as described previously for passaging. Cells were then resuspended in 1mL of medium and the density of cells was counted using a haemocytometer. Approximately $2x10^6$ cells were used per egg. These cells were placed into separate epedorf tubes and again centrifuged to form a pellet. The remaining medium was then removed leaving only 5uL of medium per $2x10^6$ cells. The cells and medium were mixed prior to implantation on to the surface of the CAM.

The eggs were removed from the incubator individually and the surface of the CAM was lightly traumatized. A 1cm² piece of sterilized lens tissue was applied to the surface of the CAM and immediately removed to lightly traumatise the surface. The appropriate NB cell line was then placed on to this area of the CAM before resealing the egg with adhesive tape and returning it to the incubator.

3.2.2.Implantation enhanced with and transforming growth factor-β, trypsin and cancer associated fibroblasts

Whilst investigating methods of enhancing NB cell invasion of the CAM several adjustments to the above method were trialled.

Trypsin and TGF-β

In the case of trypsin and transforming growth factor-β (TGF-β) cells were pelleted and counted according to the previous method. Immediately prior to implantation on to the CAM each $2x10^6$ cells had 5µL of either trypsin, TGF-β (10 ng/mL concentration) or a 50:50

mixture of both added to the cells. The cells were mixed as previously described and implanted on to the CAM surface.

Cancer associated fibroblasts (CAFs)

Fibroblasts were cultured from the shredded E8 chick heart tissue as previously described. After 3 days the cells were trypsinised and centrifuged to form a pellet. The number of cells was counted. These cells were then mixed with BE(2)-C cells at a 5:1 BE(2)-C to fibroblast cell ratio. The cell mixture was resuspended in 1mL medium and returned to a 75cm² culture flask. Cells were incubated together for 2 days prior to implantation onto the CAM.

3.3.Dissection and analysis of tumours

At E14 eggs were once again removed from the incubator individually and assessed under florescent light on a Leica M165 FC fully apochromatic corrected stereo microscope with 16.5:1 zoom optics. The visual field was maximized by breaking away shell surrounding the egg "window". Eggs were examined thoroughly for the presence of tumour formation and fluorescently labelled cells. Fluorescence was GFP and dsRed and images were captured using a Leica DFC425 C microscope camera alongside the computer software package, Leica V4.0.

Dissection of any resultant tumours was achieved using size 5 dissection tweezers and dissection scissors. Tumours were placed into PBS before being weighed and stored in RNAlater, or fixed.

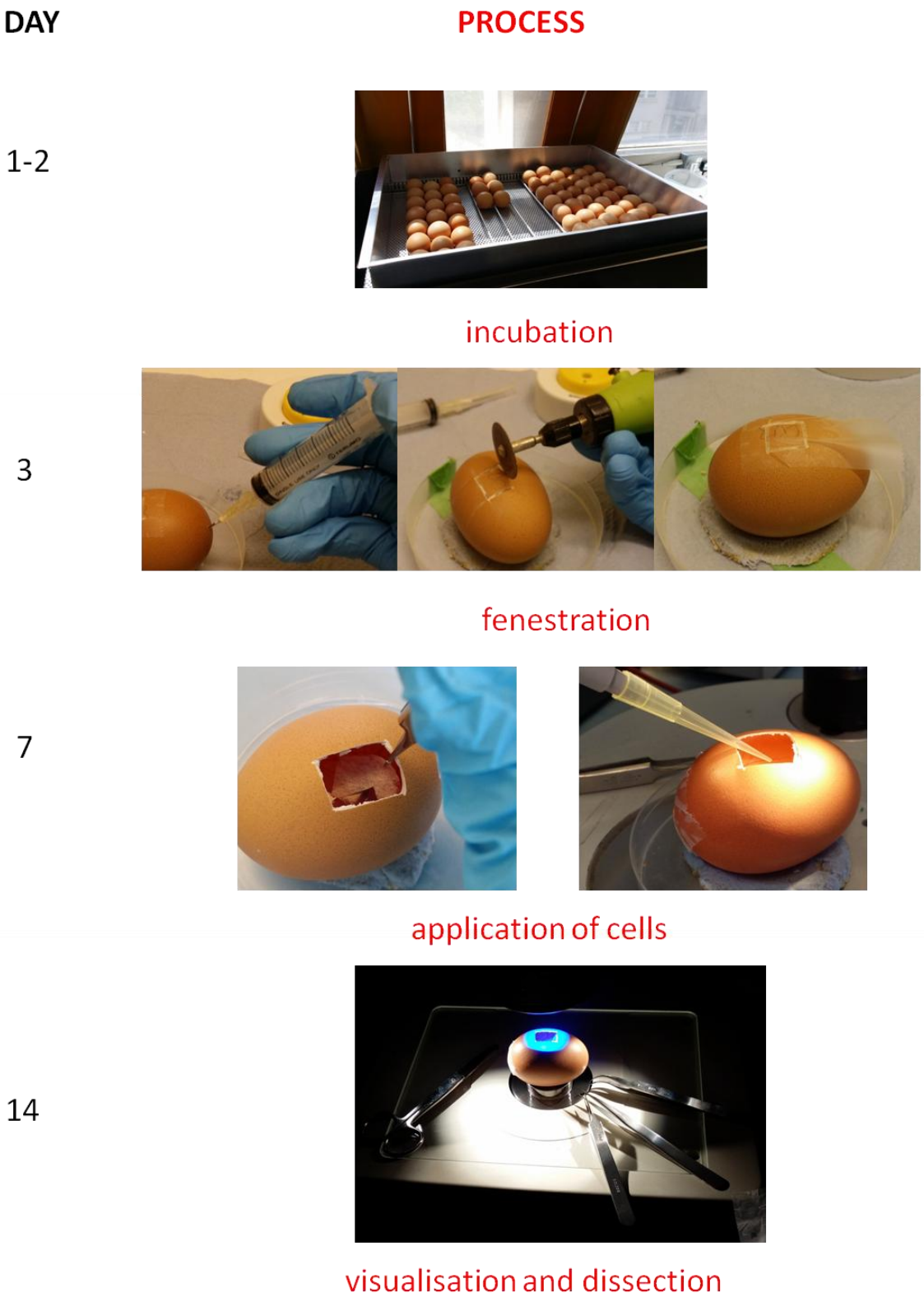

Figure 9 - a visual display of the steps taken in chick embryo experimentation. Eggs were initially incubated for 48 hours prior to the removal of albumin, and subsequent "windowing" of the shell. After 7 days the CAM was lightly traumatised using lens tissue and NB cells were placed on to this portion of the CAM. Visualisation and dissection of any resultant tumours occurred at day 14.

3.3.1.Predicting tumour formation

In order to test therapeutic compounds in the model tumour formation must be predicted prior to E14 tumour dissection. In order to assess this, eggs were prepared, incubated and cells were implanted as previously described. Each egg was then numbered and at E8, E10, E11, E13 and finally E14 eggs were reopened and assessed for the presence of tumour formation. The results were recorded at each stage.

3.3.2.Frozen sections

After dissection, tissues were fixed in 4% PFA at 4˚C for 20 minutes. Tissue was then washed 3 times with DPBS and placed in a 20% sucrose solution overnight. Tissues were then mounted on labelled 2cm diameter cork discs in Cryo-M-Bed embedding compound (Bright) and stored at -80˚C. 12 µm sections were cut using a cryostat and collected on Menzel Gläser Superfrost Plus glass slides (Thermo Scientific). Slides were stored at -80˚C prior to staining.

3.3.3.Paraffin sections

Paraffin embedding was carried out by Halleh Shahidipour, University of Liverpool. Samples were fixed in 10% Formalin up to 12 hours prior to dehydration for 48 hours in a plastic cassette. Later samples were aligned appropriately within a metal mould which rested upon a cold surface while hot paraffin wax was poured in using a Thermo SHANDON HISTOCENTRE. Once the sample was fully covered in wax it was left to cool down and set over 24 hours. Samples were stored at room temperature until sectioning.

Prior to sectioning, samples were cooled on a block of ice. After approximately 40mins, samples were fitted onto a microtome (SHANDON) equipped with S35 Feather microtome blade (JDA-0100-00A). Sections were trimmed at 20µm until the sample was uncovered at which point 4µm sections were cut in continuous ribbons' consisting of 4 – 8 sections. Ribbons were placed upon the surface of a waterbath (Fisher Scientific) preheated at 35 – 40°C and individual sections were then separated using 125mm fine point curved forceps. Sections were subsequently transferred to microscope slides (APES coated slides, Leica) which were stored upright in wooden racks and placed in a small oven to dry for at least 24 hours.

3.3.4.Immunofluorescence in pre-fixed samples

Frozen sections

12µm frozen tumour sections were prepared and collected on to Menzel Gläser Superfrost Plus glass slides as described in section 3.3.2. Slides were removed from - 80˚C and placed with tissue sections facing up. Slides were then washed once with DPBS before 0.1% Triton X-100 was added and left at room temperature for 10 minutes to permeabilize the cell membrane. Slides were then washed 3 times with DPBS. DPBS was removed and a hydrophobic ring was drawn around each tissue sample using a Dako pen. 2% BSA was then added to each ring and left for 1 hour at room temperature. BSA was removed and the primary antibody added to each slide at the appropriate concentration (see Table 6). Primary antibodies were left on slides overnight protected from light at 4˚C. Secondary antibodies were left for 1 hour at room temperature. A drop of Dako fluorescent mounting medium was applied to each sample before the addition of a cover slip to each slide. Slides were again stored at 4˚C and protected from light until analysis.

Cell Culture

Cells to be stained were grown on 13mm glass cover slips in 24 well plates. For IMR-32 (which adhere less readily) cover slips were first coated with a 1:100 dilution of Matrigel and left to dry for 1 hour. Cells were seeded at 40-60% density 24 hours prior to staining.

Cover slips were removed from medium and cells were fixed using 100µL of 4% PFA for 10 minutes. PFA was then removed and cells were washed 3x with DPBS. 100µL of 2% BSA was then added to each slide and left for 1 hour at room temperature. Following the removal of the BSA primary antibodies were added at the appropriate concentration and left, protected from light, at 4˚C overnight. The application of secondary antibodies and mounting was carried out as for frozen sections.

Controls

For each experiment a negative control in which the primary antibody was omitted from the staining proceedure was included. Due to difficulty in obtaining material to act as a positive control these were not included in experiments.

Target Name	Host species	Primary Antibody Dilution	Clonity	Manufacturer
GFP	Rabbit	1:500	Polyclonal	Abcam (Ab290)
MYCN	Mouse	1:20	Monoclonal	Abcam (Ab16898)
Ki67	Mouse	1:100	Monoclonal	Dako (F0788)
NSE	Rabbit	1:500	Polyclonal	Abcam (ab53025)
NF70	Mouse	1:500	Polyclonal	Chemicon (MAB5294)
GAP43	Rabbit	1:250	Monoclonal	Abcam (ab75810)
Robo2	Rabbit	1:250	Polyclonal	Abcam (ab85278)

Table 6 - antibodies used during immunostaining and their respective dilutions.

Antibody	Dilution	Source
Goat anti-mouse Alexa Fluor 488 (green)	1:500	Invitrogen, A11001
Goat anti-mouse Alexa Fluor 568 (red)	1:500	Invitrogen, A11004
Goat anti-rabbit Alexa Fluor 488 (green)	1:500	Invitrogen, A11034
Goat anti-rabbit Alexa Fluor 594 (red)	1:500	Invitrogen, A11012

Table 7 = secondary antibodies used during this project.

3.3.5.EdU administration

EdU is a novel thiamine analogue incorporated into dividing cells. It was used during the project to assess drug delivery in the chick embryo.

Topical administration

Eggs were incubated and prepared as described previously and cells were applied to the CAM at E7. At E13 the eggs were taken from the incubator and the adhesive tape covering the pre-cut window was removed. 200µL of 2mM or 4mM EdU was dripped on the surface of the CAM. The eggs were gently rotated 20-30˚ to allow the liquid to spread over the

surface of the CAM. The eggs were then resealed with adhesive tape and returned to the incubator for a further 24hours.

IV administration

IV administration of EdU was completed by Rachel Carter (University of Liverpool). Borosilicate glass capillary tubing (thin wall with filament, Warner Instruments) was pulled under heat to a thin taper (settings: heat 580, velocity 15, pull 130, time 15, pressure 20; Sutter Instrument Co.), and the resulting needles snapped using dissecting forceps to an appropriate diameter. At E13 8µL of 10mM EdU was injected into the CAM vasculature under a stereo microscope.

3.3.6.EdU detection

EdU was detected in tissue dissected from the chick at E14. Tissue was frozen and sectioned as previously described. A Click-iT® EdU Alexa Fluor® 488 Imaging Kit (Life Technologies) was then used according to the manufacturers protocol.

3.4.Retinoic Acid

3.4.1.Administering Retinoic Acid to the chick embryo model

A selection of eggs were weighed and an average of 50g per egg was calculated. 10% of this value was deduced to allow for the weight of the shell giving 45grams as the final value . Retinoic acid doses of 30mg/kg were used throughout experiments.

9 - cis retinoic acid (sigma) was diluted in DMSO to make 0.16M aliquots and stored at -80˚C. The final concentration of RA was obtained by diluting the stock solution first in a 1x volume of DMSO and then in PBS to make up a final volume of 200µL/egg.

Eggs were taken from the incubator and the adhesive tape covering the window in the shell was removed. 200µL of RA was carefully administered topically to the surface of the CAM using a micropipette. Fresh adhesive tape was again placed over the window and the eggs were returned to the incubator. This procedure was repeated at approximately the same time each day for 3 days.

3.4.2.RNA Extraction

RNA extraction was completed using the RNeasy Mini Kit (QIAGEN). All reagents were stored in a dedicated RNase-free area and experiments were carried out in a dedicated area of the lab.

Cells

Cells were first trypisinised and pelleted as for passaging. The supernatant was then removed and the pellet disrupted by gentle tapping of the tube. 350µL of the buffer RLT was then added to the cells. The cells were repeatedly drawn up and down using a 19G needle and 1mL syringe to simultaneously disrupt and homogenise the cells. A 1x volume of 70% ethanol was subsequently added to the lysate and mixed by pipetting. 700µL of the resultant liquid and precipitate was transferred to an RNeasy spin column and spun for 15s at 8000 x g. The flow through was then discarded and 700µL of buffer RW1 was added to the column. The column was spun again at 8000 x g for 15s. 500µL of the buffer RPE was then added to the column and spun as before. Finally a new collection tube was used and 40µL of RNase free water was applied directly to the columns membrane before spinning for 1 minute at 8000 x g.

RNA was immediately stored on ice and analysed using a luminometer. RNA was then aliquoted and stored at -80˚C.

Tumours

Tumours dissected from the chick model were placed in RNAlater (QIAGEN) and stored at 4˚C for up to 2 weeks prior to RNA extraction.

The tissue was first removed from the RNAlater and transferred to a clean RNase free falcon tube. Liquid nitrogen was used to freeze the tissue before a pestle and mortar was used to disrupt it. RNA was then extracted as per the above protocol.

3.4.3.Reverse transcription

First strand cDNA synthesis was completed using a GoScript reverse transcription system (Promega) according to the manufacturers protocol. A total of 1µg of RNA was used per reaction. Where the addition, or the volume, of a reagent was optional details can be seen below (Table 8).

Reagent	Volume per reaction (µL)
Oligo(dT)15 primers	1
MgCl2	2
Recombinant RNasin® Ribonuclease Inhibitor	0.5

Table 8 - Reagents and corresponding volumes used during reverse transcriptase that were not already stated in the manufacturers protocol.

3.5.qPCR

3.5.1.Reference gene selection

Reference genes were incorporated into the experiment to allow the normalised relative quantification of target genes to be calculated. A literature search was conducted which yielded a paper by Vandesompele *et al* examining the reliability of several commonly used reference genes in neuroblastoma cells. From this paper we chose ubiquitin C (UBC), glyceraldehyde-3-phosphate dehydrogenase (GAPDH) and hypoxanthine phosphoribosyltransferase 1 (HPRT1) as the most suitable candidates and therefore primers were sought for these genes (Vandesompele, Baudis et al. 2005).

3.5.2.Target gene selection

In a paper published in 2012 Sung *et al* described the effects of retinoic acid on several neuroblastoma cell lines in culture. We selected the three genes having the largest fold increase/decrease from this paper; Kruppel-like factor 4 (KLF4), roundabout, axon guidance receptor, homolog 2 (ROBO2), stathmin-like 4 (STMN4). We also included MYCN due to its significance in neuroblastoma differentiation.

3.5.3.Designing primers

An initial search for suitable primers was conducted. Primer sequences were identified in published papers using the same target or reference genes in qPCR experiments. Any sequences found were located within the FASTA gene sequence and only primers spanning introns were considered. The size of the intron and the PCR product was calculated. Primer sequences were entered into the NCI primer basic local alignment search tool (BLAST) in order to determine their melting temperature and to ascertain the presence and strength of

secondary structures. Where suitable published sequences were not available primers were designed using the NCI primer-BLAST tool. Data relating to the selected primers can be seen in Table 9.

Primer Name		Sequence	Product Length	Intron Length	Tm	Secondary	GC %	Reference
UBC	FW	ATTTGGGTCGCGGTTCTTG	93	812	67	none	52.6	(Vandesompele, Baudis et al. 2005)
	RV	TGCCTTGACATTCTCGATGGT			67	very weak	47.6	
HPRT1	FW	TGACACTGGCAAAACAATGCA	53	4797	68	weak	42.8	(Vandesompele, Baudis et al. 2005)
	RV	GGTCCTTTTCACCAGCAAGCT			67	weak	52.3	
GAPDH	FW	AATCCCATCACCATCTTCCA	43	130	64	None	45	(Vandesompele, Baudis et al. 2005)
	RV	TGGACTCCACGACGTACTCA			65	Weak	55	
ROBO2	FW	GATGTGGTGAAGCAACCAGC	306	990	60	weak	55	(Sung, Boulos et al. 2013)*
	RV	TGGCAGCACATCTCCACG			60	weak	61.1	
STMN4	FW	CCTAGCAGAGAAACGGGAACA	178	1254	60	none	52.4	(Sung, Boulos et al. 2013)*
	RV	GGCGTGCTTGTCCTTCTCTT			61	weak	55	
KLF4 (4)	FW	CGCCGCTCCATTACCAAGAGC	301	1101	64	weak	61.9	Designed using primer blast tool
	RV	CGGTCGCATTTTTGGCACTG			61	none	55	
MYCN 2	FW	CACAAGGCCCTCAGTACCT	95	2639	60	none	61	(Malakho, Korshunov et al. 2008)
	RV	ACCACGTCGATTTCTTCCTCT			59	weak	50	

Table 9 - details of the primers used in qPCR experiments. Tm is the melting temperature of the primer, secondary refers to the presence and strength of primer secondary structures, GC is the number of G's and C's in the primer as a percentage of the total bases. Data was obtained from the NCI primer-BLAST tool. *Primer sequences were obtained through direct contact with authors.

After suitable primer sequences were identified, primers were ordered from Sigma Aldrich. Once the primers were received they were reconstituted in PBS, and stored at -20˚C in small 10mM aliquots to avoid freeze-thawing.

3.5.4.Primer optimisation

Temperature

Temperature gradients were used to determine a suitable range of temperatures for qPCR. Primers were ranked according to their melting temperature and then paired. Each pair was tested on a single plate at a temperature gradient +/- 5˚C from the mean melting temperature of the two primers. A PCR protocol was designed to incorporate the temperature gradient (Table 10), before the individual primer pairs were tested (example can be seen in Figure 10).

qPCR Protocol design

Protocols were designed according to the recommendations of the ITaq SYBER green mastermix manufacturer (BioRad) specifically for the CFX Connect system (details seen in Table 12). The steps of the protocol used can be seen in Table 10 and an example used during primer optimisation of KLF4 and STMN4 can be seen in Figure 10.

.

Step		Details
1	Polymerase activation and DNA denaturation	95˚ C 30 seconds
2	Amplification (Denaturation)	95˚ C 5 seconds
3	Amplification (Annealing/Extension + plate read)	Gradient or 60˚C after optimization 30 seconds
4	Amplifiaction (Cycles)	40
5	Melt curve	65˚C to 95˚C 0.5˚C increment 5 seconds/step

Table 10- details of qPCR protocol

Feature	CFX Connect System
Capacity	96 wells
Light source	3 LEDs in optics shuttle
Optical detection	3 photodiodes
Excitation range	450–535 nm
Detection range	515–580 nm
Multiplex capability	Up to 2 targets
Maximum gradient span	24°C
Maximum ramp rate	5°C/sec
Real-time PCR software	CFX Manager software

Table 11 - The CFX Connect qPCR system details - table highlighting the specifications of the BioRad CFX Connect system used throughout qPCR experiments. Adapted from www.biorad.com

Example: KLF4 and STMN4

Mean primer melting temperature of 60˚C. Gradient 55˚C to 65˚C

A

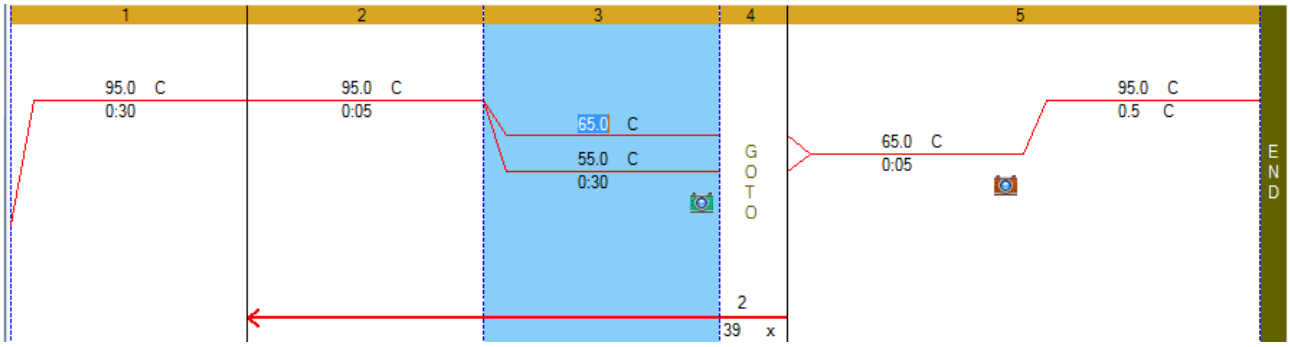

B

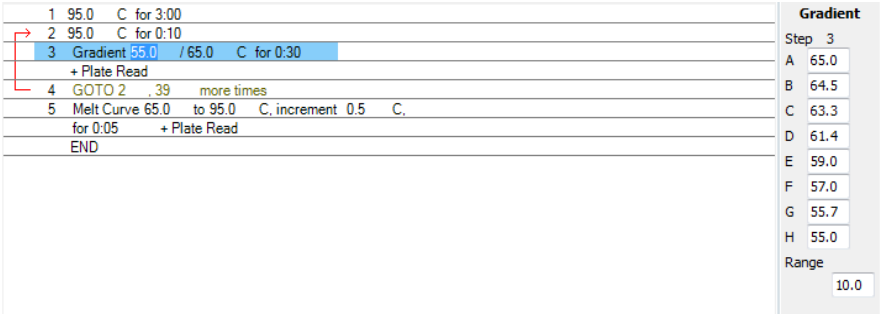

Figure 10 - An example PCR protocol with a temperature gradient of 55˚C to 65˚C. Numbers 1 - 5 across the top of A correspond to the stages displayed in B. The actual temperatures in the 8 rows (A-H) of the plate can be seen under the heading "Gradient" in B.

Controls

During primer optimization, and whenever new RNA/cDNA was used, a non-reverse transcriptase control added to the plate. For all experiments a no-template control was included.

Plate design

96 well plates (BioRad) were used throughout the qPCR experiments. The plate below demonstrates a generic plate used in primer optimization (Figure 11). Two primers and their controls were used in duplicate per plate.

	1	2	3	4	5	6	7	8	9	10	11	12
T1	NRT	NRT	Primer	Primer	NTC	NTC	NRT	NRT	Primer	Primer	NTC	NTC
T2												
T3												
T4												
T5												
T6												
T7												
T8												

Figure 11 - Plate design for optimization of primers NRT; no reverse transcriptase NTC; no template control. T1 - 8 refer to a temperature gradient.

3.5.5.qPCR Reaction Mix

The components of the qPCR reaction can be seen here (Table 12) and remained constant between experiments.

Reagent	Final concentrations	Volumes/well
ITaq Universal SYBER Green supermix (2x)	1x	5uL
Primers	500nM each	0.5uL each
cDNA	100ng	variable
Water	-	variable
Final Volume per well	10uL	10uL

Table 12 - table displaying the components of the reaction mix for qPCR experiments.

3.5.6.Retinoic Acid Experiments

Experimental design

Each experiment was carried out using 3 biological and 3 technical repeats. The plate design for experiments can be seen below (Figure 12)

GAPDH	NTC	NTC	NTC	RA	RA	RA	NTC	NTC	NTC	control	control	control
HPRT1												
KLF4												
MYCN												
ROBO2												
STMN4												
UBC												

Figure 12- Plate design in qPCR experiments NTC; no template control, RA; cDNA from cells treated with retinoic acid, Control; cDNA from cells cultured with control medium

The reagents were prepared using the same concentrations as stated in Table 12. All reagents were thawed to room temperature prior to use. Master mixes were prepared wherever possible and great care was taken to ensure accurate pipetting. 10uL of each mix was pipetted into each well prior to the application of a clear seal. A CFX Connect (BioRad) thermocycler was used for all experiments (Table 11).

Analysis

An initial inspection of both the amplification plot and melt curve ensured that there were no obvious anomalous results. Fold change in target gene expression was calculated relative to the control. Results were normalised to three housekeeping genes (GAPDH, HPRT1 and UBC) to allow for differences in the quantity of starting material and reaction kinetics.

After initially checking data subsequent qPCR data analysis was carried out using Bio-Rad CFX Manager 3.0 software. Normalised relative expression of target genes was calculated using the ΔΔCq analysis mode. Data from 3 biological replicates was used in each instance. Error was calculated using standard deviation.

P values were also calculated using the CFX Manager software. The formulas used by the software are displayed below:

$$\text{p-value} = 1 - A$$

Where:

$$A = \int_{x=-t}^{t} = \frac{\Gamma\left(\frac{v+1}{2}\right)}{\sqrt{v\pi}\,\Gamma\left(\frac{v}{2}\right)}\left(1+\frac{x^2}{v}\right)^{-\frac{v+1}{2}}$$

$$v = \text{Count}\left(\text{NE}_{\text{sample (Experimental)}}\right) + \text{Count}\left(\text{NE}_{\text{sample (Control)}}\right) - 2$$

- Γ = gamma function
- t = t-statistic

$$t = \frac{\left|Mean\left(NE_{sample(expt)}\right) - Mean\left(NE_{sample(control)}\right)\right|}{\sqrt{\frac{\left(Count\left(NE_{sample(expt)}\right)-1\right)*SD\left(NE_{sample(expt)}\right)^2 + \left(Count\left(NE_{sample(control)}\right)-1\right)*SD\left(NE_{sample(control)}\right)^2}{Count\left(NE_{sample(expt)}\right)+Count\left(NE_{sample(control)}\right)-2}} * \sqrt{\left(\frac{1}{Count\left(NE_{sample(expt)}\right)} + \frac{1}{Count\left(NE_{sample(control)}\right)}\right)}}$$

- Mean = Arithmetic mean
- NE = Normalized expression
- Count(x) = Size of list x
- SD = Sample standard deviation

3.6.MLN8237

Cells cultured with MLN8237 had RNA extracted, cDNA synthesised and qPCR performed according to the same protocol as retinoic acid based experiments.

4.Results

This project aimed to investigate the chick embryo as a potential *in vivo* model for therapeutic research. Many factors such as its degree of natural immunodeficiency and ease of access make the chick embryo amenable to this form of cancer research. Exploration of the chick embryo as a potential xenograft model for a wide variety of cancers is already underway. We hypothesised that the chick embryo and its chorioallantoic membrane could provide an informative and practical model for neuroblastoma research. We investigated the potential of this model to provide a novel means to test therapeutic compounds on neuroblastoma cells in an *in vivo* setting.

4.1.Aims:

To establish the chick embryo as a new model system for therapeutic research in neuroblastoma.

- To establish and optimise a protocol for the xenografting of different neuroblastoma cells on to the surface of the CAM, focusing on "high risk" MYCN amplified cell lines.
- To determine a suitable mode of drug delivery to tumours forming beneath the CAMs surface.
- To determine a suitable time window during which drugs may be delivered to tumours and allowed to exert their effects.
- To establish a suitable means of measuring the effects exerted by therapeutic compounds on neuroblastoma tumours formed in the model.
- To test therapeutic compounds within the chick embryo model.

4.2.Growing tumours on the CAM

Previous studies have demonstrated the suitability of the CAM for tumour xenografting (Balciuniene, Tamasauskas et al. 2009, Balke, Neumann et al. 2010, Klingenberg 2014, Yang 2014). In the context of neuroblastoma, work by others within our laboratory has

demonstrated that the SKNAS cell line could form tumours within this environment (Rice 2013). However, SKNAS is a non-MYCN amplified neuroblastoma cell line. MYCN amplification is the most robust independent prognostic factor for unfavourable outcome in neuroblastoma (Rubie, Hartmann et al. 1997). Cells with amplification therefore represent much of the high risk disease for which new treatments are needed. Thus in addition to the SKNAS cell line, we set out to investigate the ability of several MYCN amplified lines to form tumours within the model.

Fluorescently labelled Kelly, BE2C (MYCN amplified) and SKNAS (non-MYCN amplified) cells were placed on to the surface of the lightly traumatised CAM and then incubated at 38˚C, 40% relative humidity for 7 days. After 7 days the eggs were examined under UV light and the findings were recorded.

Upon examination one of three outcomes was observed. In a large proportion of the experiments carried out with MYCN amplified cell lines the neuroblastoma cells could be seen as a flat mass on the surface of the CAM (Figure 13A). Here it appeared as though the cells had failed to invade the CAM, remaining on its surface. This observation was also made with the SKNAS cells, however at a much lower frequency. In rare instances no cells were identifiable on the surface of the CAM or beneath it. Where cells had formed tumours, the CAM often had an area of dried blood on its surface suggesting that blood vessel trauma may be integral to the invasion of these cells (Figure 13B).

Tumours formed in the model were identifiable just under the surface of the CAM as distinct masses of variable size (~100µm - 5mm in diameter) and morphology (Figure 14). Large tumours were occasionally distinguishable without fluorescence however the vast majority of tumours were only identifiable under UV light. In most instances one tumour had formed however in rare cases multiple smaller masses could be seen (Figure 14b-ii). Tumours were highly vascular with blood vessels clearly identifiable on their surface (Figure 14b-iii).

4.2.1.Characterising tumours

In order to further characterise tumours forming in the model the masses were dissected out of the egg. After an initial inspection the tumours were put into paraffin sections and haematoxylin and eosin (H&E) staining was performed so that the histological appearance of the tumour could be observed.

Dissection was simple to perform and tumours remained intact during the procedure. Dissected tumours were observed as discrete masses which had a smooth outer surface (Figure 15). An intricate network of blood vessels typically covered the tumours (Figure 15-i). Paraffin sections demonstrated that the tumours were solid masses made up of densely packed tumour cells (Figure 16).

4.2.2.Quantifying Tumour Formation

In order to quantify the efficiency of tumour formation in the model the outcome (tumour formation or no tumour formation) was recorded for each cell line during dissection. In each case the number of eggs with tumours identified at E14 was divided by the number of eggs surviving until this time giving the "success rate" of the cell line.

The initial success rates for individual cell lines ranged from 23 - 66% (Figure 17) with reproducible levels of efficiency seen for each cell line during repeated experiments. The MYCN amplified cell lines were significantly less successful that the non-amplified SKNAS line with success rates averaging half that of the SKNAS.

A

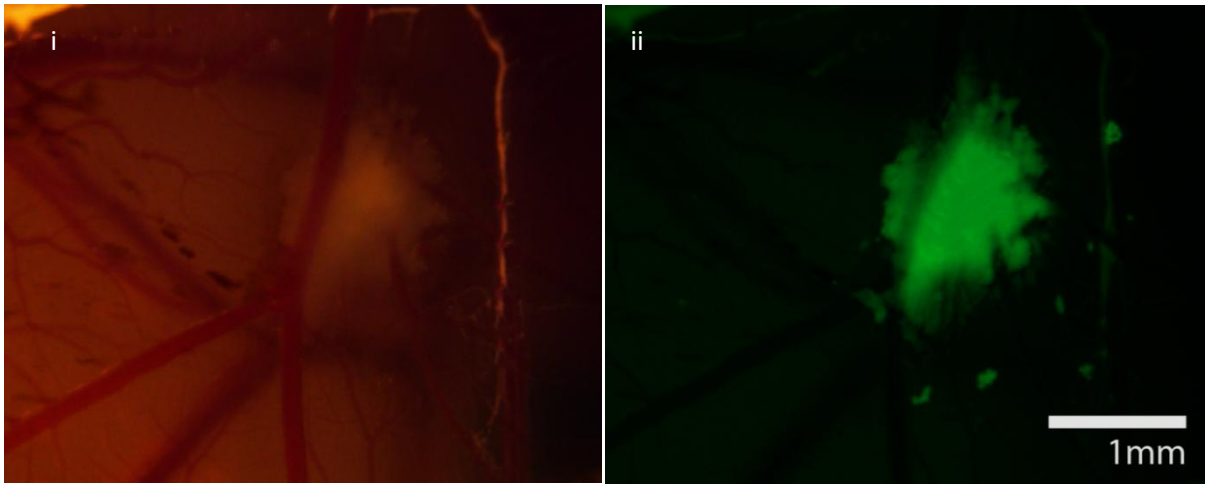

.

B

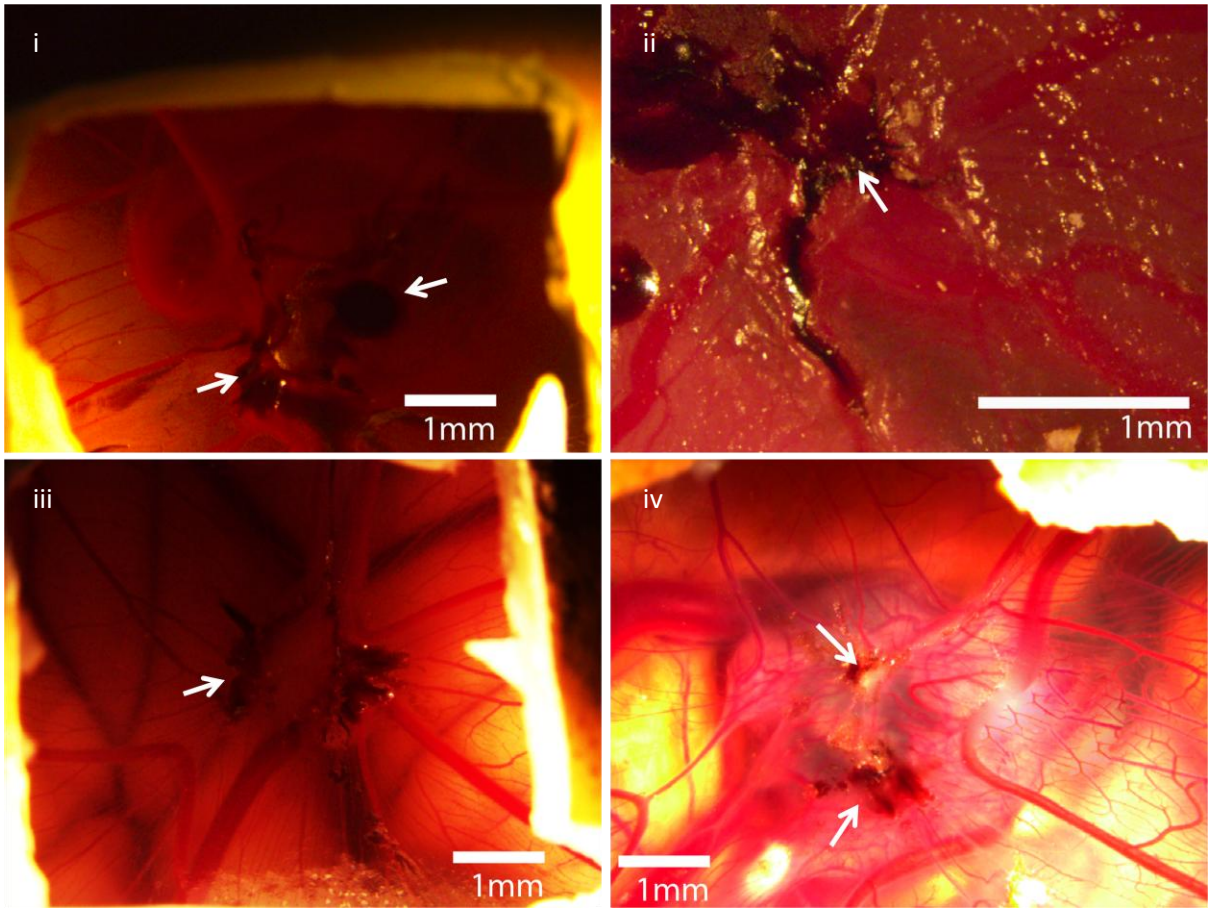

Figure 13 - Neuroblastoma cells on the CAM. A: A patch of flat BE(2)-C cells seen on the surface of the CAM at E14. i - bright field ii - GFP. Here we hypothesised that these cells have failed to invade the CAM and consequently remained on its surface B; Images demonstrating the presence of the blood spot (highlighted by the white arrows) on the surface of the CAM of eggs with tumours forming within them. The blood spot was rarely seen on the surface of CAMs where tumours had not formed and therefore may suggest that blood vessel trauma is key to promoting invasion.

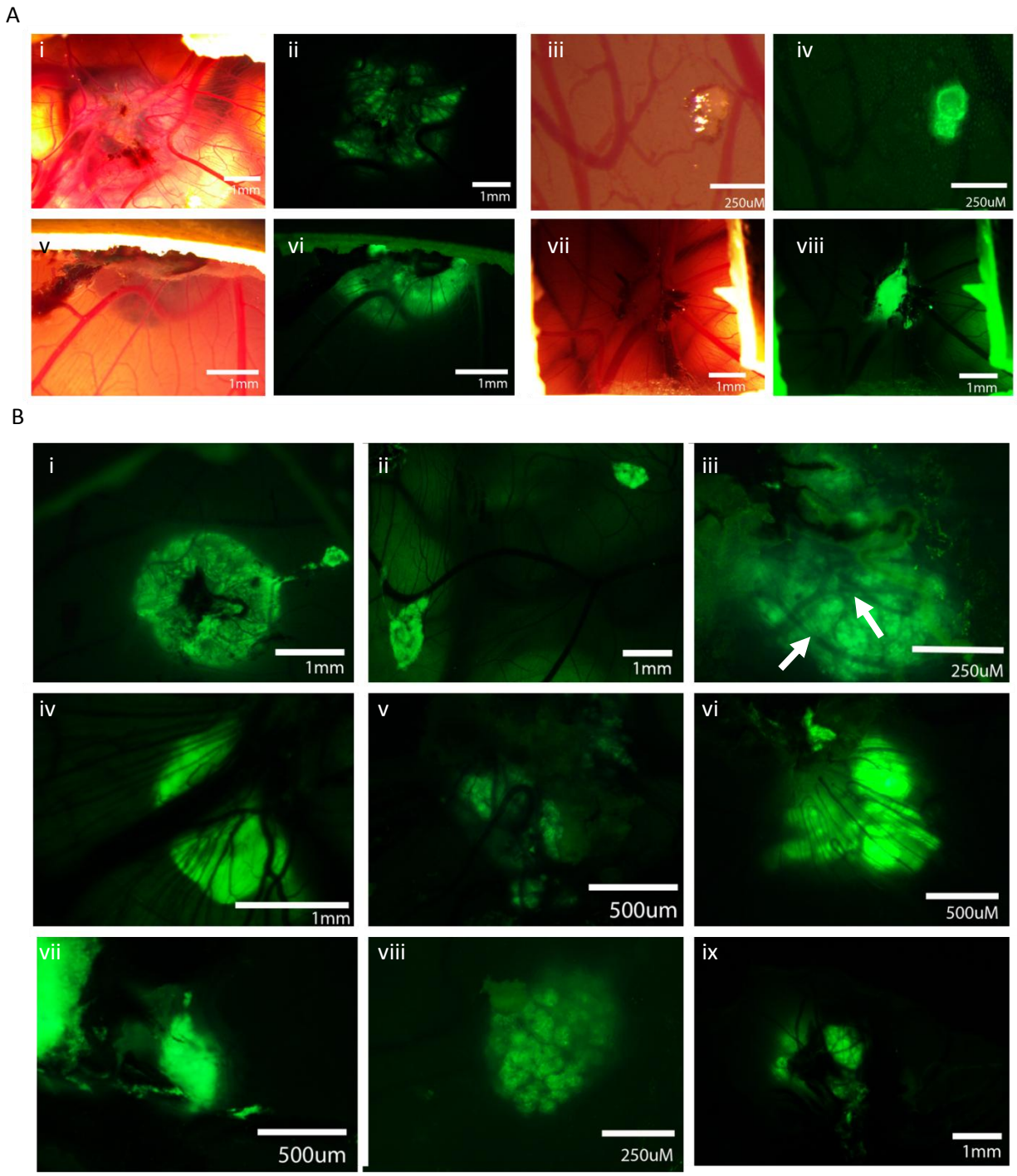

Figure 14 - **Tumours formed in the model**. A: Bright-field and GFP images of 4 tumours beneath the surface of the CAM at E14. Images A - i,ii, vii and viii are BE(2)-C tumours, iii and iv are Kelly and v and vi are SKNAS. B: GFP images displaying the variable size and morphology of tumours forming within the model. i and ii are IMR-32 tumours, iii, iv and v are BE(2)-C, vi and vii are SKNAS and viii and ix are Kelly. Image B-iii highlights the blood vessels seen on the surface of tumours (white arrows)

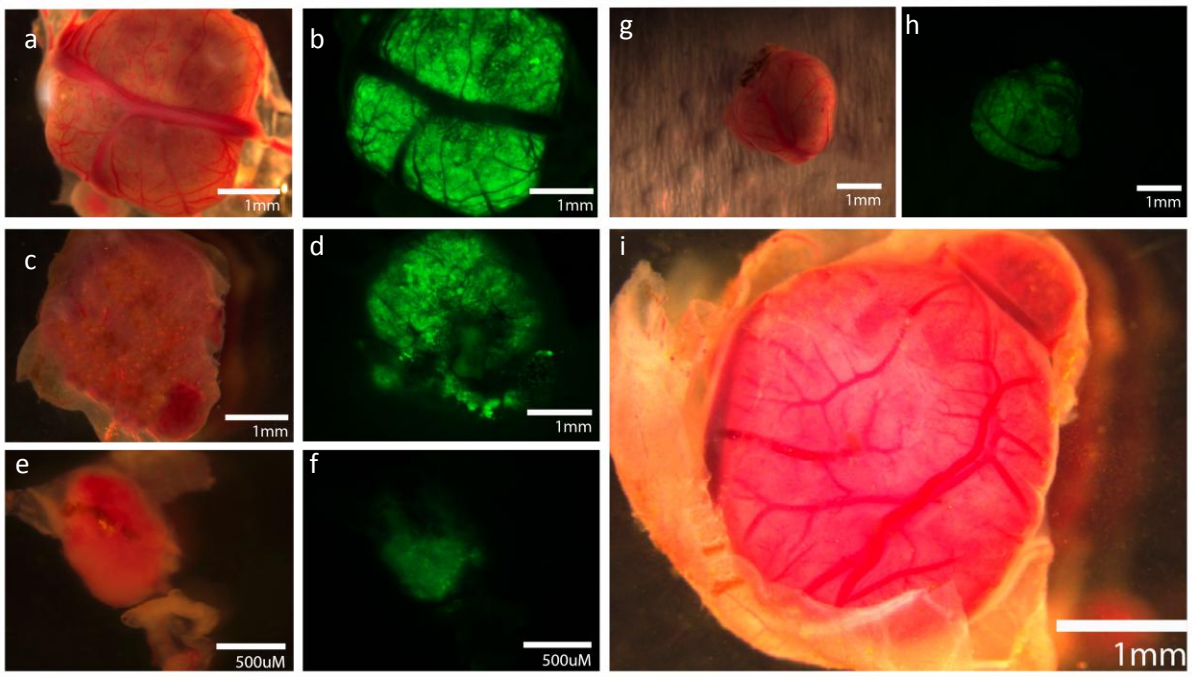

Figure 15 - Tumours after dissection. Paired bright-field and GFP images of tumours after dissection (a-h). a,b, c, d, g and h are BE(2)-C tumours. e and f are kelly. Image I is a large BE(2)-C tumour.

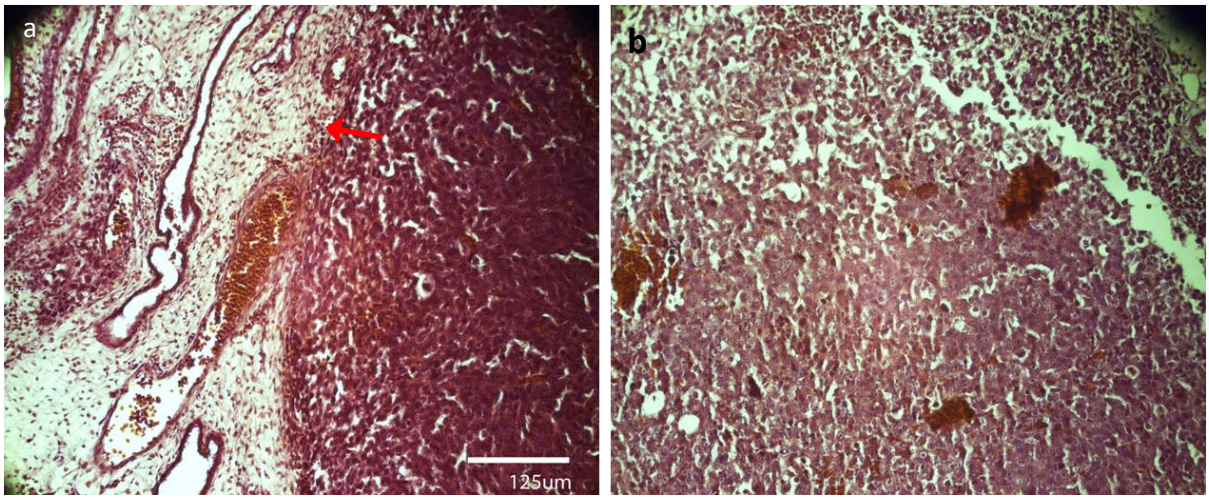

Figure 16 - H&E staining of an SKNAS tumour formed in the model. The large cells of the tumour are seen to be densely packed. A - Image demonstrating the relationship between the tumour (right) and the CAM (left). (red arrow highlights the boarder) B - Image showing the histology of the tumour.

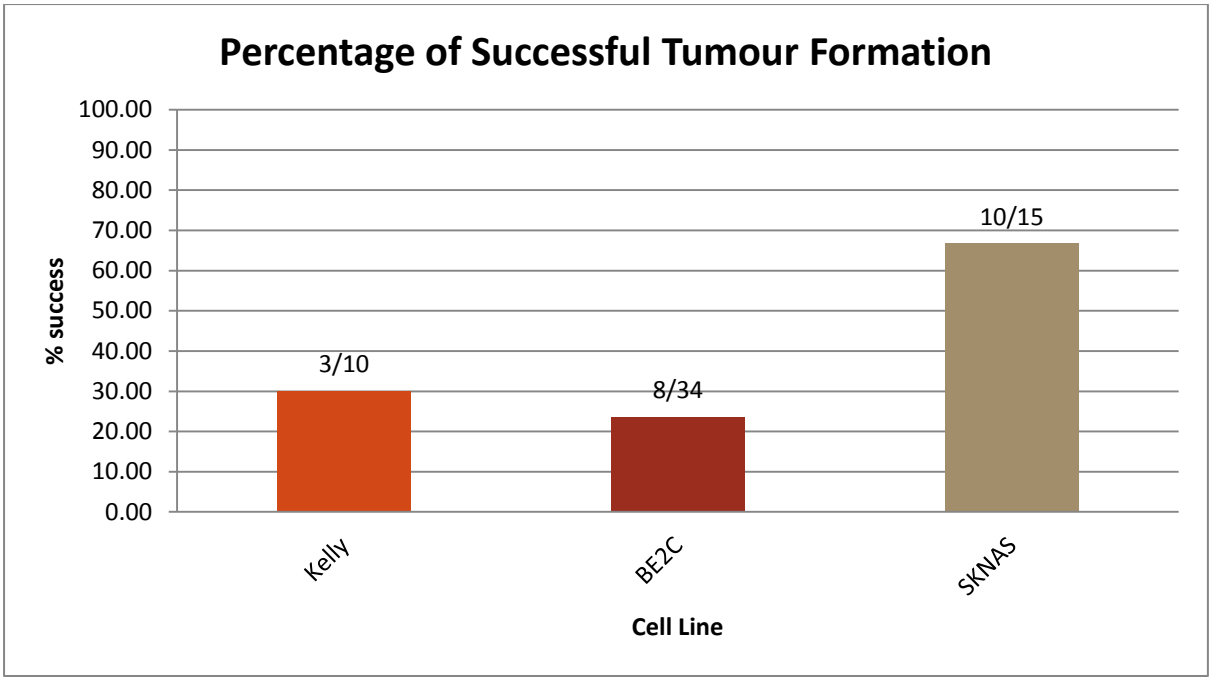

Figure 17 - The success of neuroblastoma cell lines at forming tumours in the chick embryo. Percentage success was calculated by dividing the number of eggs with tumours at E14 by the number of embryos surviving until that time. The fractions above the bars represent the actual number of tumours formed/the actual number of eggs surviving until E14.

4.3.Increasing Tumour Formation

4.3.1.Mixing Cell Lines

Due to the high yield of tumours forming from SKNAS cell line, and the low yields observed in the MYCN amplified ones, we explored the effect that mixing cell lines might have on tumour formation. We hypothesised that combining the MYCN amplified cells with the SKNAS cells prior to implantation on to the CAM may improve the rate of tumour formation in the MYCN amplified lines. Cells were applied to the CAM as for previous experiments however in this instance a 50:50 mixture of either Kelly:SKNAS or BE(2)-C:SKNAS cells was placed on to the surface of the CAM. In order to allow the distribution of the different cell lines to be observed after implantation one GFP and one dTomato labelled cell line was used.

Mixing lower yield cell lines with the higher yield SKNAS line aided tumour formation (Figure 18). The rate of formation for both the MYCN cell lines doubled reaching that of the SKNAS cells alone. Tumours forming from mixed cell populations were seen to contain both cell lines (Figure 19). However for the purposes of future experiments single cell lines were required and so this approach was not investigated further.

4.3.2.Trypsin, TGF-β and Fibroblast Culture

In order to increase the yield of tumours formed from the low success MYCN amplified cell lines further methodological variances were investigated. We hypothesised that lack of tumour formation was the result of failure of some tumour cells to invade the CAM. In an attempt to overcome this, four experimental conditions were generated. One group of neuroblastoma cells was co-cultured with chick fibroblast cells for 3 days prior to implantation on to the CAM (Figure 20). In the other three conditions neuroblastoma cells were placed on to the CAM with either trypsin, TGF-β or a combination of both.

TGF-β has been shown to modulate of the immune system and tumour microenvironment promoting tumour cell invasiveness and metastasis (Katz, Li et al. 2013). Trypsin is a protease which cleaves peptides on the C-terminal side of lysine and arginine amino acid residues and therefore we asserted that it may aid the penetration of xenografted tumour cells through the superficial epithelial cell surface of the CAM (Sigma). CAFs form an essential part of the tumour microenvironment and are reported to increase the invasive

potential of malignant cells (Choi, Lee et al. 2014). We therefore hypothesised that each of these conditions might aid the neuroblastoma cells in invading the CAM.

TGF-β alone or in conjunction with trypsin did not increase the yield of tumours further than trypsin alone. All of the eggs in which the neuroblastoma-fibroblast co-culture cells were used did not survive until E14 and therefore this line of investigation was not pursued further. The addition of trypsin to cells was the most successful variation of the method resulting in a two fold increase in the yield of tumours (Figure 21). Using Fishers exact test this result was demonstrated to be statistically significant (p value <0,05). This method was therefore adopted for future experiments.

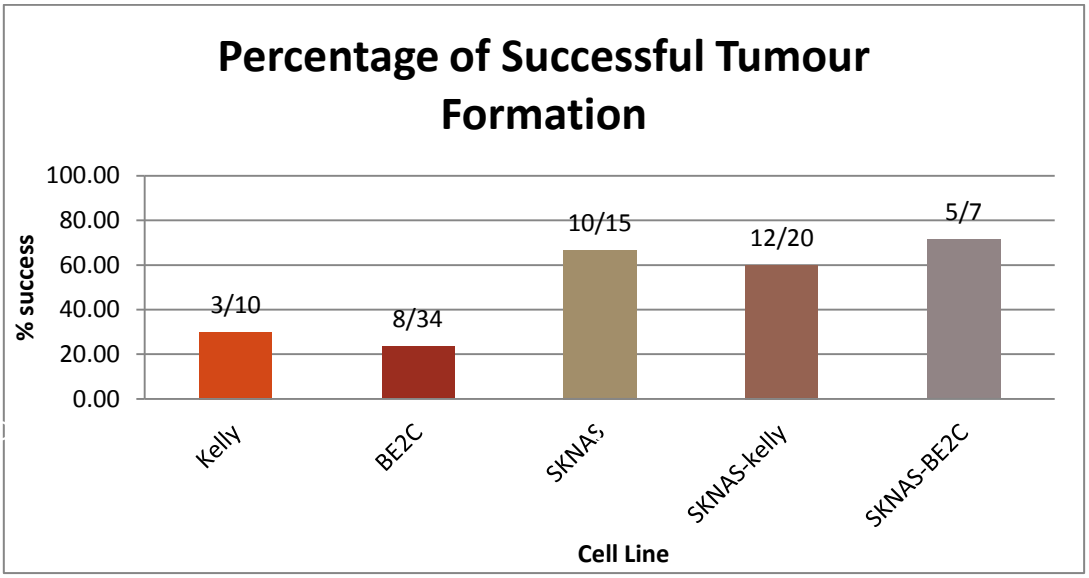

Figure 18 - **The success of mixed and single neuroblastoma cell lines at forming tumours in the chick embryo.** Percentage success was calculated by dividing the number of tumours with tumours at E14 by the number of embryos surviving until that time. The fractions above the bars represent the actual number of tumours formed/the actual number of eggs surviving until E14.

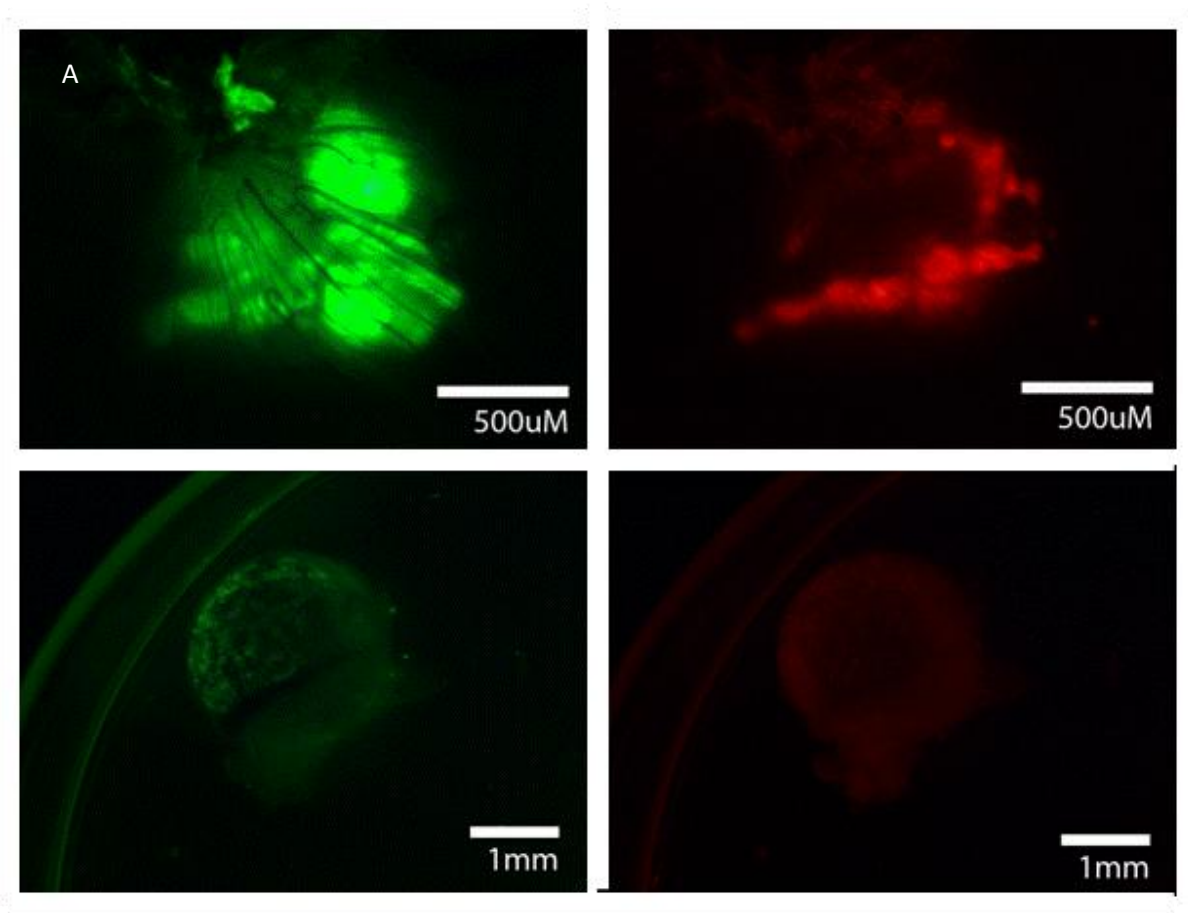

Figure 19 - Mixed cell line tumours. GFP and dTomato images of tumours formed using mixed cell lines showing the distribution of the different cell lines within the tumour. A and B are images of an SKNAS-Kelly tumour. Kelly is GFP labelled (A) and SKNAS is dTomato labelled (B). C and D are images of an SKNAS-BE2C tumour. BE2C is GFP labelled (A) and SKNAS is dTomato labelled (D).

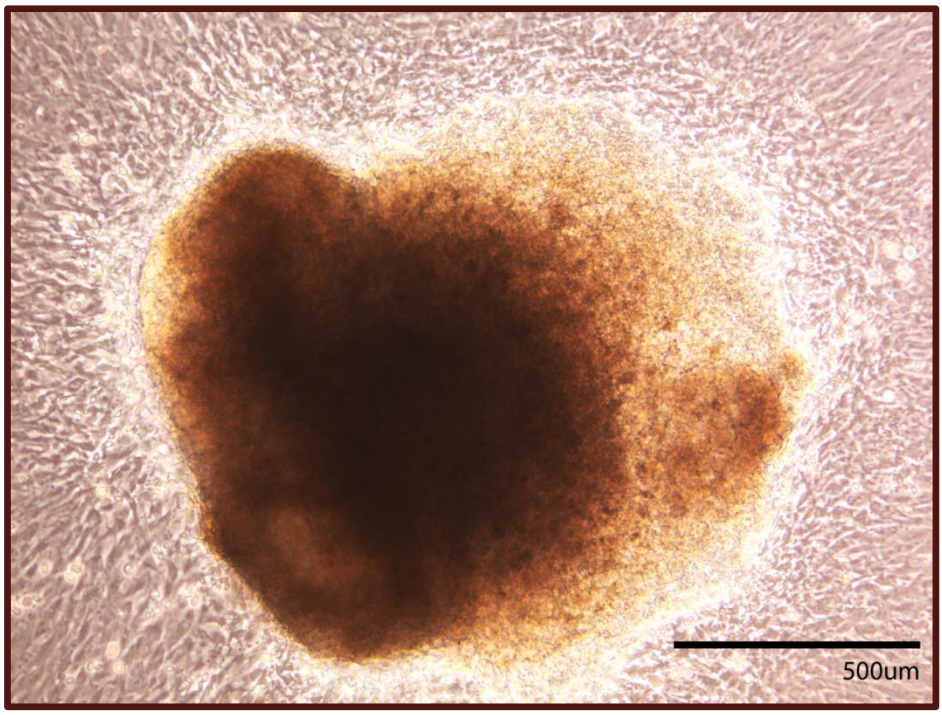

Figure 20 - Fibroblasts (seen peripherally) growing from a piece of dissected chick embryo heart (dissected at E8) in culture. Fibroblasts were then co-cultured with BE2C cells for 3 days prior to implantation on the CAM.

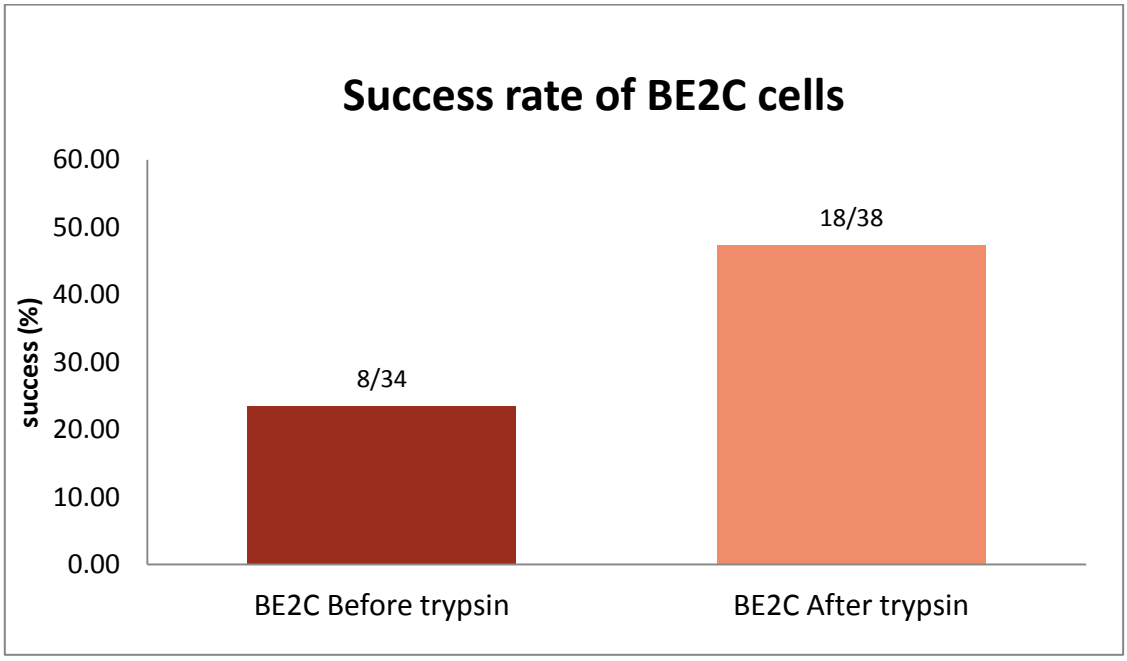

Figure 21 - The success of BE2C tumour formation before and after the addition of trypsin. Fractions above the bars represent the actual number of tumours dissected to date (numerator) and the number of embryos surviving until E14 (denominator). The Fishers exact test statistic is 0.0496. The result is significant at $p<0.05$.

4.4.Drug Delivery

For the chick embryo to be effective as a therapeutic model drugs must be delivered to tumour cells successfully. One key advantage of the chick model is its simplicity, and so a delivery method would ideally not compromise this feature. We therefore sought a method that would be easy to perform and not compromise embryo survival whilst effectively delivering compounds throughout tumours.

An initial literature search into potential drug delivery methods for the model yielded an interesting and informative paper by Vargas *et al*. In this paper various methods of drug delivery were discussed (Figure 22).

In order to retain the simplicity of the model we decided to explore topical administration of compounds on to the surface of the CAM. We hypothesised that compounds applied in this manner would diffuse into the CAM vasculature and therefore penetrate throughout the tumour. In order to investigate this hypothesis we used EdU. EdU is a novel thiamine analogue incorporated into dividing cells and therefore should be seen throughout the rapidly dividing tumour.

200µL of either 4mM or 2mM EdU was added to the surface of the CAM 24hrs prior to dissection of the underlying tumour. As a positive control EdU was also injected into the vasculature of the CAM (carried out by Rachel Carter, University of Liverpool). If, as we hypothesised, EdU diffused into the embryonic circulation, we would also expect it to be incorporated into the rapidly dividing cells of the chick embryo. Therefore during dissection embryonic liver was also removed for EdU testing.

Following EdU detection 3 samples from slides representing the centre of the tumour were visualised. A total of nine tumours were assessed. For both topical and IV administration of EdU, 70-90% of GFP cells were found to be EdU labelled (Table 13). EdU staining was observed throughout the tumour with no noticeable absent areas (Figure 23). T- tests were performed on the values obtained from cell counting and there was no significant difference in drug penetration between the two modalities (P value 0.73). Similarly reducing the concentration of EdU did not appear to significantly hinder delivery of the drug (P value 0.16).

EdU was also detected throughout the embryo's liver further supporting our hypothesis that substances applied to the surface of the CAM diffused into the embryo's circulation (Figure 24).We therefore concluded that topical administration was an effective mode of drug delivery in this model.

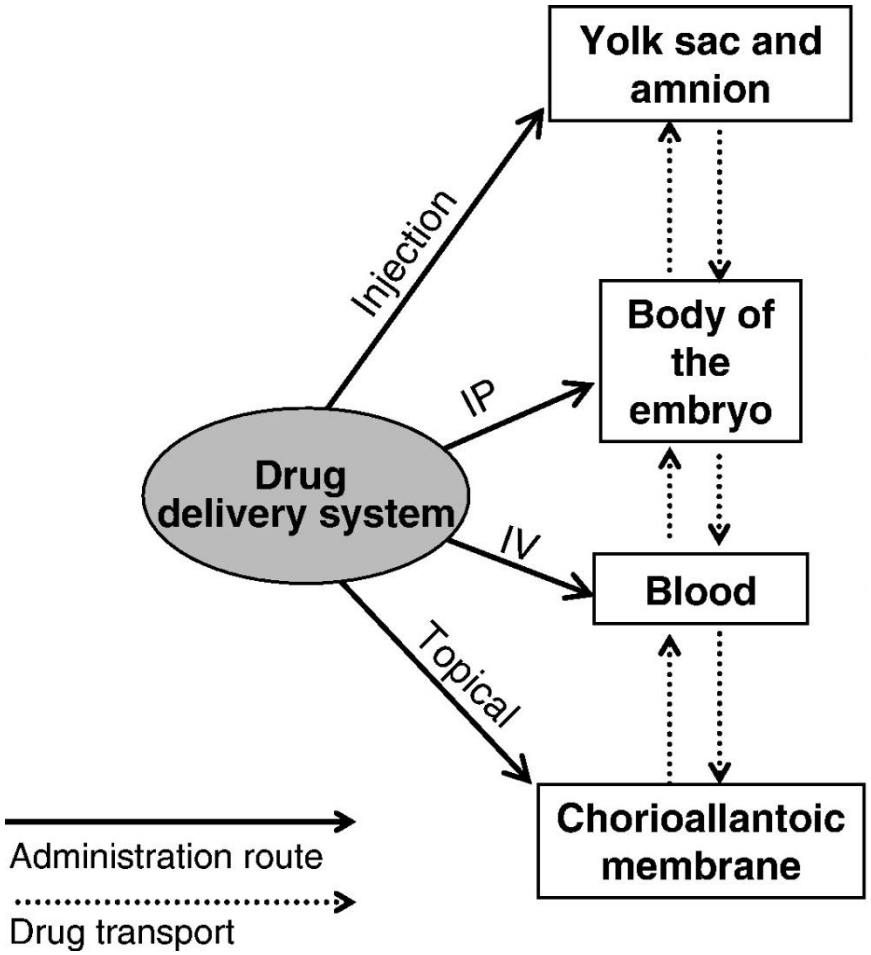

Figure 22 - **The different approaches to drug delivery in the chick embryo model**. IV - intravenous IP - intraperitoneal. This diagram displays the various methods that can be used to deliver drugs to the chick embryo model as well as outlining the expected diffusion pathways of these drugs. Topical administration on to the CAM can be seen to diffuse into the blood stream. Adapted from Vargas *et al*, 2007.

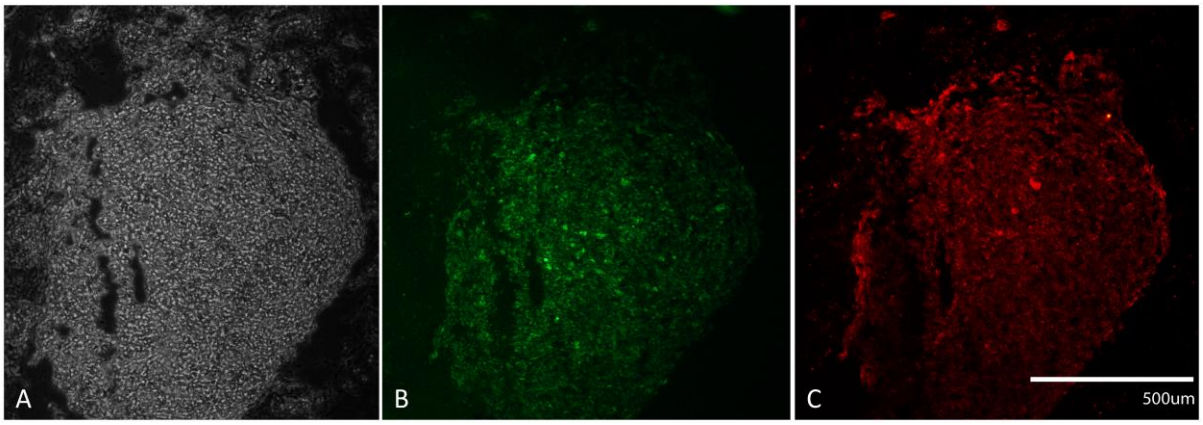

Figure 23 - EdU staining following topical application. EdU staining in an SKNAS tumour dissected from beneath the CAM 24 hours after topical EdU application. A - phase image showing the densely packed cells of the tumour. B - GFP antibody staining showing human neuroblastoma cells. C - EdU detection. Images shown are representative.

Tumour	Mode of administration	EdU Concentration	Volume of EdU	Mean EdU cell count	Mean GFP cell count	Percentage of GFP cells also EdU labelled (%)
1	Topical	4µM	200µL	272	366	90.8
2	Topical	4µM	200µL	248	260	87.5
3	Topical	2µM	200µL	241	259	85.1
4	Topical	2µM	200µL	300	322	89.2
5	Topical	2µM	200µL	243	276	82.7
6	Topical	2µM	200µL	196	213	84.2
7	IV	10µM	8µL	164	175	81.3
8	IV	10µM	8µL	205	208	86.2
9	IV	10µM	8µL	199	228	79.8

Table 13 - table displaying the results of EdU and GFP counts performed 24 hours after administration.

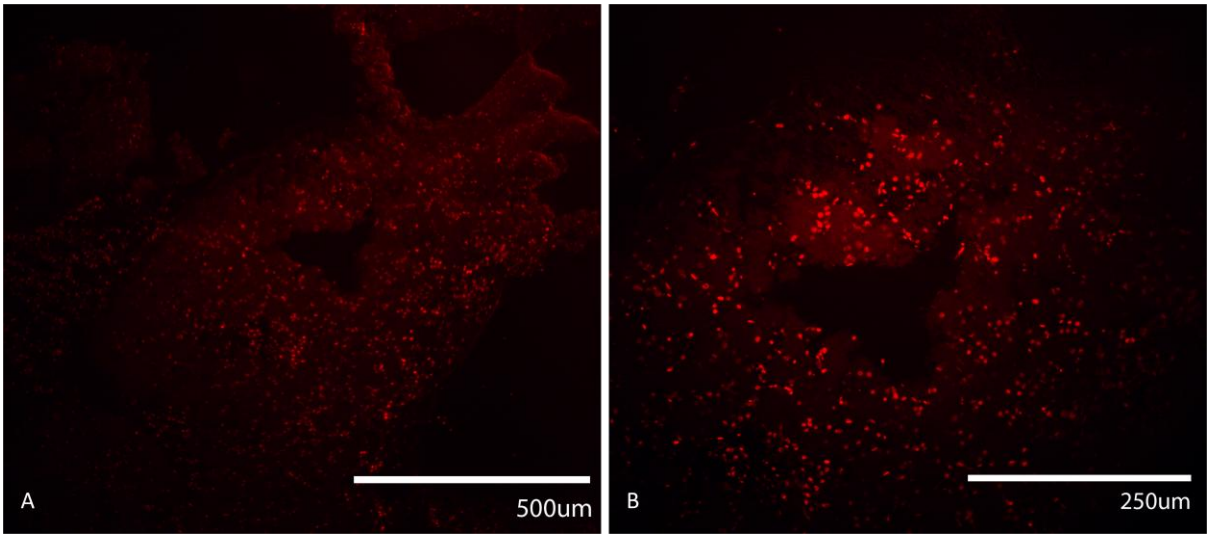

Figure 24 - EdU detected in the chick embryo liver. EdU staining performed on sections of the chick embryo liver 24 hours after topical application of EdU on to the CAM. Staining can be seen clearly throughout the liver.

4.5.Detecting a Suitable Time Window

In order for compounds to be tested within the model there must be a suitable time window for them to be applied to the CAM and allowed to take effect. In order to ascertain whether tumour growth at E14 could be predicted at an earlier stage, eggs were reopened and evaluated at E9, E10, E11 and E12. Eggs were marked as positive (tumour) or negative (no tumour) and correlation between early predictions and E14 results were evaluated.

Tumours were found to be visible in 90% of cases by E11 (Table 14) allowing a 72 hour window for the application of therapeutic compounds to the CAM. Tumours that were missed at this stage were either due to a large blood spot obscuring the tumour, or a peripherally located tumour that was difficult to see. Earlier on, the main challenge to prediction was differentiating between cells beneath the CAM and those cells forming a flattened mass on its surface.

Embryonic Day	Correct Prediction (%)
E9	30
E10	50
E11	90
E12	90

Table 14 - The reliability of predicting tumour formation from E9-12. Embryonic day refers to the number of days since initial egg incubation. Correct prediction refers to the percentage of tumours correctly identified in eggs by visual inspection under UV light prior to the day of dissection.

4.6.Detecting therapeutic effects

We had now established that neuroblastoma cells were able to invade the CAM and form tumours beneath its surface. That this growth could be reliably predicted to provide a 72 hour window for potential drugs to be administered and take effect, and that drugs applied topically to the CAM would penetrate throughout these tumours. We now sought a suitable method of detecting and quantifying the effects of drugs to be used in the model.

Tumours were grown on the CAM and either frozen or paraffin sections were prepared. Immunostaining for several differentiation and proliferation markers was conducted (Table 15).

We encountered several problems with the use of frozen sections. The heterogeneity of malignant cells means that expression of mature neuronal markers might be expected in some of the tumour cells. However expression of these markers was not observed at all in sections. A lack of availability of tissues to act as a positive control in experiments meant that determining whether these observations represented a failure of the immunostaining process or a lack of expression was not possible. Furthermore markers such as ki67, did not appear to consistently represent the expected cellular location when used in frozen sections. Paraffin sections were therefore investigated as a potential alternative method. However, here again similar problems were encountered with several of the markers.

Further research into these difficulties indicated that others had failed to identify reliable antibodies for several of these genes. Some had therefore used qPCR as an alternative and more reliable method of quantifying changes in gene expression and we therefore decided to utilize it.

4.6.1.qPCR

The next stage in the development of this model was to use qPCR to examine the effects of a well-established therapeutic compound. Retinoic acid (RA) is a differentiation agent causing neuroblastoma cells to display a more mature neuronal phenotype. It has been extensively researched and is currently employed in the standard treatment of patients with high risk neuroblastoma.

13-cis-retinoic acid is a derivative of vitamin A (retinol). It is a naturally occurring substance of which levels are tightly controlled during development. RA binds to heterodimers of retinoic acid receptors (RAR) or the retinoid X receptor (RXR), which in turn bind to retinoic acid response elements (RARE) located in the 5' upstream regions of target genes. RA is recognised to modulate the expression of many protein coding genes and non-coding RNA sequences in this fashion and it is these changes that are believed to initiate the process of differentiation in neuroblastoma cells (Marill, Idres et al. 2003).

In a paper published in 2012 Sung *et al* demonstrate several changes in gene expression in IMR-32 cells following the culture with retinoic acid (RA). We identified 3 genes from this paper which demonstrated the greatest fold change; krupel like factor 4 (KLF4), stathmin-like 4 (STMN4) and roundabout, axon guidance receptor, homolog 2 (robo2). KLF4 is a member of the KLF zinc-finger-containing transcription factor family. High expression of KLF4 has been associated with a less differentiated phenotype and therefore levels would be expected to decline during retinoic acid treatment. ROBO2 and STMN4 are both associated with axon guidance. During differentiation their levels would therefore be expected to rise. In addition to these genes Sung *et al* reported a decrease in MYCN expression. Others have shown previously that down-regulation of *MYCN* precedes retinoic acid induced differentiation and it has been suggested that retinoic acid can directly regulate *MYCN* expression at the transcriptional level (Westermark, Wilhelm et al. 2011). The MYCN protein is its self a transcription factor believed to be a key regulator of differentiation in neuroblastoma and therefore we also chose to include it in our research. We hypothesised that changes in MYCN expression may be responsible for the changes observed in other genes.

A literature search indicated that UBC, HPRT1 and GAPDH were the three most stably expressed housekeeping genes in neuroblastoma cell lines and therefore these were the reference genes used in all experiments to allow for accurate normalisation of gene expression (Vandesompele, Baudis et al. 2005).

Marker	Type of marker	Expected Levels	Observed Levels	Expected Location	Observed Location
Ki67	Proliferation marker	High	High	nuclear	Mixed
NSE	Differentiation marker	Low	absent	Cytoplasm and cell membrane	-
NF70	Differentiation marker	Low	absent	cytoplasmic	-
GAP43	Differentiation marker	Low	High	cytoplasmic	cytoplasmic
Robo2	Differentiation marker	Low	absent	Cell membrane	-

Table 15 - **Table outlining the different markers explored in frozen sections of tumours grown in the chick model**. Levels refer to the levels in the cells of the tumour, location refers to the sub-cellular location of the marker. NSE; neuron specific enolase, NF70; *Neurofilament* 70, GAP43; growth associated protein 43, Robo2; Roundabout, axon guidance receptor, homolog 2.

Primer Name		Sequence	Product Length	Intron Length	Tm	Secondary	GC %	Reference
UBC	FW	ATTTGGGTCGCGGTTCTTG	93	812	67	none	52.6	(Vandesompele, Baudis et al. 2005).
	RV	TGCCTTGACATTCTCGATGGT			67	very weak	47.6	
HPRT1	FW	TGACACTGGCAAAACAATGCA	53	4797	68	weak	42.8	(Vandesompele, Baudis et al. 2005).
	RV	GGTCCTTTTCACCAGCAAGCT			67	weak	52.3	
GAPDH	FW	AATCCCATCACCATCTTCCA	43	130	64	None	45	(Vandesompele, Baudis et al. 2005).
	RV	TGGACTCCACGACGTACTCA			65	Weak	55	
ROBO2	FW	GATGTGGTGAAGCAACCAGC	306	990	60	weak	55	(Sung, Boulos et al. 2013)*
	RV	TGGCAGCACATCTCCACG			60	weak	61.1	
STMN4	FW	CCTAGCAGAGAAACGGGAACA	178	1254	60	none	52.4	(Sung, Boulos et al. 2013)*
	RV	GGCGTGCTTGTCCTTCTCTT			61	weak	55	
KLF4 (4)	FW	CGCCGCTCCATTACCAAGAGC	301	1101	64	weak	61.9	Designed using primer blast tool
	RV	CGGTCGCATTTTTGGCACTG			61	none	55	
MYCN 2	FW	CACAAGGCCCTCAGTACCT	95	2639	60	none	61	(Malakho, Korshunov et al. 2008)
	RV	ACCACGTCGATTTCTTCCTCT			59	weak	50	

Table 16 - details of the primers used in qPCR experiments. Tm is the melting temperature of the primer, secondary refers to the presence and strength of primer secondary structures; GC is the number of G's and C's in the primer as a percentage of the total bases. Data was obtained from the NCI primer-BLAST tool.(Malakho, Korshunov et al. 2008)*Primer sequences were obtained by directly contacting the authors of (Sung, Boulos et al. 2013).

4.6.2.Optimising qPCR

Before experiments could be conducted primers for the four target genes and three reference genes were designed and optimised.

Primer sequences were identified in published papers using the same target or reference genes in qPCR experiments. Where suitable published sequences were not available primers were designed using the NCI primer-BLAST tool.

In order to optimise the temperature of the qPCR reaction a temperature gradient spanning 10˚C was used to evaluate each primer. This evaluation was also aided by the inclusion of no-reverse transcriptase (NRT) and no-template (NT) controls in the experimental design. As a result, an amplification curve and melt curve for each primer at the given range of temperatures was obtained. An example plot is shown for KLF4 (Figure 25).

Initially examining the appearance of this plot demonstrated a smooth amplification curve with no obvious anomalous results (Figure 25a). Further analyses identified the line (and corresponding temperature) from which the lowest Ct value of 15.4 was obtained. The melt curve demonstrated the presence of a single product (Figure 25b). This plot also allowed the presence of products in the control wells to be excluded (Figure 25c). In cases where there were products within, or close to the intended target primers were redesigned and tested.

From these observations overall impression of the best temperature and the range of acceptable temperatures for the primer was made. Once the process had been repeated for each primer an overall temperature for the qPCR reaction was calculated (Figure 26).

Suitable temperatures ranges spanned 4-10˚C with the lowest acceptable temperature for any primer being 50˚C and the highest reaching 63˚C (Figure 26). The single temperature of 60˚C was chosen as a suitable universal temperature for future experiments.

In order to ensure the suitability of the chosen temperature a single plate containing all of the primers was run at 60˚C. Each primer displayed a single clear melt curve peak which was not seen in the NRT control confirming the suitability of this temperature (Figure 27).

4.6.3.Primer efficiency

To ensure the qPCR reaction was adequately optimised the efficiency of primers was assessed using both sample and control cDNA. A five point dilution scale of cDNA concentrations was generated spanning the range used throughout experiments. Each primer was subsequently assessed using this scale. The results were plotted on individual graphs where the y axis was the log to base 10 of the dilution factor (Figure 28). The m value ($y = mx+c$) of these plots was used to calculate the efficiency (E) of the primer according to Equation 1. This process was repeated for each primer using both sample and control cDNA (Table 17).

Efficiencies ranged from 94.7% to 99.1% (Table 17) indicating that the qPCR reactions were suitably optimised. No significant difference was observed between the control and sample cDNA and therefore would not need to be accounted for later on during analysis of qPCR data.

A

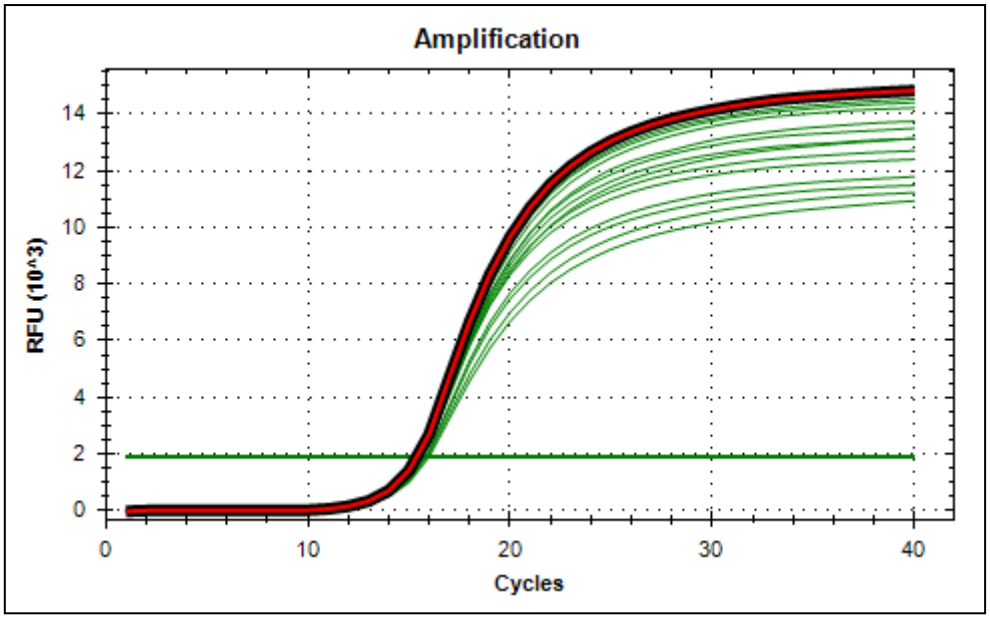

B

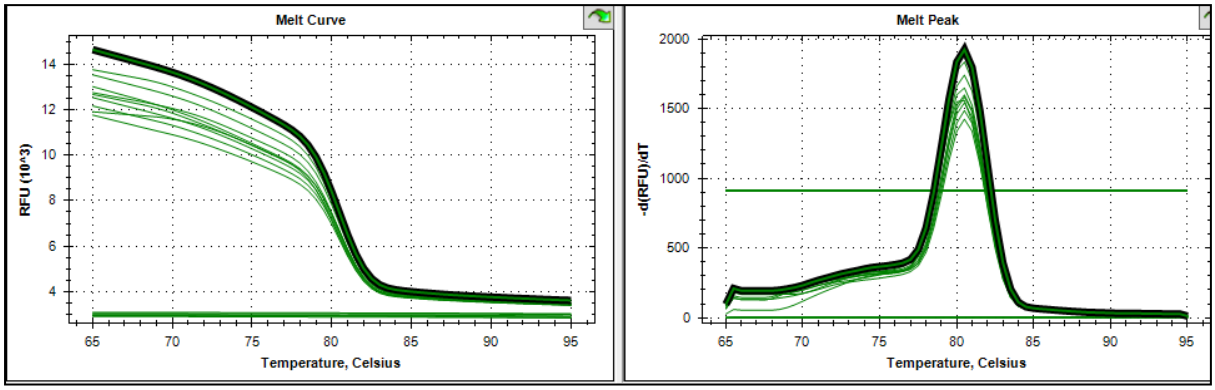

C

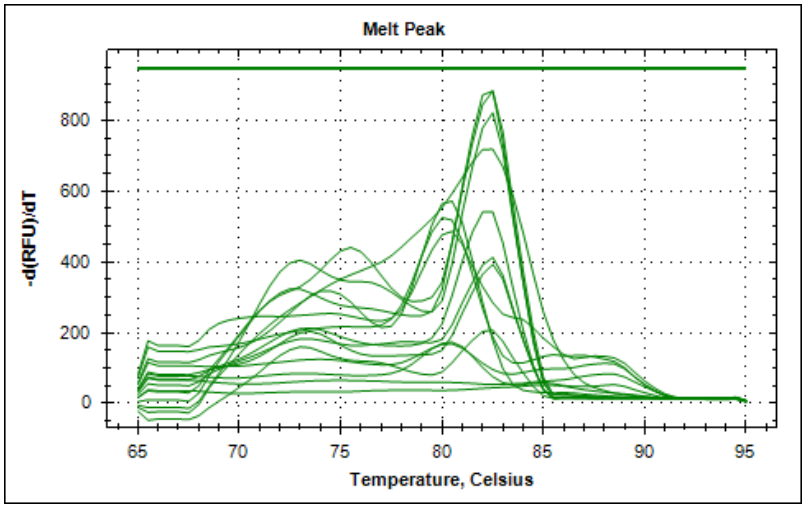

Figure 25 - Optimisation of qPCR. An example of primer optimisation using KLF4. A : KLF4 amplification plot showing the smooth curve. Highlighted is the amplification curve with the lowest Ct value. B: melt curve for KLF4 showing one clear product. Highlighted is the amplification curve with the highest peak. C: Melt curve of the NRT control wells. The green line above the plot indicates the threshold for detection. The melt curves do not cross this indicating that the KLF4 primer is not amplifying the genomic DNA at a level that is significant.

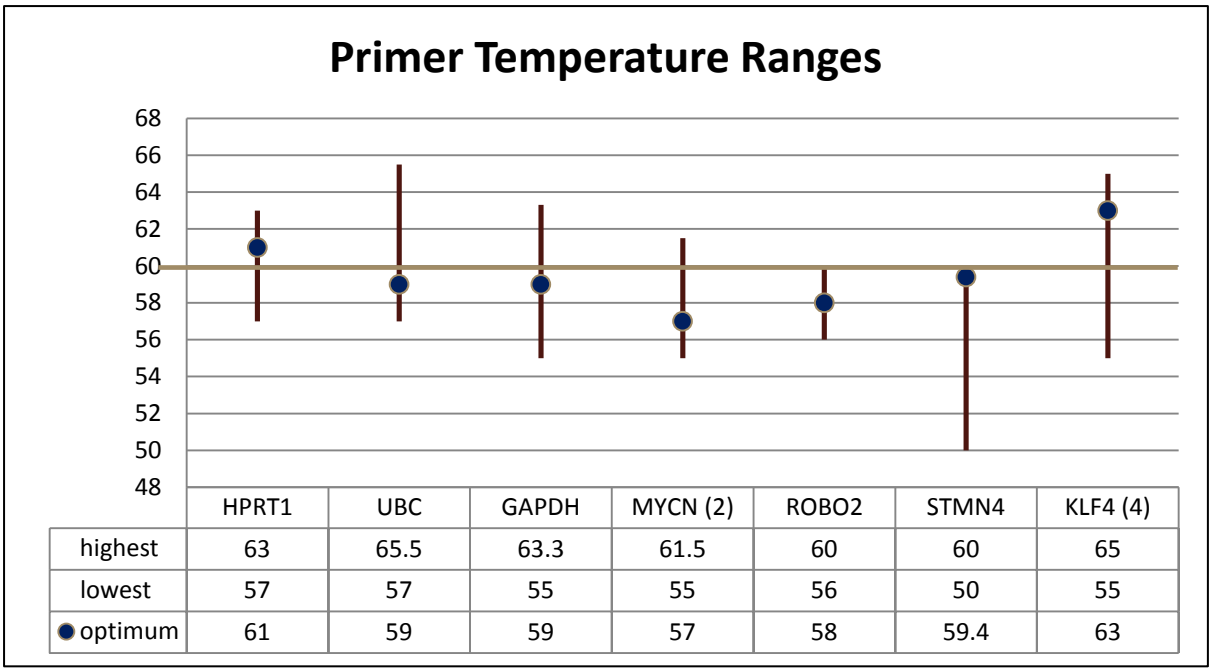

	HPRT1	UBC	GAPDH	MYCN (2)	ROBO2	STMN4	KLF4 (4)
highest	63	65.5	63.3	61.5	60	60	65
lowest	57	57	55	55	56	50	55
optimum	61	59	59	57	58	59.4	63

Figure 26 - Primer Optimisation. A graph showing the range of acceptable temperatures (brown) and optimum temperature (blue) for each primer. The green line indicates the temperature of 60˚C which was used in future experiments.. The table below indicates the actual temperature values recorded from temperature gradients.

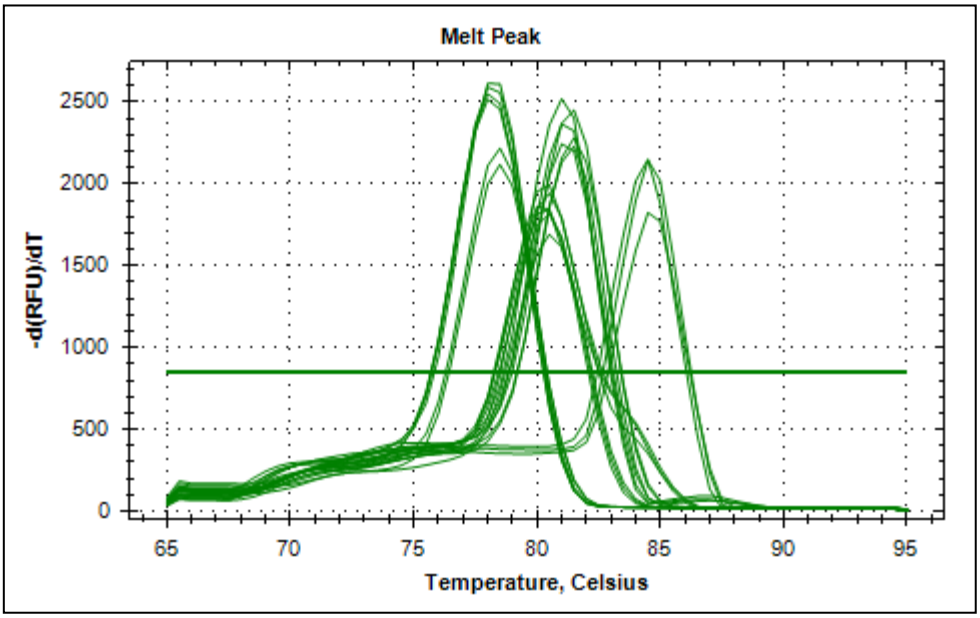

Figure 27 - Amplification curve for all 7 primers at 60˚C showing smooth reaction and the clear melt curve peaks.

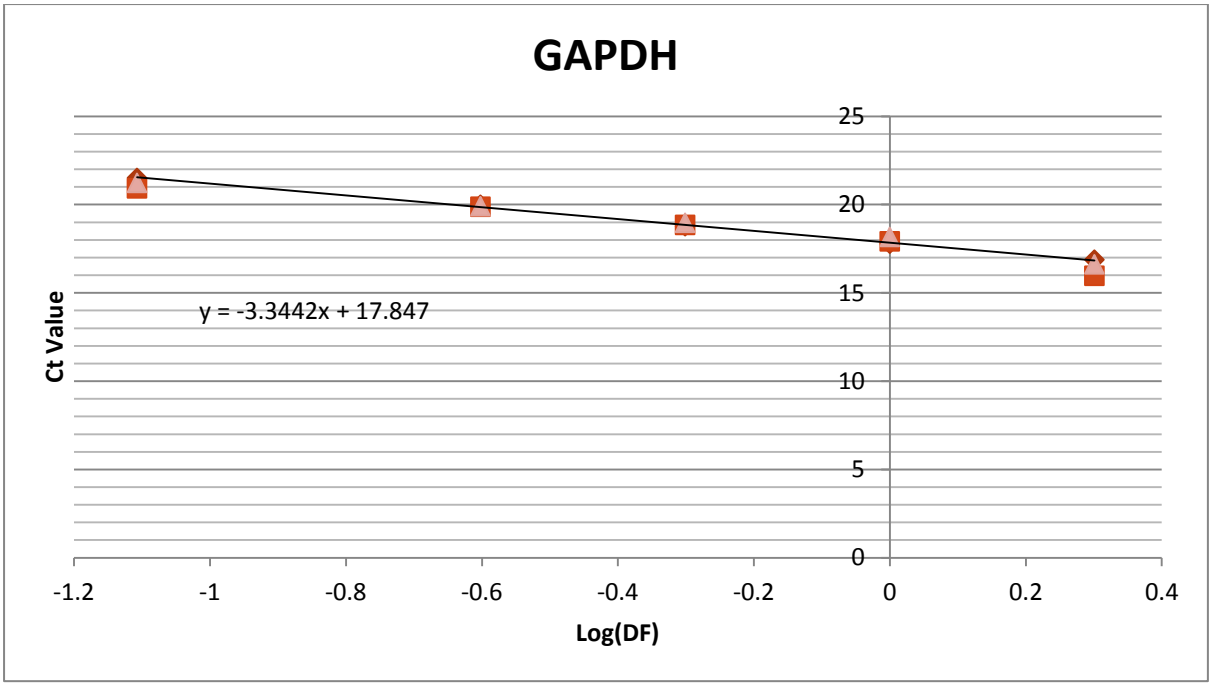

Dilution Factor	0.125	0.25	0.5	1	2
Log10(DF)	-1.11	-0.602	-0.301	0	0.301

Figure 28 - GAPDH dilution series. A curve showing the Ct values (Y axis) obtained at different dilutions of cDNA (X axis) for the GAPDH primer. A logarithmic scale is used for the X axis values allowing a linear relationship to be observed. The equation of the line can be seen on the graph.

$$E = (10^{[-1/m]}-1)x100$$

Equation 1 - equation for calculating the efficiency (E) of primers. The m value (y = mx+c) was taken from plots of 5 point dilution series.

Primer	Equation	m value	1/m	Efficiency (%)
GAPDH	y = -3.3442x + 17.847	-3.34	0.299	99.1
HPRT1	y = -3.4566x + 23.484	-3.46	0.289	94.7
KLF4	y = -3.4261x + 31.35	-3.43	0.292	95.8
MYCN	y = -3.3925x + 17.858	-3.39	0.295	97.1
ROBO2	y = -3.3847x + 25.831	-3.39	0.295	97.4
STMN4	y = -3.3705x + 21.584	-3.37	0.297	98.0
UBC	y = -3.3842x + 18.236	-3.38	0.296	97.5

Table 17 : Primer efficiency. A table displaying the reaction efficiency (E) of each primer. The equation for each primer was derived from graphs of the 5 point dilution series'. The efficiency was calculated according to the formula $E = (10^{[-1/m]}-1)x100$

4.7.Retinoic Acid in Cell Culture

Experiments using retinoic acid were initially conducted in culture with both IMR-32 and BE(2)-C cells. Both of these cell lines display MYCN amplification and therefore represent high risk disease. IMR-32 was the cell line used in the paper by Sung *et al* which was the basis of our gene selection. BE(2)-C cells are a well characterised cell line with which our lab has experience and therefore were also included.

4.7.1.Morphology

Cells were cultured with medium containing 10μM RA for 3 days. Cells were observed daily and the morphological appearance of the cells was noted. The results were compared with control cells cultured with DMSO.

Morphological changes in both cell lines were observed after 24hrs of retinoic acid treatment. Neurite outgrowth (defined as a process whose length equals or exceeds the cell body diameter) the appearance of axonal processes continued to increase throughout the 72 hour period of observation (Figure 29).

4.7.2qPCR

After 3 days the RNA was extracted from control and RA treated cells and cDNA was subsequently synthesised. qPCR was performed to detect changes in target gene expression. Results were normalised using 3 housekeeping genes (GAPDH, HPRT1 and UBC) in order to account for differences in RNA quantity and variability of reaction kinetics. Expression levels of target genes were calculated relative to controls. Each experiment was conducted using 3 technical repeats. Similarly 3 biological repeats were used for both IMR-32 and BE2C cell lines.

In each experiment results were initially examined for any obvious anomalous results before relative normalised expression was calculated. For each gene the mean of the three technical replicates was calculated (

Table 18). The difference in the Ct value (ΔCt) for treated and control cells was calculated by subtracting the mean Ct for the treated cells from the mean Ct for the control cells for each gene (

Table 18). Relative expression was then calculated using $2^{\Delta Ct}$. In order to normalise expression according to the change observed in the reference genes (GAPDH, HPRT1 and UBC) the geometric mean of their $2^{\Delta Ct}$ values was calculated. The $2^{\Delta Ct}$ values of the target genes were then divided by this number to give normalised relative quantification (NRQ). Where expression was less than 1 (representing a negative change) the reciprocal was calculated to make the values easier to interpret (

Table 18).

In order to plot values graphically a log to base 2 of the unadjusted NRQ values was calculated making the positive and negative changes in gene expression symmetrical and converting the NRQ value of 1 (1 fold change - no change) to zero. Error bars were added showing the standard deviation (SD) (Figure 30). For all experiments this process was carried out for each biological replicate (see appendix for individual results of all RA experiments) before results were combined (Figure 31)

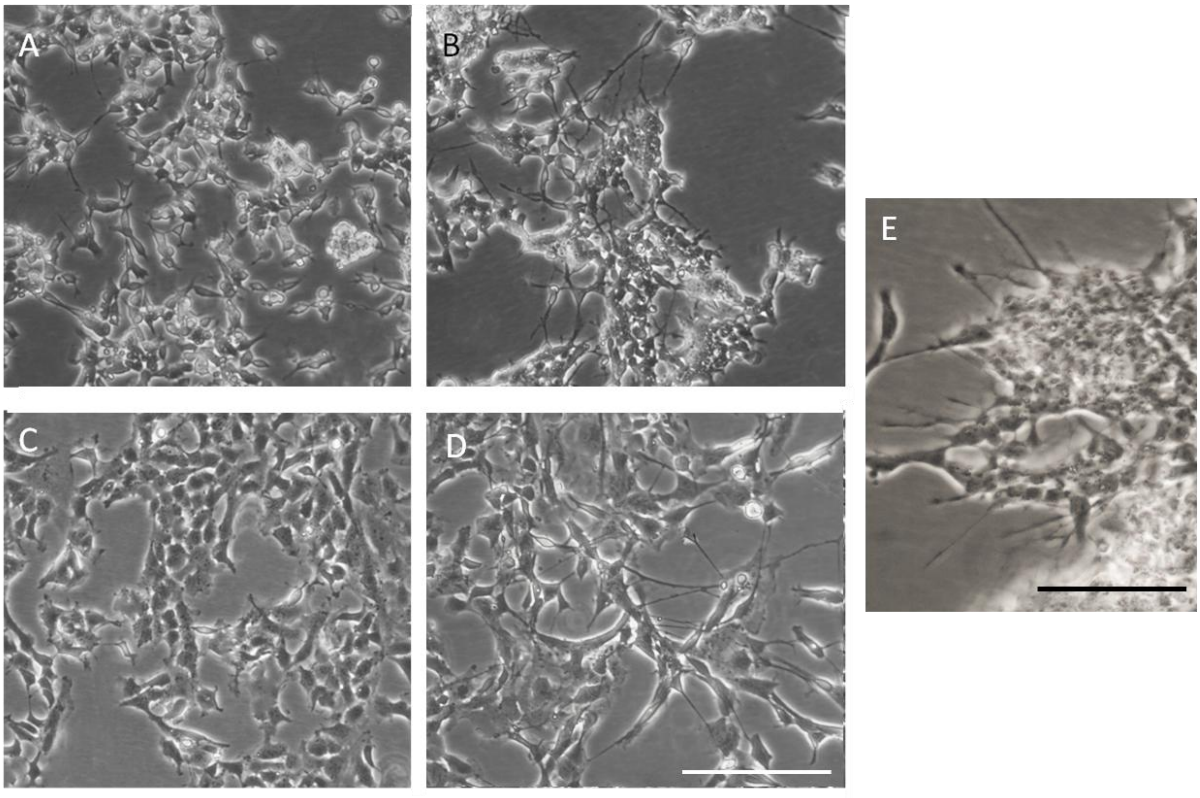

Figure 29 - Changes in cell morphology after three days of RA treatment. A and B are IMR-32 cells, C and D are BE(2)-C cells. A and C are images taken of the control cells and B and D are the treatment groups.

Morphological changes indicative of differentiation are seen in both cell lines. Neurite outgrowth and axonal processed can be seen. E highlights some of these features in IMR-32 cells. The white scale bar is represents 250µm. The black scale bar is 125µm.

	GAPDH	HPRT1	UBC	MYCN	KLF4	ROBO2	STMN4
Control							
replicate 1	19.0	24.6	19.9	18.8	31.5	25.5	23.3
replicate 2	18.5	24.1	19.8	18.8	32.2	25.3	23.0
replicate 3	18.1	23.6	19.6	18.7	32.5	24.8	22.8
Mean	18.5	24.1	19.7	18.8	32.1	25.2	23.1

	GAPDH	HPRT1	UBC	MYCN	KLF4	ROBO2	STMN4
RA							
replicate 1	18.5	24.6	19.5	20.2	33.4	23.9	19.8
replicate 2	18.7	24.4	19.6	20.1	34.5	24.2	19.7
replicate 3	18.1	24.1	19.6	18.1	33.1	23.1	19.6
Mean	18.5	24.3	19.6	19.5	33.7	23.7	19.7

	GAPDH	HPRT1	UBC	MYCN	KLF4	ROBO2	STMN4
ΔCt	0.0833	-0.260	0.130	-0.673	-1.59	1.48	3.35
$2^{\Delta Ct}$	1.06	0.845	1.09	0.627	0.332	2.78	10.2
Geomean	0.989						

NRQ				0.634	0.336	2.81	10.3
Adjusted NRQ				-1.58	-2.98	2.81	10.3

Table 18 - Calculating normalised relative expression using qPCR data. Initially the mean Ct value of three technical repeats was calculated for each gene, both in treated and control groups. The ΔCt was then generated by calculating the differences between the control and treated Ct mean for each gene. Relative quantification was calculated using the formula $2^{\Delta Ct}$ before normalisation using the geometric mean of the housekeeping genes (GAPDH, HPRT1, UBC) $2^{\Delta Ct}$ values. The reciprocal of any negative changes was calculated to give the Adjusted NRQ. GEOMEAN; geometric mean, NRQ, normalised relative quantification.

A

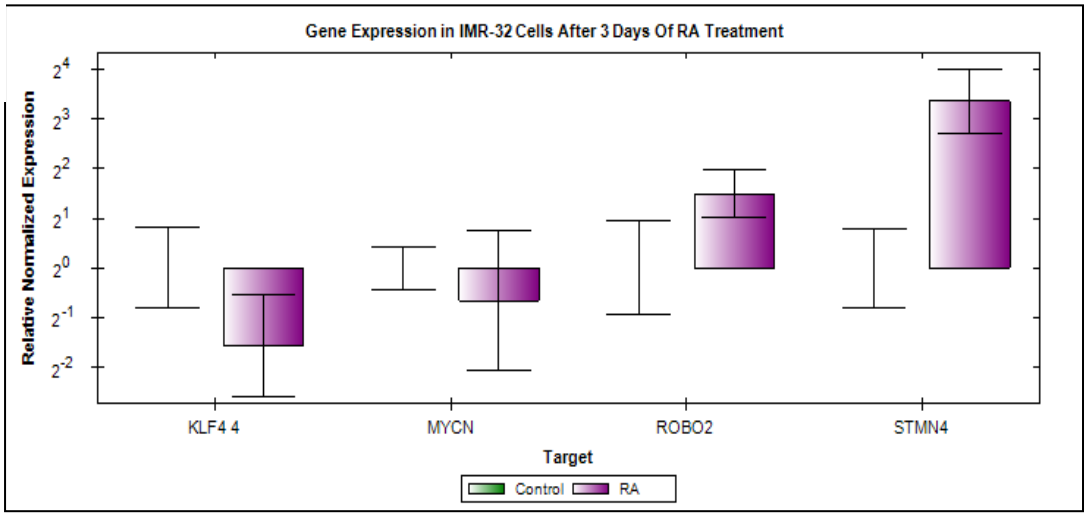

B

	KLF4	MYCN	ROBO2	STMN4
Adj NRQ	-2.98	-1.58	2.82	10.3
SD	0.175	0.517	0.542	2.92
Regulation	No change	No change	No change	Up regulated

Figure 30 - **Results of a single qPCR experiment.** A; a graph displaying the results of a single qPCR experiment in IMR-32 cells following 3 days of RA treatment. The error bars display the standard deviation (SD). B: a table providing a summary of the values obtained from the experiment. The adjusted normalised quantification (Adj NRQ) describes the actual change in the gene expression relative to the control. Regulation describes the overall statistically significant change in gene regulation. The error bars of the control are displayed to the left.

A

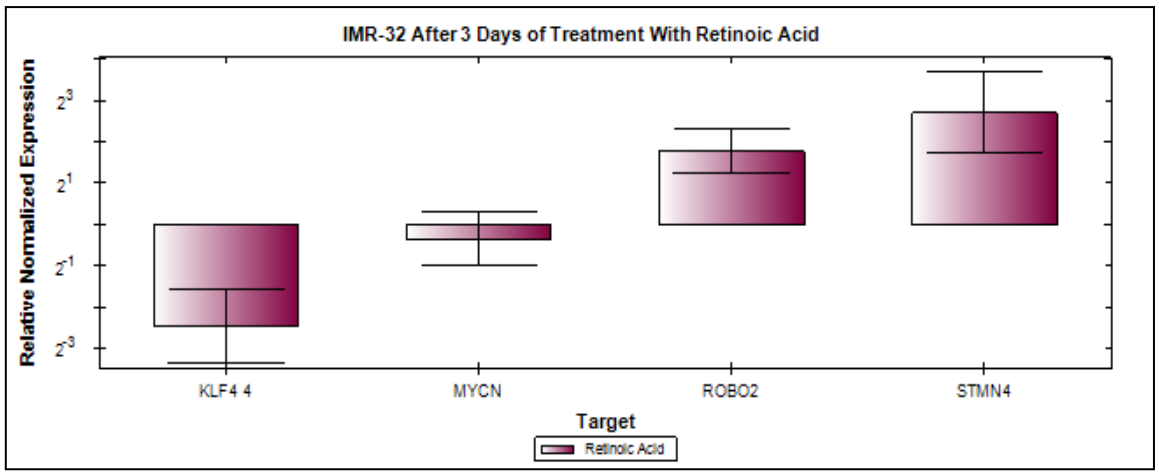

B

	KLF4	MYCN	ROBO2	STMN4
Adj NRQ	-5.53	-1.28	3.41	6.52
SD	0.152	0.446	1.512	2.42
Regulation	Down regulated	No change	No change	Up regulated

C

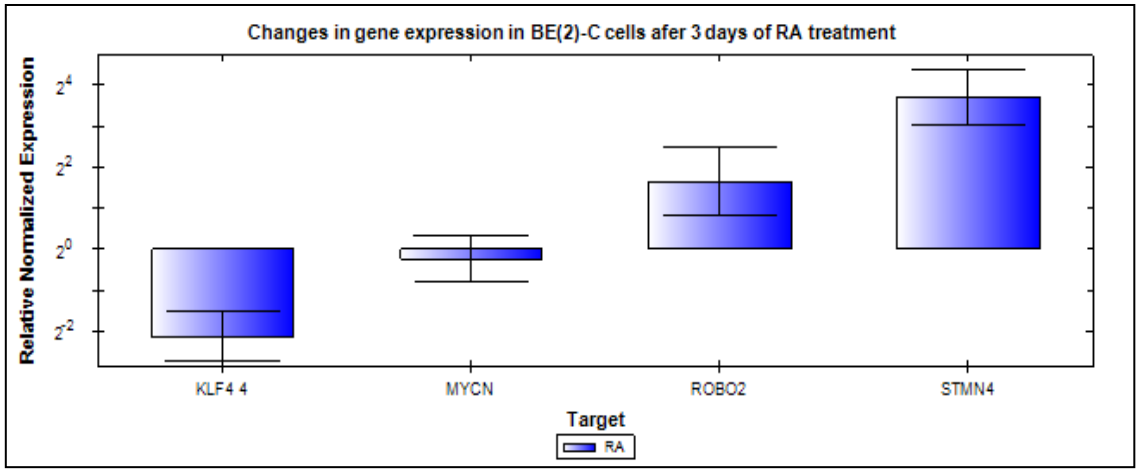

D

	KLF4	MYCN	ROBO2	STMN4
Adj NRQ	-4.89	-1.17	3.37	14.6
SD	0.152	0.410	2.52	3.93
Regulation	Down regulated	No change	No Change	Up Regulated

Figure 31 - Graphs showing the level of target gene expression in IMR-32 (A) and BE2C (C) cells after 3 days of RA treatment. Graphs display the results of three biological repeats. Results are displayed relative to control. Error bars were calculated using standard deviation (SD). Tables give a summary of the QPCR data for the 4 target genes for IMR-32 (B) and BE2C (D).

In both BE2C and IMR-32 cell lines the expression of KLF4 was reduced following 3 days of retinoic acid treatment (-5.53 fold change in IMR-32, -4.89 fold change in BE2C). In both cases down regulation of KLF4 was statistically significant (P-Values; IMR-32 <0.001, BE2C <0.05)(Figure 31). MYCN expression, which was also expected to fall, showed no overall significant change. Within the biological replicates for each cell line MYCN appeared to fall slightly or remain at a similar level as the control (Figure 31).

ROBO2 expression was 3.41 fold and 3.37 fold higher in the retinoic acid treated cells in IMR-32 and BE2C cells respectively. However due to error present in both the sample and the control (example Figure 30) this result was not found to be statistically significant after analysis. Within the biological repeats of each cell line one the three experiments carried out showed statically significant up regulation of the ROBO2 gene. STMN4 consistently showed the greatest level of change in both cell lines. In IMR-32 cells the change in STMN4 expression was 6.70 fold higher than in the control. Overall analysis determined that this gene was significantly up regulated (P-Value <0.01). This result was mirrored in the BE2C cells with significant up regulation observed (P-Value <0.0001) and an average fold change of 14.60 after RA treatment (Figure 31).

4.8.RA in the chick embryo model

After completing RA experiments in cell culture the same cell lines were used to generate tumours in the chick embryo. Where tumours were evident at E11 RA was administered topically to the surface of the CAM every 24hrs at the dose of 30mg/kg. Control tumours were treated with DMSO at the same final concentration. At E14 tumours were dissected and stored in RNAlater until RNA extraction and cDNA synthesis. qPCR was performed to detect and change in expression of the target genes in this model.

The application of retinoic acid to the chick embryos did not significantly alter the survival rate and on inspection no gross defects were observed in the embryos. Normalized relative

expression from 3 biological replicates showed a decrease KLF4 in both IMR-32 and BE2C (-4.22 and -3.44 fold respectively) (Figure 32). This down regulation was statistically significant in the IMR-32 tumours (p value <0.05) but not in the BE(2)-C cell line. MYCN showed a modest decrease in expression (BE(2)-C -2.17, IMR-32 -2.93 fold change) however similar to the results observed in culture these results did not reach statistical significance and therefore no overall change could be determined. In the BE(2)C cells both ROBO2 and STMN4 were both significantly unregulated in response to RA treatment (ROBO2 5.91, STMN4 5.02 fold increase, p values <0.05). However in IMR-32 cells ROBO2 showed a modest (2.09 fold change) increase which was not significant enough to distinguish up regulation of this gene. Within the biologic repeats up regulation of ROBO2 did reach statistical significance in one of the three experiments. STMN4 showed an overall 4.40 fold increase in expression (p value <0.05). These data are summarised in Figure 32.

A

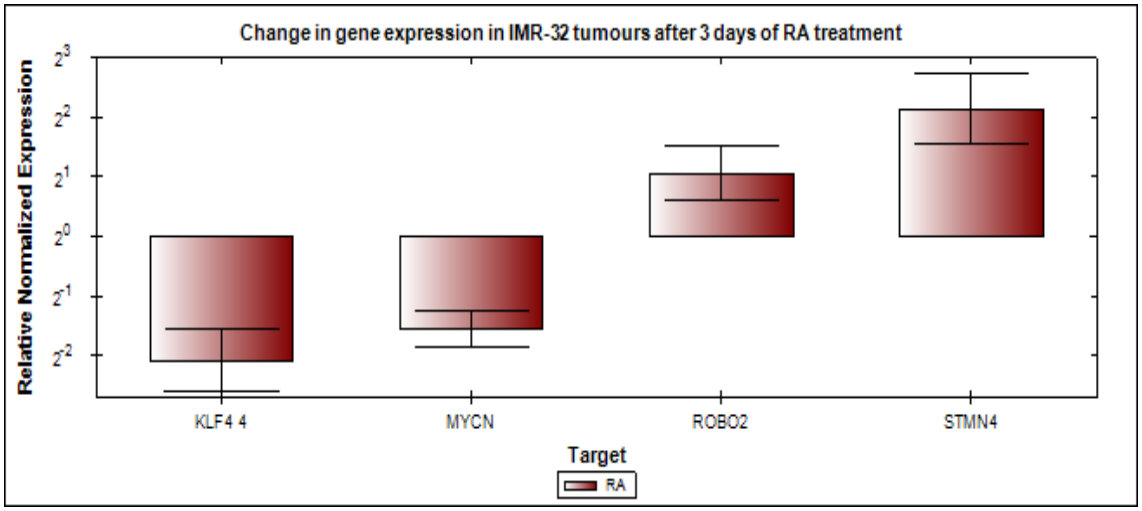

B

	KLF4	MYCN	ROBO2	STMN4
Adj NRQ	-4.22	-2.93	2.09	4.40
SD	0.107	0.0828	0.781	2.27
Regulation	Down regulated	No change	No change	Up regulated

C

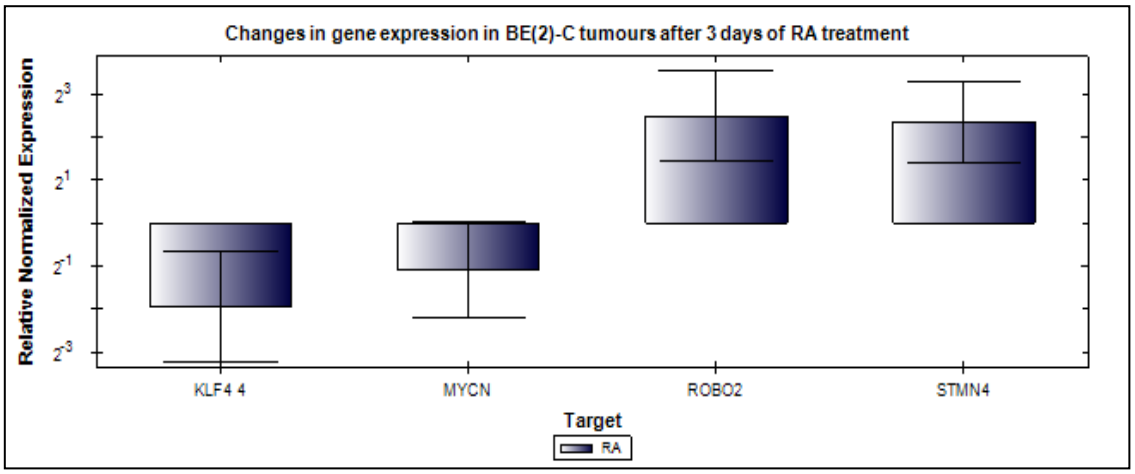

D

	KLF4	MYCN	ROBO2	STMN4
Adj NRQ	-3.44	-2.17	5.91	5.02
SD	0.373	0.546	2.09	1.46
Regulation	No change	No change	Up regulated	Up regulated

Figure 32 - Graphs showing the level of target gene expression in IMR-32 (A) and BE2C (C) tumours after 3 days of RA treatment. Graphs display the results of three biological repeats. Results are displayed relative to control. Error bars were calculated using standard deviation (SD). Tables give a summary of the QPCR data for the 4 target genes for IMR-32 (B) and BE2C (D).

4.9.Further Investigation of RA

Due to the limited significance of the changes observed in the expression of some target genes further experimentation with RA was conducted in cell culture. We hypothesised that increasing the length of time the cells were cultured with RA would increase the level of differentiation and therefore changes observed in the target genes.

The same procedure was implemented as described previously, however in this instance cell culture experiments were extended to last 6 days. Cell morphology was observed daily over the 6 day period before RNA extraction, cDNA synthesised and qPCR performed.

A similar pattern of morphological change was observed in both of the neuroblastoma cell lines however these changes became more pronounced over the 6 day period. A much more dramatic effect was seen in the IMR-32 cells where a higher number of longer processes could be seen (Figure 33).

Following cell culture with RA for 6 days significant down regulation of KLF4 was observed (IMR-32 p-value <0.01, BE(2)-C p-value <0.05). A 5.88 fold decrease was seen in the IMR-32 to cells and an 8.15 fold decrease in the BE(2)-C. Similarly a decrease in MYCN expression was also observed (-4.63 and -4.22 in the IMR-32 and BE(2)-C cells respectively). After analysis the down regulation of MYCN was statistically significant (p values <0.01). ROBO2 and STMN4 were up regulated in both of the cell lines with greater change seen in the IMR-32 cell line with 6.41 and 9.46 fold increases in these two genes respectively compared to a 5.06 and 7.64 fold change in the BE(2)-C. Up regulation of the two genes was statistically significant in each instance (ROBO2 p-value <0.05, STMN4 p-values <0.01) (Figure 34).

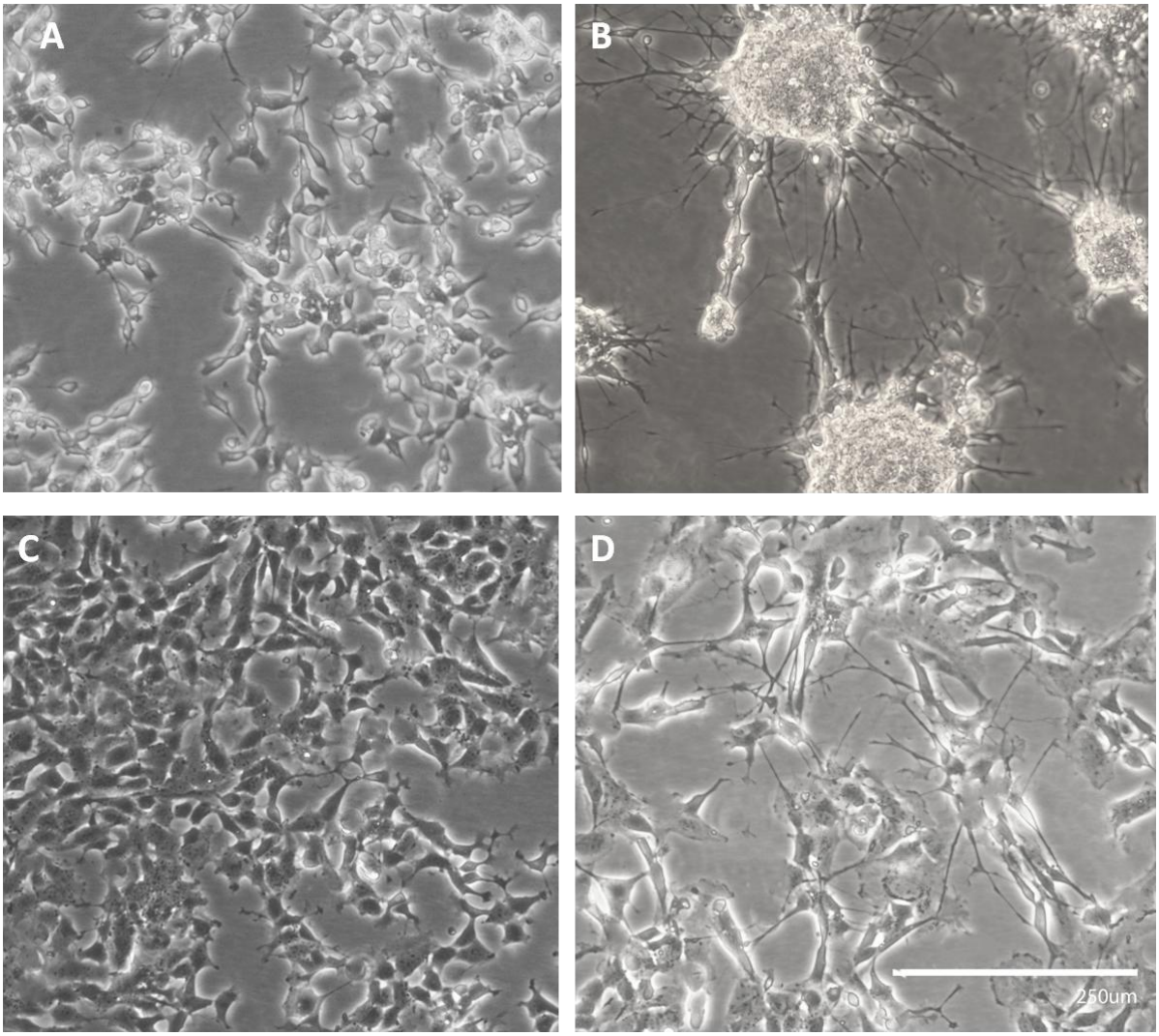

Figure 33 - **Appearance of cells after 6 days of RA treatment.** IMR-32 are on the top row, BE(2)-C are on the bottom row. Images A and C are control cells. B and D are cells treated with 10µM RA.

A

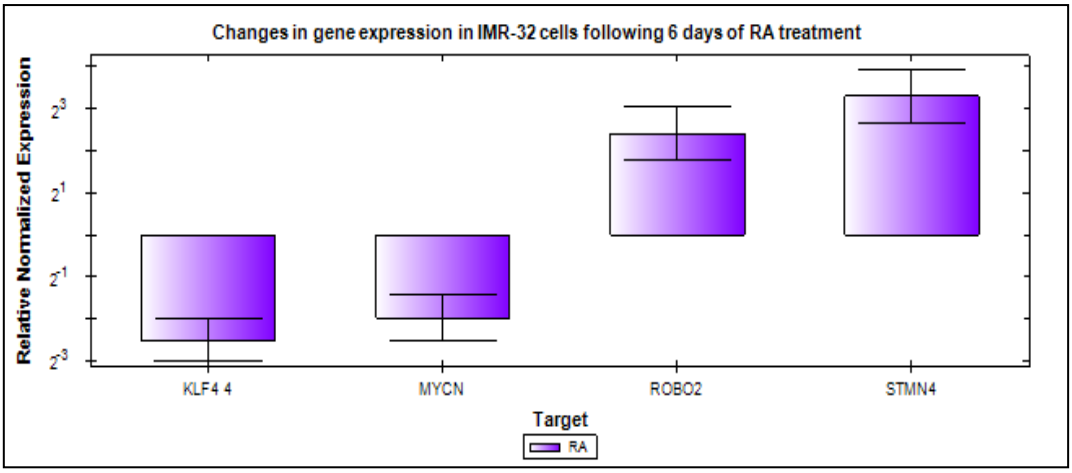

B

	KLF4	MYCN	ROBO2	STMN4
Adj NRQ	-5.88	-4.63	6.41	9.46
SD	0.074	0.115	2.90	3.39
Regulation	Down regulated	Down Regulated	Up regulated	Up regulated

C

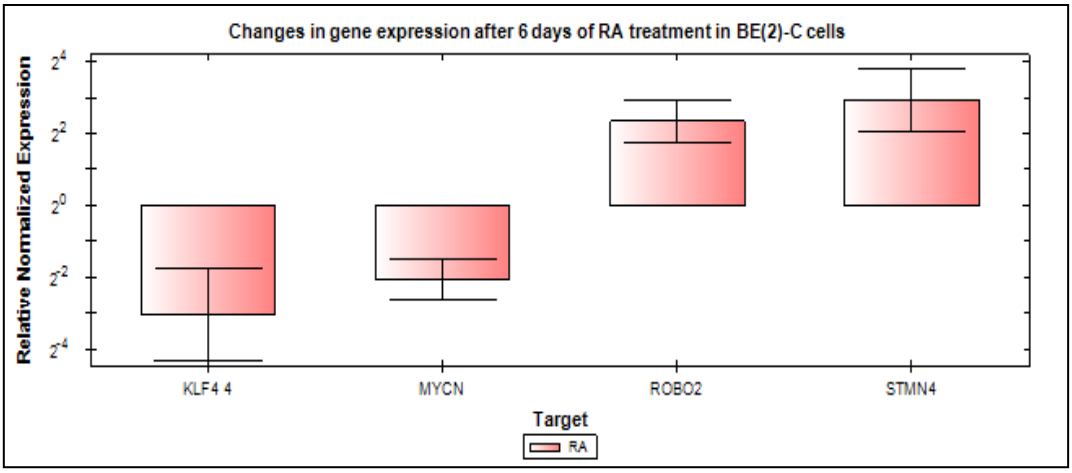

D

	KLF4	MYCN	ROBO2	STMN4
Adj NRQ	-8.15	-4.22	5.06	7.64
SD	0.179	0.116	2.47	3.29
Regulation	Down regulated	Down Regulated	Up regulated	Up regulated

Figure 34 - Graphs showing the level of target gene expression in IMR-32 (A) and BE2C (C) cells after 6 days of RA treatment. Graphs display the results of three biological repeats. Results are displayed relative to control. Error bars were calculated using standard deviation (SD). Tables give a summary of the QPCR data for the 4 target genes for IMR-32 (B) and BE2C (D).

4.10.Future directions

Following experimentation with RA, investigation into the effects of another compound, MLN8237, was initiated.

Aurora kinases are key regulators of cell cycle progression and over expression of Aurora kinase A and B is seen in a wide variety of human cancers. Several small molecule inhibitors of Aurora kinases have entered clinical trials. MLN8237 is a second generation Aurora kinase A inhibitor. Aurora kinase A has been shown to stabilise the MYCN protean by direct physical interaction with MYCN and the E3 ubiquitin ligase FBXW7 (Otto, Horn et al. 2009). The role of the MYCN transcription factor in regulating many genes in neuroblastoma cells, and its consequent role as a key prognostic factor for this malignancy, makes it an important therapeutic target. Furthermore, if as we and others have hypothesised, down regulation of the MYCN gene is the initiating factor in the differentiation of neuroblastoma cells, destabilisation of the N-Myc protein would similarly be expected to result in differentiation of these cells.

4.10.1.Preliminary work with MLN8237

In order to investigate the effects of MLN8237 IMR-32 and BE(2)-C cells were cultured with 1µM, 4µM and 10µM concentrations of the compound for 3 days. Cells were examined daily for changes in cell morphology and growth.

After 3 days the cells at the10µM concentration displayed evidence of toxicity and cell death. In the 1 µM medium no morphological changes were apparent. At 4µM some minor evidence of differentiation was present in cells in the form of small spike like processes (Figure 35). However due to the limited response observed we decided to extend the length culture up to 6 days. After 6 days a more pronounced effect on cellular morphology was seen (Figure 35).

Cell proliferation appeared to be reduced in the treated cells relative to control. We therefore performed Ki67 staining on these cells to quantify this effect. Cell counts were performed comparing the number of Ki67 stained cells to the number of DAPI stained cells in the treated and control cells (Figure 36). Overall a 14% decrease was observed in the level of Ki67 staining in the BE(2)-C cell line and a 20% decrease in IMR-32 cell line.

In order to determine if MLN8237 caused changes in gene expression associated with differentiation, cells cultured with the compound had their RNA extracted and cDNA synthesised. qPCR was performed using the same target and housekeeping genes as previous experiments.

Similar to the low degree of change in cellular morphology which was observed after 3 days of MLN8237 treatment, changes in the expression of target genes were also limited. In both cell lines the changes in gene expression were not statistically significant. STMN4 showed the largest change of any gene with a 2.51 fold increase observed seen in the IMR-32 cell line, however as previously stated this change was not statistically significant and no overall change could be determined (Figure 37).

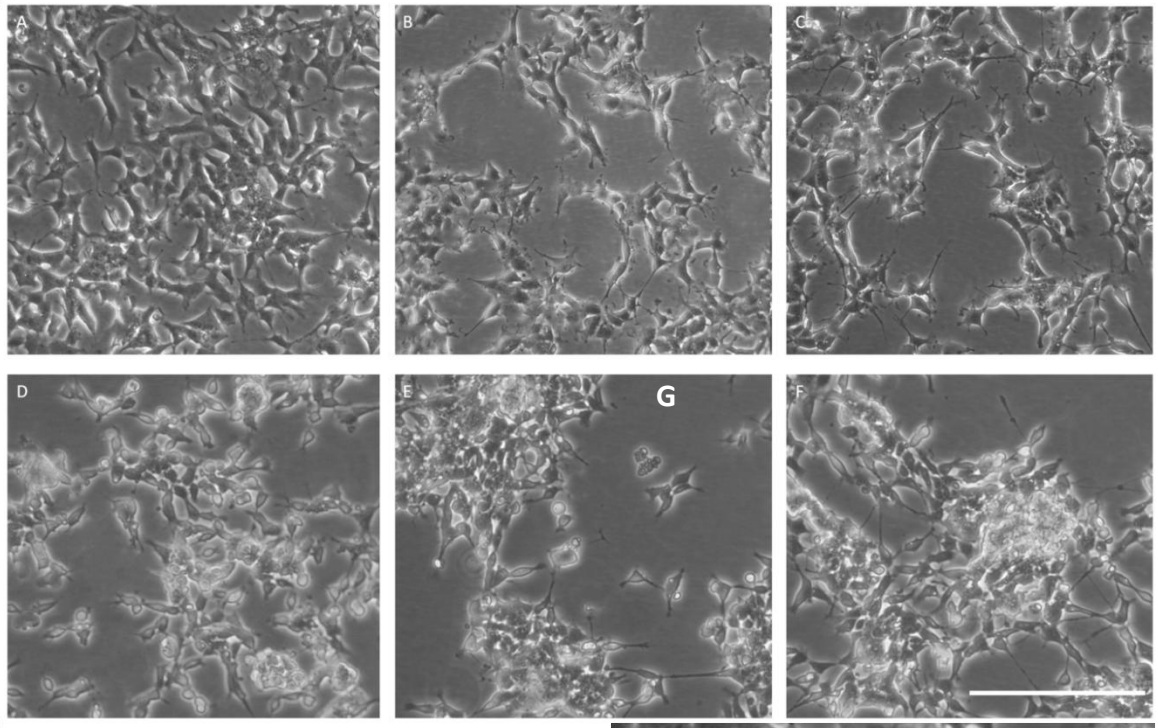

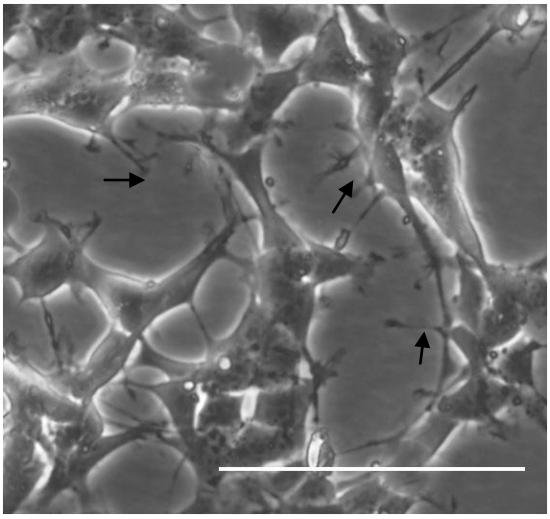

Figure 35 - Morphological changes after treatment with MLN8237. Top row are IMR-32 cells, bottom row are BE(2)-C. B and E represent cells after 3 days of treatments with MLN8237. C and E represent 6 days. A and D are control cells (DMSO) after 7 days. Scale bar represents 250µm. G: Image highlighting the presence of small processes protruding from neuroblastoma cells (black arrows) after 3 days of MLN8237 treatment. Scale bar represents 250µm.

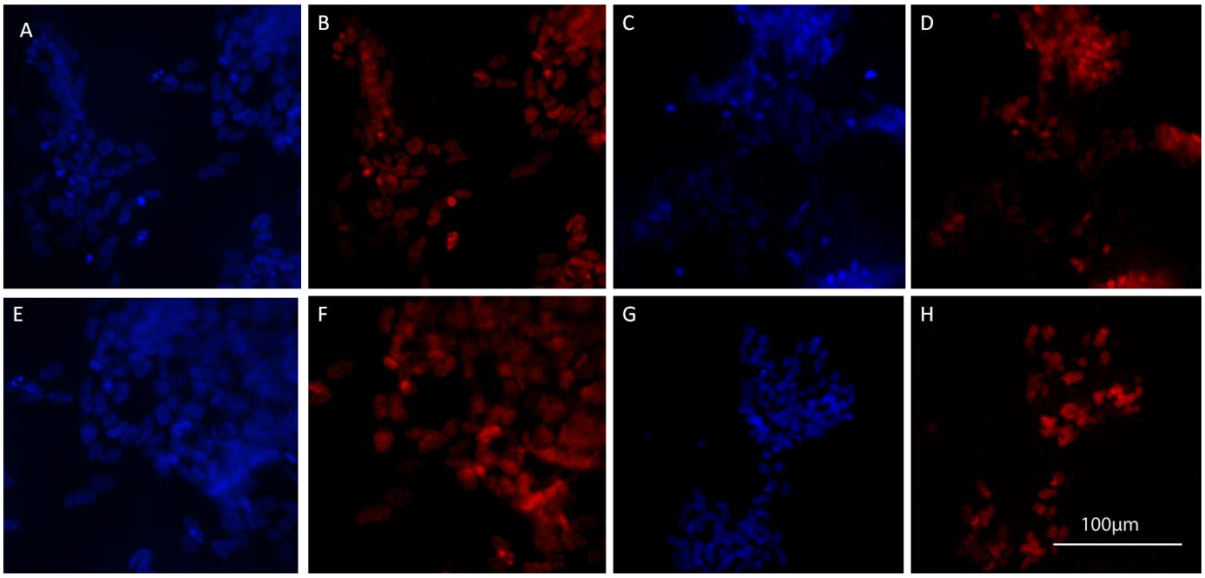

I

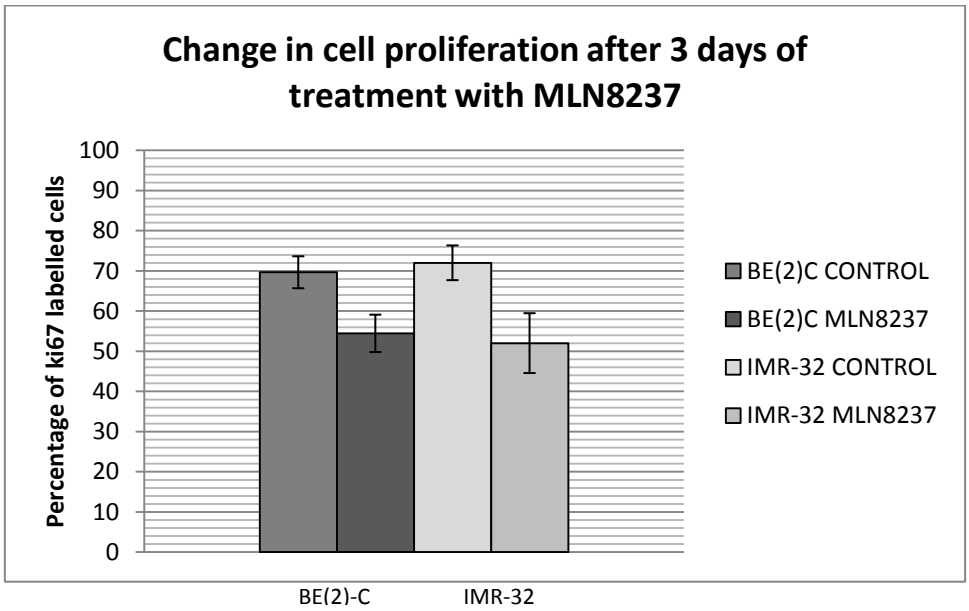

Figure 36 - Changes in proliferation after MLN8237 treatment. Ki67 staining in BE(2)-C (A-D) and IMR-32 (E-F) cells treated with MLN8237 for 3 days. A, B, E and F are control cells treated with DMSO alone. A reduction in the amount of Ki67 staining was observed in both cell lines. I: graph representing the percentage of ki67 stained cells in both IMR-32 and BE(2)-C cell lines comparing untreated and treated cells. Error bars show the standard deviation.

A

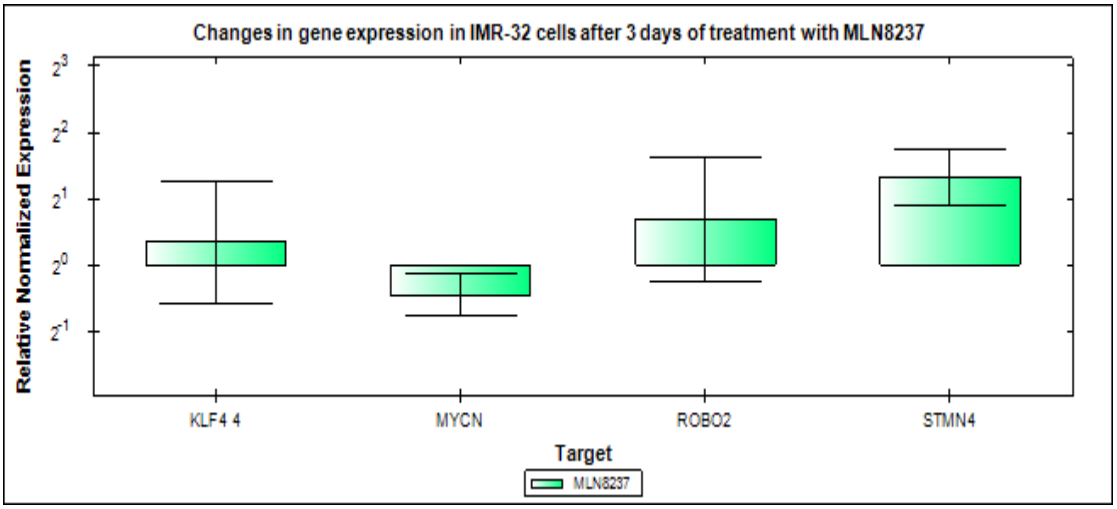

B

	KLF4	MYCN	ROBO2	STMN4
Adj NRQ	1.27	-1.37	1.61	2.51
SD	1.14	0.181	1.46	0.854
Regulation	No change	No change	No change	No change

C

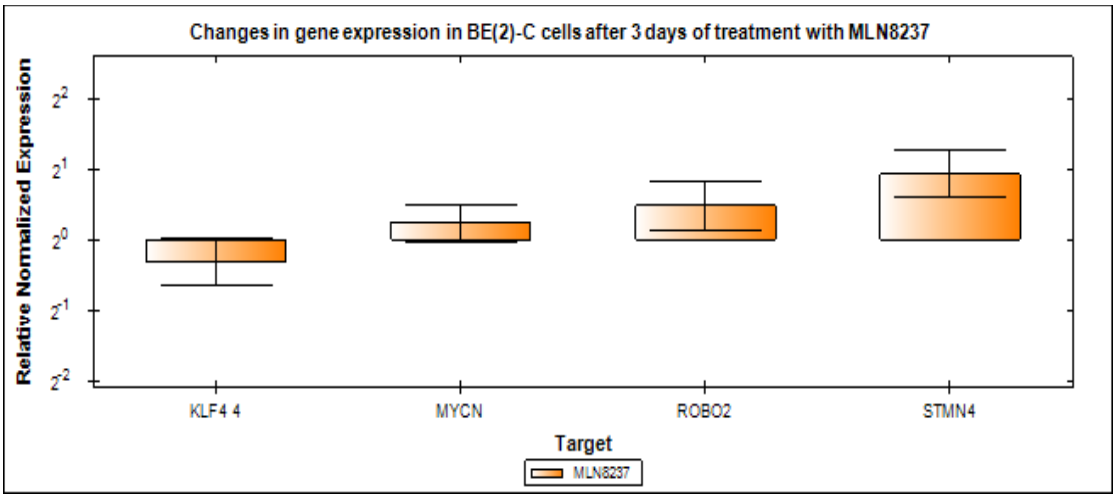

D

	KLF4	MYCN	ROBO2	STMN4
Adj NRQ	-1.25	1.18	1.39	1.89
SD	0.202	0.241	0.391	0.504
Regulation	No change	No change	No change	No change

Figure 37 - Graphs showing the level of target gene expression in IMR-32 (A) and BE2C (C) cells after 3 days of treatment with MLN8237. Graphs display the results of three biological repeats. Results are displayed relative to control. Error bars were calculated using standard deviation (SD). Tables give a summary of the QPCR data for the 4 target genes for IMR-32 (B) and BE2C (D).

5.Discussion

During this project we aimed to establish the ability of the chick embryo to act as a therapeutic model system for neuroblastoma research. We endeavoured to build on the work of others using the CAM, to demonstrate the ability of neuroblastoma cells to successfully form tumours within the model. We hoped to show that we could deliver drugs effectively to tumour cells in this system, and then detect the effects exerted by these drugs in a quantifiable way. Ultimately we hoped to validate the model by confirming the efficacy of existing standard therapy on neuroblastoma tumours within chick embryo model.

5.1.1.Growing tumours on the chick CAM

We used an *in ovo* shell-window technique throughout chick embryo experiments which has been used by others for similar means (Ribatti, Vacca et al. 1996, Wang, Wang et al. 2009). This method allows the CAM to be visualised and manipulated throughout embryonic development. Although *ex-ovo* techniques allow continual monitoring of the embryo and access to a greater area of the CAM, they can also greatly compromise survival (Lokman, Elder et al. 2012) and were deemed unnecessary. We were able to establish the presence of a tumour just 4 days after cells were placed on to the CAM, as well as being able to monitor tumours throughout treatments. The ability to perform continuous visual monitoring in this manner confers significant advantage over murine models where tumours must be palpable, or complex imaging modalities must be employed to detect and monitor tumour growth (Young, Ileva et al. 2009, Puaux, Ong et al. 2011).

Various methods, such as collagen inplants (Deryugina and Quigley 2008), plastic rings (Balke, Neumann et al. 2010), and matrigel grafts (Klingenberg 2014) have been used by others to graft cells onto the chick CAM. Here we simply applied the cells directly on to CAMs surface demonstrating that, in the case of NB cells, this added manipulation and complexity may not be necessary. We applied cells to the CAM at E7, allowing 7 days for tumour growth. Others using this model generally applied cells or tumour explants to the CAM at a later stage, around E9 or E10. This is largely due to the high degree of new vessel formation occurring prior to this stage, which may have confounded the results of those conducting research into angiogenesis itself. However some found that this period did provide them with greater embryo survival and tumour formation (Wang, Wang et al. 2009,

Yang 2014). Our work demonstrates that good levels of tumour formation can achieved at this earlier stage. It allows completion of embryo studies can be carried out prior to E14 which under current UK regulation is the deadline for keeping embryos without appropriate licensing. This may make the model more accessible to a wider range of laboratories, however greater rates of tumour formation may be observed at a later date. In the context of the embryo's 21 day developmental time frame, earlier tumour formation provides the potential for a longer window of compound administration and the consequent effects to be realised in tumours within the model. In either case the short time frame of the experiments carried out in this model allows results to be obtained at a much quicker rate than other more commonly used murine models.

Implantation of several neuroblastoma cell lines on to the surface of the chick chorioallantoic membrane allowed us observe the ability of the cells to form tumours in this environment. We observed variable rates of successful of tumour formation. The SK-N-AS cell line consistently formed tumours in the model, however the Kelly and BE(2)-C cells had much lower yields. These results were in keeping with other studies that also observed variable levels of cell line specific success when investigating the propensity of malignant cell lines to form tumours in the chick embryo model (Balke, Neumann et al. 2010).

Interestingly, of the neuroblastoma cell lines used in experiments, the MYCN amplified Kelly and BE(2)-C cells showed lowest rates of tumour formation. Clinically the presence of MYCN amplification denotes high risk disease (Westermark, Wilhelm et al. 2011). Thus these are the cells that are known to be more aggressive and therefore would be expected to form tumours more readily. Moreover in representing high risk disease these are the cells that new therapies are required to treat, thus not being able to include them in the model would represent a serious disadvantage.

Mixing the low yield Kelly or BE(2)-C cells with the SKNAS cells prior to implantation of the cells on to the CAM increased their rate of tumour formation. Furthermore, the use of different florescent labels allowed us to observe that both the SK-N-AS and the BE(2)-C/Kelly cells were present beneath the surface of the CAM in the resultant tumours. Although this methodology was unsuitable for future experimental analysis, it did demonstrate that

beneath the surface of the CAM the low yield cell lines were in fact able to survive and grow as tumours within model.

Where tumours did not form in the model, cells were seen on the surface of the CAM rather than beneath it as mass. This observation, along with the success of the mixed cell lines, led us to hypothesise that the lack of tumour formation displayed by these cells may represent their failure to invade the superficial epithelial layer of the CAM. Degradation and penetration of basement membranes and their underlying stroma are hallmarks of tumour invasion and metastasis (Stetler-Stevenson, Aznavoorian et al. 1993). Matrix metalloproteases (MMPs) are a large family of Zn^{2+}-dependent neutral endopeptidases. MMPs show proteolytic activity for many components of the extra-cellular membrane and are among the proteases believed to be involved in tumour invasion and metastases.

The levels of MMPs and their regulators have been studied in a several neuroblastoma cell lines (Sugiura, Shimada et al. 1998, Bjornland, Bratland et al. 2001, Noujaim, van Golen et al. 2002, Waheed Roomi, Kalinovsky et al. 2013). A paper by Sugiura *et al* identified that a high levels of certain MMPs are found to be secreted by a number of NB cell lines (LA-N-I. LA-N-2, LA-N-5, LA-N-6, IMR-32, SK-N-BE(2) SK-N-SH and HT1080). However it was also found that these enzymes are almost exclusively found in an inactive proform (Sugiura, Shimada et al. 1998). Interestingly in another study, Bjornland *et al* reported that the SKNAS cell line had the highest expression of MMPs of all the cell lines in the study (SK-N-AS, IMR-32, SK-N-DZ, SK-N-FI) (Bjornland, Bratland et al. 2001). In line with this finding, this group also showed that, of the cell lines studied, SKNAS was the only cell line with mRNA detected for the biological activator of the MMP. These results were further supported by a display of increased motility and invasiveness of the SKNAS cell line in *in vivo* experiments. Others have reported correlation between the results of *in vitro* motility and invasiveness studies, and tumour formation on the chick embryo CAM (Lokman, Elder et al. 2012). These findings may therefore explain why the SKNAS cell line was consistently the most successful in forming tumours in the chick embryo.

The above findings may also explain why the addition of trypsin, which is also a proteolytic enzyme, to the low yield NB cell lines significantly aided them in tumour formation. In general tumours forming in the chick embryo model were observed to be highly vascular.

After the addition of trypsin the MYCN amplified BE(2)-C cell line consistently formed very large, highly vascularised tumours. This suggests that once aided in invading the surface of the CAM the aggressive phenotype of these cells was more accurately reflected. The BE(2)-C tumours were often haemorrhagic in nature. In a similar fashion neuroblastoma commonly presents in patients as haemorrhagic tumours or tumours surrounded by haematoma (EE 1997, EE 2007). Other studies utilising the chick embryo as a xenograft model have also demonstrated that human malignancies implanted on the CAM reproduce many characteristics of primary disease (Hagedorn, Javerzat et al. 2005, Wang, Wang et al. 2009, Sys, Van Bockstal et al. 2012, Klingenberg 2014). Our data may also suggest that NB cell lines used in the model faithfully reproduce characteristics of the primary disease.

These results demonstrate that human neuroblastoma cells, like many other malignancies (Khanna, Jaboin et al. 2002, Hagedorn, Javerzat et al. 2005, Subauste, Kupriyanova et al. 2009, Wang, Wang et al. 2009, Balke, Neumann et al. 2010, Sys, Lapeire et al. 2013, Yang 2014), are able form tumours in this model. We have also shown that with the addition of trypsin the success of neuroblastoma cells in forming tumours can be greatly enhanced. This finding may have significance, not only in establishing the chick embryo as a suitable in vivo model system for neuroblastoma, but may aid research into other malignancies being used in the model.

5.1.2.Drug Delivery

EdU administered topically to the surface of the CAM could be detected throughout underlying tumour as well as being observed throughout the chick embryo's liver. There was no obvious gradient observed (as might be seen with simple diffusion) and no areas where EdU was absent. We inferred from these observations that substances applied topically had the capacity to reach the blood stream of the chick embryo. Although not accounting for differences in the physicochemical properties of drugs such as in molecular weight, shape, charge and aqueous solubility which determine the rate of diffusion through tissue, this result allowed us to feel confident that compounds administered in this way could reach cells throughout the tumours growing in the model. As a practical and simplistic method, topical administration has been the most widely utilised mode of administering compounds to the CAM to date (Hagedorn, Javerzat et al. 2005, Vargas, Zeisser-Labouebe et al. 2007). However up until now, compounds administered in this model have been designed to affect

angiogenesis which may therefore exhibit a much more localised effect on the CAM vasculature. Here we expanded the context in which topical administration can be deemed appropriate.

Upon analysis of the tumours dissected after EdU administration there were no areas where EdU staining was obviously absent, however 10-30% of cells were not EdU labelled. Within the 3D tumour environment the presence of pockets of poorly perfused tumour cells which are consequently hypoxic, poorly nourished, express a more aggressive phenotype and also proliferate at a slower rate, has been widely reported (Minchinton and Tannock 2006). The presence of non-EdU labelled cells upon analysis may therefore reflect the more realistic 3D in vivo tumour cell environment which is not seen in cell culture experiments.

5.1.3.Retinoic Acid.

After 3 days of culture with RA both IMR-32 and BE(2)-C cells displayed morphological changes such as neurite formation. Such changes have been widely reported within the literature (Sidell 1982, Sidell, Altman et al. 1983, Wu, Fang et al. 1998) and are characteristic of differentiation. Changes in the level of target gene expression after exposure to RA were detected using qPCR. Against our expectations, the level of MYCN expression remained largely unchanged after 3 days of RA treatment in culture. However, after 6 days MYCN expression in both IMR-32 and BE(2)-C cells in culture fell by around 4 times relative to that of the control.

MYCN is a transcription factor known to regulate expression of many target genes (Gherardi, Valli et al. 2013). It is thought to be directly affected by RA and has been implicated as a regulator of differentiation in neuroblastoma (Wada, Seeger et al. 1992, Westermark, Wilhelm et al. 2011). Therefore to observe morphological characteristics of differentiation prior to the down regulation of this gene is somewhat unexpected. One explanation for these observations may come from a paper by Guglielmi *et al* in which the authors suggest that the presence of MYCN is necessary for differentiation to occur (Guglielmi, Cinnella et al. 2014). In contrast to several previous studies (Amatruda, Sidell et al. 1985, Thiele, Reynolds et al. 1985) , the authors describe a transient rise in the expression of MYCN in the first few days of RA induced differentiation before levels later decrease. They propose that MYCN, as a transcription factor, is necessary at the onset of

neuronal differentiation to establish the expression of a set of genes essential for subsequent phases. MYCN is known to play a role in normal development and has been implicated in the control of early differentiation steps in some tissues, including the nervous system (Guglielmi, Cinnella et al. 2014, !!! INVALID CITATION !!!). Consequently there may be some biological foundation for these findings. Our observations did not support a rise in the level of MYCN expression, however as we observed expression at 3 and 6 days alone it is possible that a rise in MYCN could have occurred prior day 3 and levels may have begun to fall again at this stage leading limited changes to be observed overall. As different cell lines were used in these works it may also be possible that different levels of MYCN expression are observed during differentiation in these cells. Clearly further work is needed to clarify the pattern of MYCN expression during this period before any such conclusions can be made.

Another explanation for these findings may be that MYCN is not initiating differentiation in these neuroblastoma cells. Transcriptional profiling has demonstrated that retinoic acid influences the expression of a large number of transcription factors (Korecka, van Kesteren et al. 2013). Many of these genes are also known to affect differentiation and therefore the changes observed in this study may represent influences exerted by other transcription factors (Korecka, van Kesteren et al. 2013). Kaplan *et al* reported induction of the TrkB neurotrophin receptor by RA. They suggested that this induction mediated biologic responsiveness to the TrkB ligands BDNF and NT-3 and the differentiation of human NB cells (Kaplan, Matsumoto et al. 1993). Unlike some NB cell lines both BE(2)-C and IMR-32 cells do express full length TrkB and therefore it is possible that differentiation is being mediated by this pathway (Scala, Wosikowski et al. 1996, Chu, Cheung et al. 2003) although TrkB expression is typically associated with a more aggressive phenotype (Scala, Wosikowski et al. 1996) (Brodeur, Minturn et al. 2009). Other studies have identified changes in key regulators of normal neural crest differentiation in response of RA treatment. Prompt down regulation of hASH-1, an early element of the differentiation pathway has been reported following RA treatment in SH-SY5Y cells (Lopez-Carballo, Moreno et al. 2002).

The key significance of the MYCN gene in neuroblastoma means that understanding the relationship between its expression and differentiation is extremely important in this field. Therefore these findings, in potentially challenging previously accepted patterns of MYCN

expression, could be highly significant. Differentiation therapy itself is integral to the treatment of patients with high risk neuroblastoma, and therefore understanding the pathways involved in mediating its effects may provide means of aiding problems such as resistance to therapy. Further work is needed to fully understand these pathways.

Following retinoic acid treatment, expression levels of KLF4 fell consistently in culture. As might be expected, the fold decrease was greater after 6 days of RA treatment than that at 3. This gene was selected for inclusion in this research based on the work of Sung *et al* who observed a ~10 fold decrease in the expression of the gene in IMR-32 cells following exposure to RA (Sung, Boulos et al. 2013). Our results further support this observation and extend it to show similar changes in the BE(2)-C cell line.

KLF4 has a key role in the regulation of many aspects of cell biology and has been implicated in the expression of stem-like properties. Using retroviral transduction it has been demonstrated that, in conjunction with other genes, KLF4 is capable of inducing mouse embryonic fibroblasts to be reprogrammed to a pluripotent state similar to that observed in ES cells (Hima Vangapandu 2009). Others have found that KLF4 is in turn regulated by N-Myc, in both tumours and stem cells. This suggests that N-Myc may enforce expression of stem-like characteristics and contribute to the undifferentiated phenotype of neuroblastoma (Cotterman and Knoepfler 2009). In keeping with this theory our results display a marked decrease in KLF4 expression in conjunction with a visibly more differentiated cell phenotype, however the relationship between these observations and MYCN expression is less clear.

Expression of ROBO2 was increased throughout all of the RA experiments, however changes only reached statistical significance after 6 days in cell culture. Again our results supported those of the Sung *et al* and extended them to demonstrate similar changes in the BE(2)-C cell line. Extensive research has been conducted on the role of Robo genes in axon guidance (Brose, Bland et al. 1999, Guthrie 2004, Long, Sabatier et al. 2004, Devine and Key 2008). Specifically, Robo2 is reported to be involved in the regulation of actin cytoskeleton and axonogenesis pathways (Sung, Boulos et al. 2013). Increased expression of this gene is in keeping with the observed morphological changes of cells under the influence of RA.

In a similar fashion STMN4 was up regulated in all of the cell culture experiments involving RA. Again this result was very similar to that published by Sung *et al*. Less is known about the role of STMN4, however it has been implicated in the destabilisation of microtubules. This is essential in the regulation of dynamic microtubules which are known to be aid growth cone advance and responses to guidance cues (Grenningloh, Soehrman et al. 2004).

Changes observed in the expression of KLF4, ROBO2 and STMN4 were largely reproducible between experiments. The plausible biological rationale behind these changes, and their correlation with the changes in morphological appearance of the cells over time, supports their significance. Furthermore as these changes have been recognised in other published works this indicates that they may provide good markers of differentiation in neuroblastoma cells.

5.1.4.Retinoic acid in the chick embryo

In order to demonstrate the suitability of the chick embryo xenograft model for therapeutic research, the model was assessed using RA.

The dose of 30mg/kg was used throughout chick embryo experiments conducted with RA. This figure was deduced from papers using the drug in xenograft mouse models where the maximum tolerated dose was approximately 60mg/kg and 50-60% of this value was observed in order to observe therapeutic effects (Shalinsky, Bischoff et al. 1995). Dose calculations used the weight of an average egg less the weight of its shell. As tumours in the model exist outside of the embryo itself it seemed logical to include the entire extra-embryonic weight in drug dose calculations. Although extrapolating drug dosing from different species is unlikely to provide optimal therapeutic levels this method does provide a bench mark for future experiments. Where new compounds are tested in panels of mouse xenograft models the maximum tolerated dose is administered in order to first establish the presence of a drug effect, before a physiologically acceptable range of doses is later determined (NCI). The high throughput nature of the chick embryo model would make it amenable to this form of therapeutic research and therefore this approach could also be adapted for future research.

As with cell culture experiments, qPCR was used to detect changes in gene expression signifying differentiation of cells. Retinoic acid administered to tumours in the chick embryo

model showed a very similar pattern of results to those of cell culture. The general pattern of positive and negative fold change was exactly the same as for culture experiments. Sight differences in the magnitude of these changes, variability and consequent statistical significance between genes were noted which may reflect the differences in the cells *in vitro* and *in vivo* environment.

The consistency of these results along with their similarity to those seen in cell culture suggests that RA was being delivered effectively to a high proportion of cells. As might be expected a small increase in the variability of results was observed in the *in vivo* studies perhaps reflecting the more variable drug exposure cells would be expected to receive in this environment. However the changes in gene expression that were observed do suggest that NB cells within the model were differentiating in response to retinoic acid exposure. Furthermore analysis of primary neuroblastoma samples has shown previously that higher levels of Robo2 and STMN4 are commonly identified in lower stage (typically more differentiated) disease and are associated with better patient survival (Sung, Boulos et al. 2013) adding to the robustness of this finding. Others have attempted to use to analyse gene expression changes in cancer cells implanted on the chick embryo CAM (Hagedorn, Javerzat et al. 2005). During tumour formation on the CAM Hagedorn *et al* identified up regulation of several genes known to be involved in human glioma tumour progression (Hagedorn, Javerzat et al. 2005). Here we have identified the inverse, that changes in genes associated with cell differentiation, can also be observed.

Many others have suggested the suitability of the chick embryo model for therapeutic research however this is the first time, outside the field of angiogenesis, that the efficacy of a known compound has been reproduced in the chick embryo model. These results are highly promising in confirming our hypothesis that the chick embryo can provide an effective therapeutic model system.

5.1.5.MLN8237

MLN8237 is a small molecule inhibitor of Aurora Kinase A (AURKA) that is currently in early phase clinical testing. AURKA plays a pivotal role in centrosome maturation and spindle formation during mitosis but has also been shown to aid the stabilisation of the N-Myc protein making MLN8237 a potentially powerful tool in the treatment of NB (Brockmann,

Poon et al. 2013). In order to expand the number of compounds explored in the chick embryo model, as well as to further investigate the role of MYCN in differentiation, we began experimentation with MLN8237.

In order to optimise and characterise the effects of this compound, experiments were conducted *in vitro* with both BE(2)-C and IMR-32 cell lines using several drug concentrations. At 4µM MLN8237 showed limited toxicity and some morphological changes to cells were visible. Small processes were visible extending from cells, suggesting some influence of the drug on differentiation. However these changes were far less pronounced than those observed with RA, even after 6 days of treatment.

Other works investigating MLN8237 have described evidence of differentiation *in vitro*. However rather than discussing the effects on cell morphology, the authors state that levels of neurofilament protein L mRNA ($NF\text{-}L$) rose demonstrating differentiation (Brockmann, Poon et al. 2013). Previous studies have found variable levels of NF-L mRNA, but not protein, are expressed in both differentiation induced and control cells. Furthermore NF-L mRNA, and some protein, has been seen to be expressed in both RA-treated and control cells within 6 h of plating, but down-regulated to baseline level thereafter in both populations (Shea, Sihag et al. 1988, Chiu, Feng et al. 1995). Others have reported the absence of this protein altogether in both cell populations (Andres, Keyser et al. 2013).Therefore the reliability of this marker as an indicator of differentiation is somewhat questionable. Although evidence of differentiation appears less prominent *in vitro*, *in vivo* studies with MLN8237 have been conducted in the Th-MYCN mouse model of NB where partial maturation of tumours was observed. This could suggest other factors such as the tumour-host interactions impact on the response of cells to this compound.

In support of the lack of morphological changes we observed in cell culture, qPCR results failed to show any significant changes in target gene expression. The largest change was observed in STMN4 expression which was 2.51 and 1.89 fold higher in the treated IMR-32 and BE(2)-C cells respectively. However, as stated these changes did not reach statistical significance.

The limited nature of these changes when compared to those observed after 6 days of RA treatment may be explained somewhat by the gene selection process. We chose genes

based on data published by Sung *et al* showing significant changes in expression following RA administration (Sung, Boulos et al. 2013). Further experiments involving the siRNA mediated knock down of MYCN and chromosome 1p transfer as means of causing differentiation of NB cells were also conducted by these authors. Each of these methods caused similar patterns of target gene expression, (as seen by up regulation, or down regulation of genes) however the magnitude of these changes was highly variable. It is therefore not surprising that a degree of variation between the two treatments used in our research should be observed. Having selected the genes observed to respond to RA with the greatest fold change, it is also not surprising that these genes show greater change following its administration here.

Our results could be interpreted to suggest that these genes are effective indicators of RA mediated differentiation alone. However, as previously stated although Sung *et al* saw differing magnitudes of change, they still demonstrated statistically significant differences in expression and observed morphological changes in these cells during each experimental condition. The lack of morphological changes observed after MLN8237 administration, coupled with the lack of statistically significant change observed in gene expression suggests that the differentiation process had not truly begun here. Despite being a negative result these findings are useful in further supporting the reliability of our target gene selection in detecting differentiation in NB cells. The lack of differentiation observed here could support the theory that MYCN levels must rise to initiate the differentiation programme or that other targets of RA are initiating in this process.

MLN8237 did produce a noticeable reduction in cell proliferation which was quantified using Ki67 staining. Overall a 14% decrease in Ki67 staining in the BE(2)-C cells and a 20% decrease in the IMR-32 cells was observed compared to controls. This result was in keeping with published results on the effects of MLN8237 where similar effects were observed over this timescale, although a much greater effect was reported in this paper after 6 days (Brockmann, Poon et al. 2013). Others have also reported that down regulation of MYCN can reduce proliferation (Shang, Burlingame et al. 2009). It is hypothesised that this effect may be mediated by MYCN induced down regulation of cell-cycle inhibitor *CDKN1A* (encoding $p21^{Cip1}$)(Brockmann, Poon et al. 2013).

Despite consistent results in relation to this compound effects on neuroblastoma proliferation further work is required to optimise the effects of this molecule before it is utilised in the chick model.

5.2.Limitation of the CAM model

All in vivo models as approximations of reality have inherent strengths and limitations. An appreciation of these limitations is important in interpreting results obtained through their use and aids decisions about which model is appropriate in which context. As a xenograft model the chick embryo involves the addition of human neuroblastoma cells into the chick embryo environment. This non-human environment may have affect on aspects of cell behaviour and interactions between tumour cells and the local microenvironment may not be faithfully recreated. The natural immunodeficiency of the chick embryo, though aiding xenografting, prevents the investigation of compounds acting in an immune mediated fashion and does not recreate the interaction between host immune system and the tumour.

The short 21 day period of chick development may also confer limitations. Firstly this limits the length of time compounds can be administered in the model. We have demonstrated that a 3 day window can be used to test compounds whilst others have grown tumours in the model until day 18 theoretically allowing 7 days of tumour treatment. Whilst this time frame may be appropriate for the more rapid screening of compounds, this makes this model unsuitable for the longer term study of therapeutic effect. Secondly the rapidly changing nature of the embryonic environment may affect factors such as diffusion across the CAM as well as the distribution of fluid within the egg (Stephanie Li Mei Tay 2011). These changes may have implications for the rate of diffusion and distribution of therapeutic compounds within the model.

The use of cell lines in this model, which although well characterised, are subject to genetic drift and may not represent primary disease accurately. They may also fail to reproduce the heterogeneity of genetic changes characteristic of primary tumours and therefore exaggerate the therapeutic effect of targeted therapies.

5.3.Future directions

The majority of work carried out in these experiments used the IMR-32 and BE(2)-C cell lines. It would be useful to extend the number and variety of cell lines used in experiments to represent a wider spectrum of disease. Others have demonstrated the successful xenografting of tissue derived from primary tumour samples on the chick embryo CAM (Sys, Van Bockstal et al. 2012, Fergelot, Bernhard et al. 2013, Sys, Lapeire et al. 2013). This opens up the exciting possibility of including both neuroblastoma cell lines and primary tumour samples in this model system and would provide an excellent means providing more robust findings on the activity of therapeutic compounds.

We identified that the addition of trypsin to cells aided them in tumour formation and hypothesised that this addition supplemented a lack of activated MMPs in these cells. Although in vivo activation of pro-MMPs is complex, in vitro activation can be achieved simply using destabilizing agents such as the organomercurial 4-aminophenyl mercuric acetate (APMA) which initiate an autocatalytic cleavage of the prodomain(Sugiura, Shimada et al. 1998). Further examination of the hypothesis that MMP inactivation is responsible for the low tumour yield of certain NB cell lines could be accomplished by activating MMPs in culture immediately before implantation of cells on to the CAM.

Tumours developing in the model shared morphological characteristics of primary neuroblastoma however further characterisation of these tumours would give a better idea of how well they represent primary disease. Sys *et al* blinded a pathologist as to the identity of tumours, and compared CAM derived and primary sarcomas to establish the level of similarity. Work has already begun to complete a similar evaluation of NB tumours from this model. When characterising tumours in the Th-MYCN transgenic murine model of neuroblastoma, staining for synaptophysin and neuron-specific enolase was conducted and this method could be reproduced here (Weiss, Aldape et al. 1997).

We saw correlation between cell morphology and the expression of target genes in cells treated with RA in culture. Histological analysis of tumours treated with RA in the model would also allow this form of comparison, and would increase confidence in these genes as markers of differentiation. Other forms of analysis such as ki67 staining and excision clonogenic assays could be used to assess the retention of proliferative potential in treated

tumours **(Khleif SN 2000)**, whereas techniques such as tunel staining could also be employed to detect apoptosis.

Further validation of this model must be completed using other therapeutic compounds. Works with MLN8237 have begun in order to further investigate the effects of MYCN reduction on differentiation in NB cells. In respect to this drug, continued optimisation in culture is required before work in the chick embryo can begin. So far work has focused on differentiation therapies for NB however exploring other forms of cancer therapy would also be important in producing a robust well characterised model system. In order to carry out such experiments using qPCR suitable candidate genes must first be identified and validated. Commercially available, optimised qPCR arrays capable of quantifying changes in large numbers of genes relating to known phenotype have been developed. This technology could provide the ability for large scale gene expression analysis following administration of compounds.

The rapid time frame, practical nature and low cost of this model system means that it could potentially provide an excellent means of *in vivo* high through-put screening of therapeutic compounds. Ultimately this model may offer the potential to replace much of the early *in vivo* screening completed in more costly xenograft murine models in initiatives such as the PPTP. Before the chick embryo is able to replace the use of xenograft models, results obtained from its use must be validated. Here we have shown that the effects of RA are reproduced in the model. However in order to replace existing models a wider degree of correlation must be demonstrated between results derived from the chick, and those from mouse xenograft models and later clinical studies.

5.4.Conclusions

Neuroblastoma is a childhood malignancy displaying a diverse range of clinical behaviours. For high risk patients mortality remains tragically, and unacceptably, very high. Thus new treatments able to target the distinct biological and molecular features of these patient's disease are urgently required. In the field of paediatric therapeutic research, preclinical models are vital. With an increasing number of potential therapeutic targets being identified, the need for economically viable, high through put in vivo models is escalating.

The chick embryo is low cost, highly practical and well characterised by centuries of research, and may provide a suitable xenograft model for work in this field.

We have demonstrated that human neuroblastoma cell lines can be grafted on to the chick CAM and form tumours. We have seen that topical administration provides a simple and effective way to deliver compounds in this model. Using elements of standard therapy we have identified three genes which reproducibility change in line with NB cell differentiation in both *in vitro* and using the *in vivo* chick embryo model.

In conclusion this project adds to existing works which highlight the suitability of the chick embryo as a model for cancer research. In addition we have created a system by which the effects of differentiation agents can be tested on human neuroblastoma tumours in this model. We hope this research may serve as blueprint for future works allowing the full spectrum of drug effects to be investigated. We hope that further development and characterisation of this model may eventually lead to its use in preclinical therapeutic research, and ultimately in helping to identify compounds offering new treatment for patients with neuroblastoma.

6.Appendix

Figure 38: IMR-32 + RA in culture

a

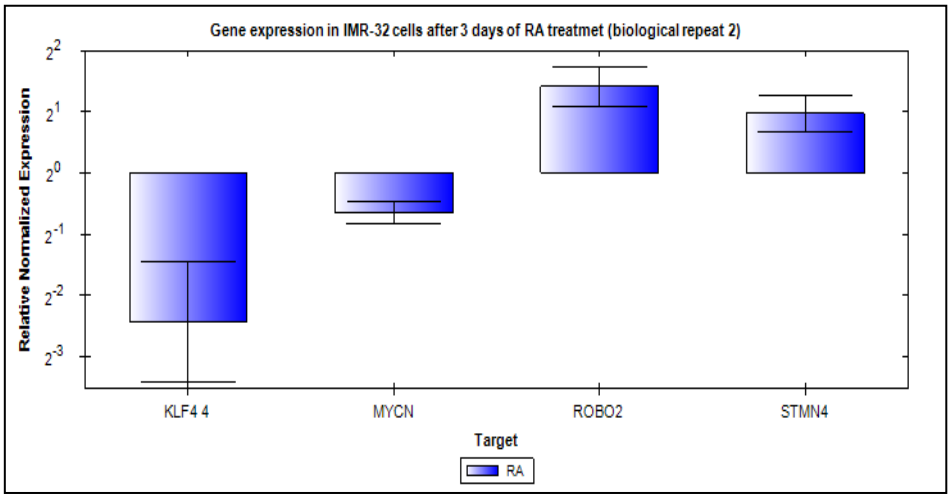

b

	KLF4	MYCN	ROBO2	STMN4
Adj NRQ	-5.42	-1.57	2.67	1.97
SD	0.183	0.0888	0.676	0.461
Regulation	Down regulated	No change	Up regulated	No change

c

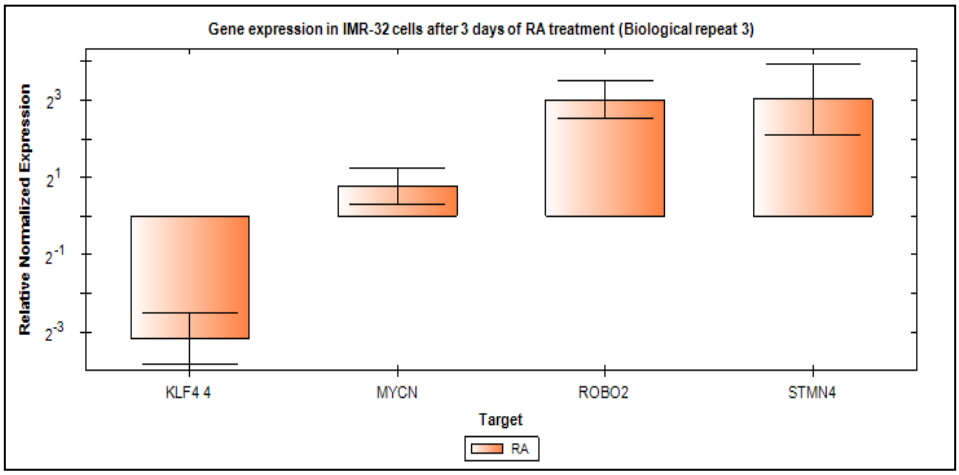

d

	KLF4	MYCN	ROBO2	STMN4
Adj NRQ	-8.97	1.71	8.01	8.15
SD	0.116	0.151	1.35	2.29
Regulation	Down regulated	No change	Up regulated	Up regulated

Figure 38 - RA in cell culture: A and C; graphs displaying the results of single qPCR experiment in IMR-32 cells following 3 days of RA treatment. The error bars display the standard deviation (SD). B and D: tables providing a summary of the values obtained from the experiments. The adjusted normalised quantification (Adj NRQ) describes the actual change in the gene expression relative to the control. Regulation describes the overall statistically significant change in gene regulation.

Figure 39: BE(2)-C + RA in culture

a

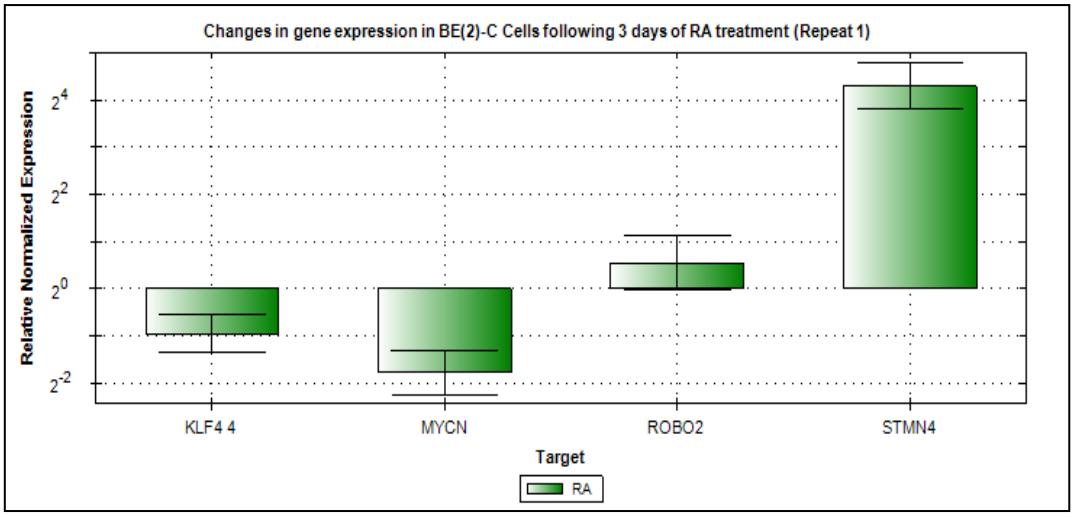

b

	KLF4	MYCN	ROBO2	STMN4
Adj NRQ	-1.93	-3.43	1.45	19.5
SD	0.165	0.112	0.715	0.992
Regulation	No change	No change	No change	Up regulated

c

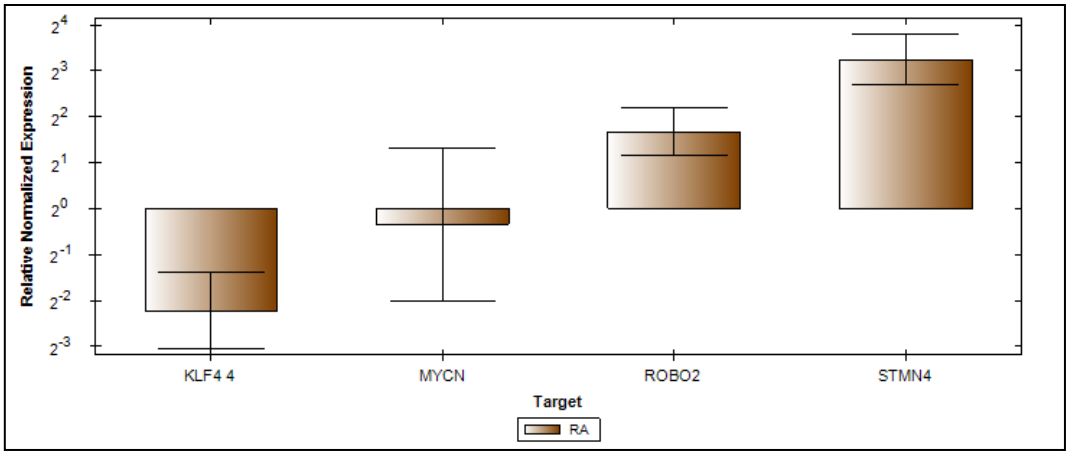

d

	KLF4	MYCN	ROBO2	STMN4
Adj NRQ	-4.52	-1.28	3.41	9.43
SD	1.57	2.10	1.15	1.63
Regulation	No change	No change	No change	Up regulated

e

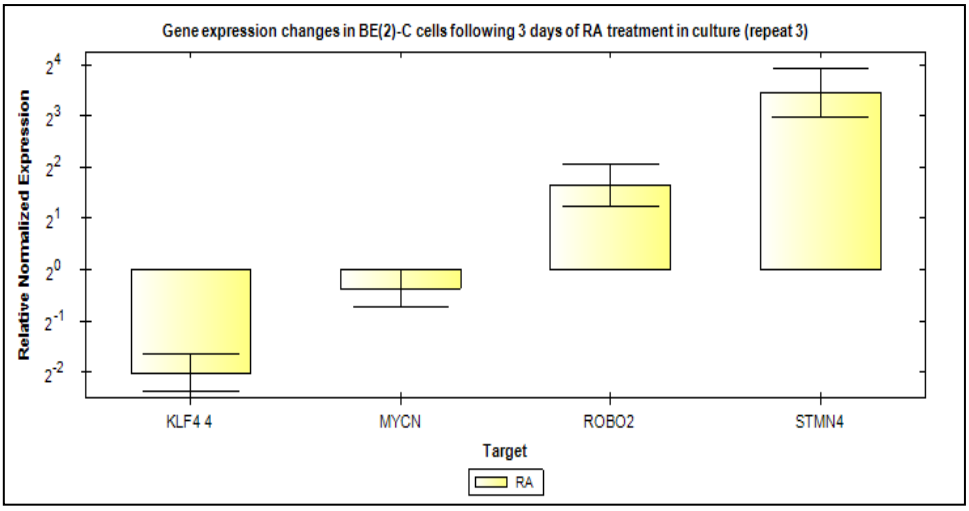

f

	KLF4	MYCN	ROBO2	STMN4
Adj NRQ	-4.02	-1.29	3.14	10.9
SD	0.07	0.22	1.04	1.35
Regulation	Down regulated	No change	No change	Up regulated

Figure 39 - RA in cell culture: a,c and e; graphs displaying the results of single qPCR experiment in BE(2)-C cells following 3 days of RA treatment. The error bars display the standard deviation (SD). B, D and F: tables providing a summary of the values obtained from the experiments. The adjusted normalised quantification (Adj NRQ) describes the actual change in the gene expression relative to the control. Regulation describes the overall statistically significant change in gene regulation.

Figure 40: IMR-32 + RA for 6 days in cell culture

a

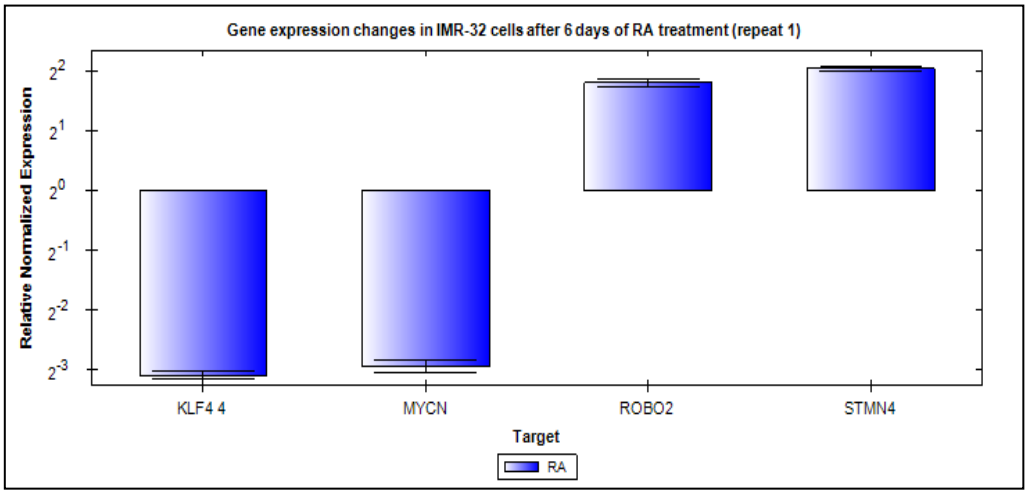

b

	KLF4	MYCN	ROBO2	STMN4
Adj NRQ	-8.52	-7.68	3.50	4.10
SD	0.0157	0.0195	0.0161	0.0146
Regulation	Down regulated	Down regulated	Up regulated	Up regulated

c

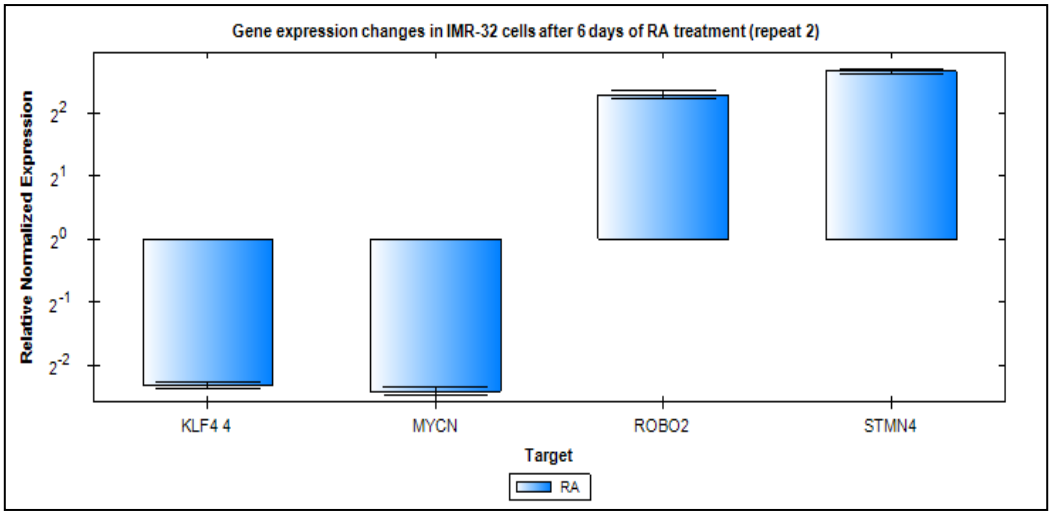

d

	KLF4	MYCN	ROBO2	STMN4
Adj NRQ	-4.95	-5.32	4.90	6.39
SD	0.0765	0.0902	0.245	0.0231
Regulation	Down regulated	Down regulated	Up regulated	Up regulated

e

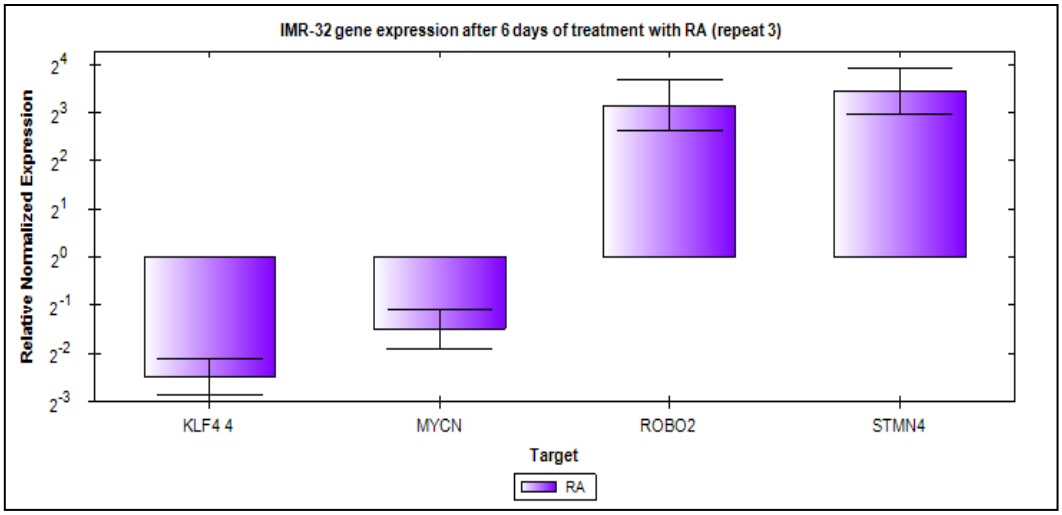

f

	KLF4	MYCN	ROBO2	STMN4
Adj NRQ	-5.64	-2.80	8.89	10.9
SD	0.0961	0.201	0.885	0.783
Regulation	Down regulated	Down regulated	Up regulated	Up regulated

Figure 40 - RA in cell culture: a,c and e; graphs displaying the results of single qPCR experiment in IMR-32 cells following 6 days of RA treatment. The error bars display the standard deviation (SD). B, D and F: tables providing a summary of the values obtained from the experiments. The adjusted normalised quantification (Adj NRQ) describes the actual change in the gene expression relative to the control. Regulation describes the overall statistically significant change in gene regulation.

Figure 41: BE(2)-C + 6 days of RA in culture

a

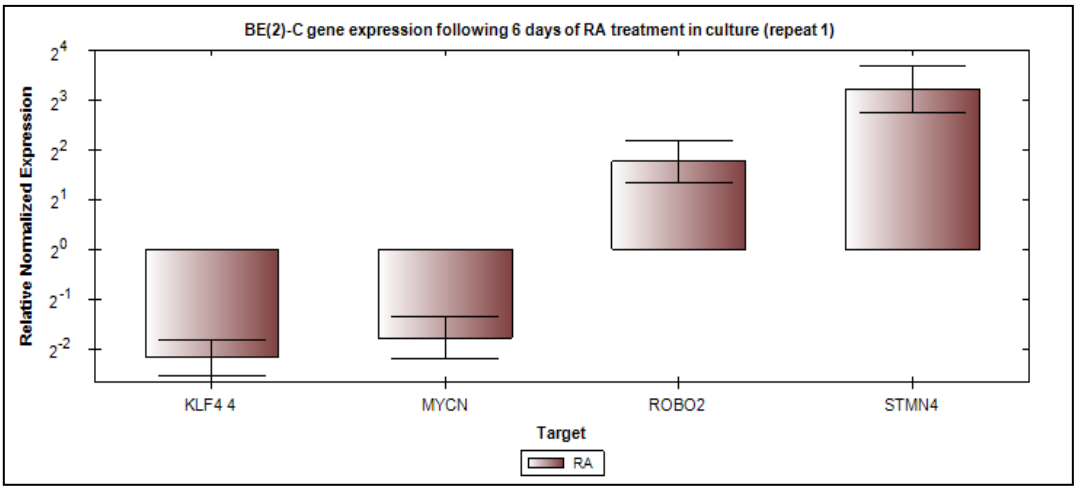

b

	KLF4	MYCN	ROBO2	STMN4
Adj NRQ	-4.52	-3.42	3.41	9.43
SD	0.0713	0.102	1.15	3.23
Regulation	Down regulated	Down regulated	Up regulated	Up regulated

c

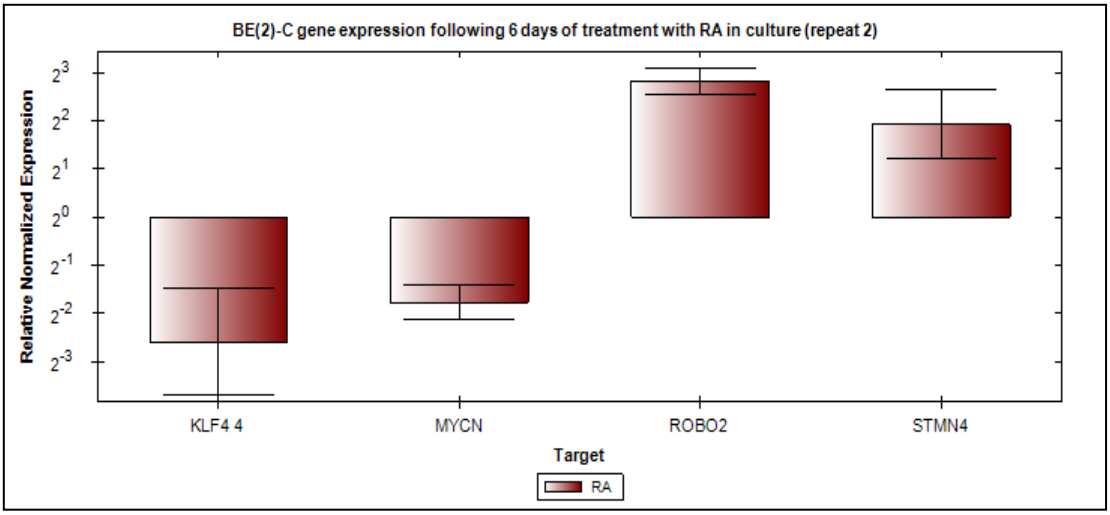

d

	KLF4	MYCN	ROBO2	STMN4
Adj NRQ	-6.04	-3.41	7.04	3.79
SD	0.193	0.0812	1.55	2.48
Regulation	Down regulated	Down regulated	Up regulated	Up regulated

e

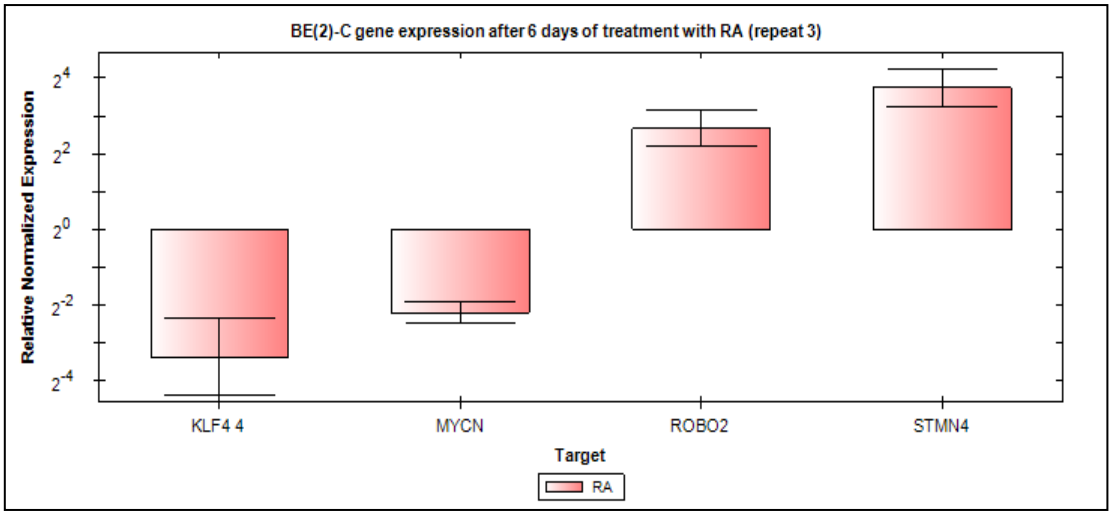

f

	KLF4	MYCN	ROBO2	STMN4
Adj NRQ	-10.20	-4.57	6.36	13.50
SEM	2.83	0.0532	1.04	1.23
Regulation	Down regulated	Down regulated	Up regulated	Up regulated

Figure 41 - RA in cell culture: a,c and e; graphs displaying the results of single qPCR experiment in BE(2)-C cells following 6 days of RA treatment. The error bars display the standard error of the mean (SEM). B, D and F: tables providing a summary of the values obtained from the experiments. The adjusted normalised quantification (Adj NRQ) describes the actual change in the gene expression relative to the control. Regulation describes the overall statistically significant change in gene regulation.

Figure 42: IMR-32 tumours treated with RA

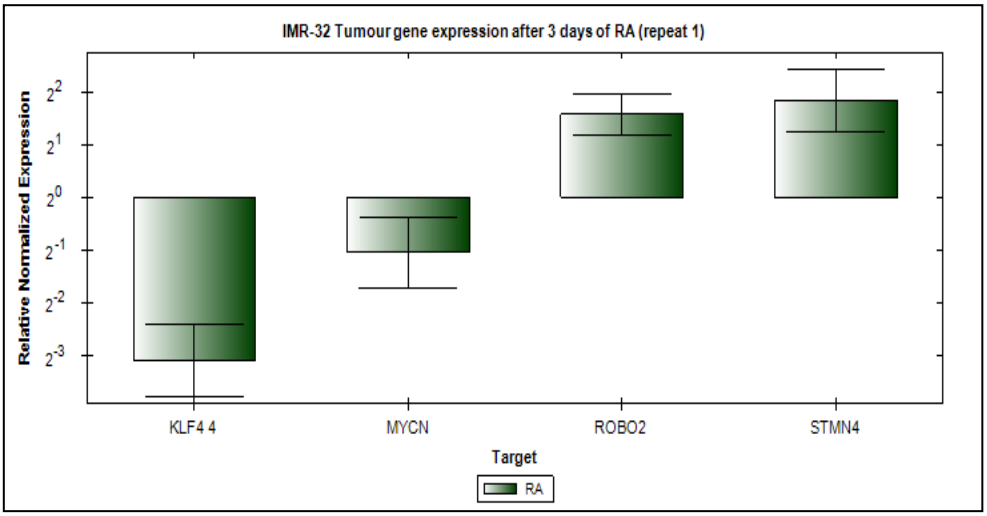

	KLF4	MYCN	ROBO2	STMN4
Adj NRQ	-8.58	-2.26	2.16	3.58
SD	0.987	0.814	1.54	1.69
Regulation	Down regulated	No change	No change	No change

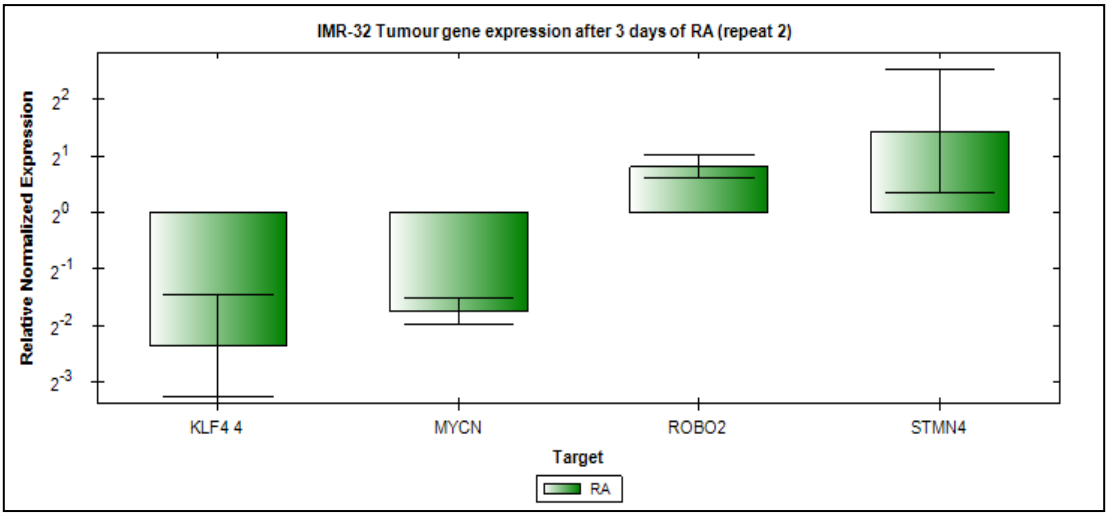

	KLF4	MYCN	ROBO2	STMN4
Adj NRQ	-5.15	-3.36	1.76	2.72
SD	1.25	0.0888	0.676	1.63
Regulation	Down regulated	Down regulated	No change	No change

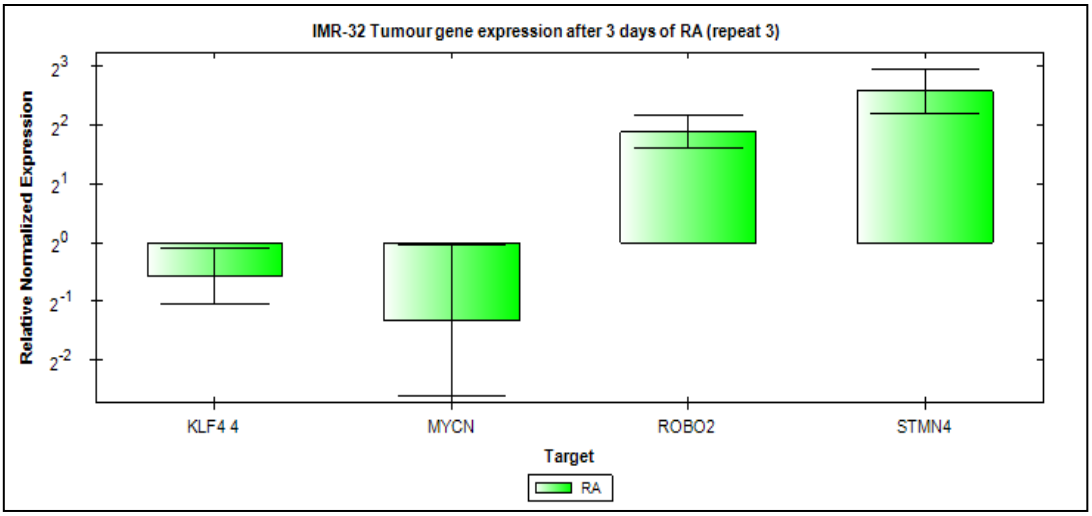

	KLF4	MYCN	ROBO2	STMN4
Adj NRQ	-1.49	-2.53	3.79	6.00
SD	0.464	1.98	0.453	0.822
Regulation	No change	No change	Up regulated	Up regulated

Figure 42 - RA in the chick embryo: a,c and e; graphs displaying the results of single qPCR experiment in IMR-32 tumours following 3 days of RA treatment. The error bars display the standard deviation (SD). B, D and F: tables providing a summary of the values obtained from the experiments. The adjusted normalised quantification (Adj NRQ) describes the actual change in the gene expression relative to the control. Regulation describes the overall statistically significant change in gene regulation.

Figure 43: BE(2)-C tumours treated with RA

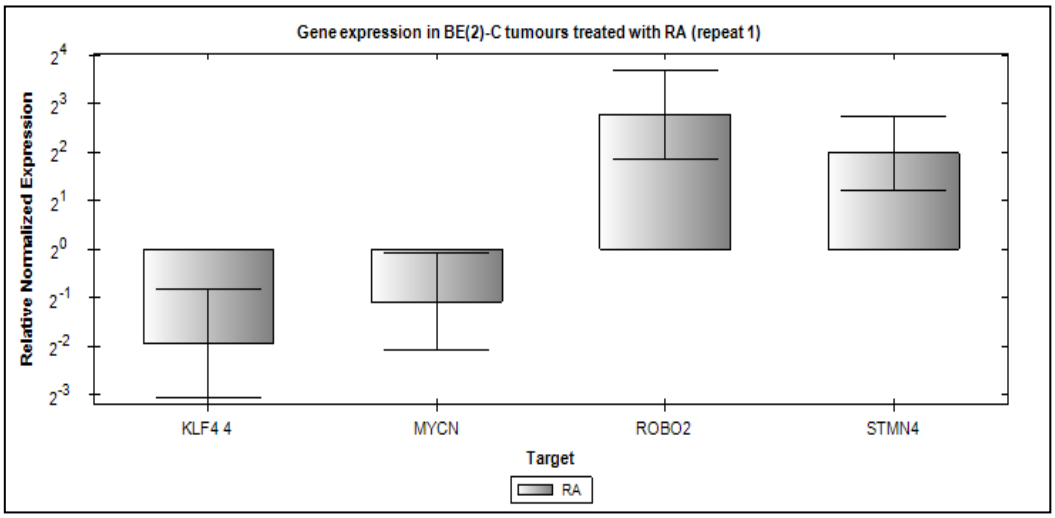

	KLF4	MYCN	ROBO2	STMN4
Adj NRQ	-3.85	-2.11	6.82	3.94
SD	0.315	0.473	2.17	2.70
Regulation	No change	No change	Up regulated	No change

	KLF4	MYCN	ROBO2	STMN4
Adj NRQ	-3.15	-1.79	5.02	5.34
SD	1.08	0.75	1.72	1.73
Regulation	No change	No change	Up regulated	Up regulated

	KLF4	MYCN	ROBO2	STMN4
Adj NRQ	-3.26	-2.24	5.64	5.24
SD	0.279	0.198	1.92	1.63
Regulation	No change	No change	Up regulated	Up regulated

Figure 43 - RA in the chick embryo: a,c and e; graphs displaying the results of single qPCR experiment in IMR-32 tumours following 3 days of RA treatment. The error bars display the standard deviation (SD). B, D and F: tables providing a summary of the values obtained from the experiments. The adjusted normalised quantification (Adj NRQ) describes the actual change in the gene expression relative to the control. Regulation describes the overall statistically significant change in gene regulation.

References

(!!! INVALID CITATION !!!).
Albanese, C., O. C. Rodriguez, J. VanMeter, S. T. Fricke, B. R. Rood, Y. Lee, S. S. Wang, S. Madhavan, Y. Gusev, E. F. Petricoin, 3rd and Y. Wang (2013). "Preclinical magnetic resonance imaging and systems biology in cancer research: current applications and challenges." Am J Pathol **182**(2): 312-318.
Alejandro Cruz, R., Tran, T.K, Holdeman, N.R , Cajavilca, C.a, Tang, R. (2013). "Horner's syndrome secondary to neuroblastoma." Clinical and Surgical Ophthalmology **31**(2): 55-58.
Alexander, F. (2000). "Neuroblastoma." Urol Clin North Am **27**(3): 383-392, vii.
Amatruda, T. T., 3rd, N. Sidell, J. Ranyard and H. P. Koeffler (1985). "Retinoic acid treatment of human neuroblastoma cells is associated with decreased N-myc expression." Biochem Biophys Res Commun **126**(3): 1189-1195.
Andres, D., B. M. Keyser, J. Petrali, B. Benton, K. S. Hubbard, P. M. McNutt and R. Ray (2013). "Morphological and functional differentiation in BE(2)-M17 human neuroblastoma cells by treatment with Trans-retinoic acid." BMC Neurosci **14**: 49.
Armstrong, P. B., J. P. Quigley and E. Sidebottom (1982). "Transepithelial invasion and intramesenchymal infiltration of the chick embryo chorioallantois by tumor cell lines." Cancer Res **42**(5): 1826-1837.
Asgharzadeh, S., R. Pique-Regi, R. Sposto, H. Wang, Y. Yang, H. Shimada, K. Matthay, J. Buckley, A. Ortega and R. C. Seeger (2006). "Prognostic significance of gene expression profiles of metastatic neuroblastomas lacking MYCN gene amplification." J Natl Cancer Inst **98**(17): 1193-1203.
Azar, W. J., S. H. Azar, S. Higgins, J. F. Hu, A. R. Hoffman, D. F. Newgreen, G. A. Werther and V. C. Russo (2011). "IGFBP-2 enhances VEGF gene promoter activity and consequent promotion of angiogenesis by neuroblastoma cells." Endocrinology **152**(9): 3332-3342.
Azarova, A. M., G. Gautam, R. E. George, A. M. Azarova, G. Gautam and R. E. George (2011). "Emerging importance of ALK in neuroblastoma." Seminars in Cancer Biology **21**(4): 267-275.
Azmi, A. (2014). "Rectifying cancer drug discovery through network pharmacology." Future Medicinal Chemistry **6**(5): 529-539.
Balciuniene, N., A. Tamasauskas, A. Valanciute, V. Deltuva, G. Vaitiekaitis, I. Gudinaviciene, J. Weis and D. G. von Keyserlingk (2009). "Histology of human glioblastoma transplanted on chicken chorioallantoic membrane." Medicina (Kaunas) **45**(2): 123-131.
Balke, M., A. Neumann, C. Kersting, K. Agelopoulos, C. Gebert, G. Gosheger, H. Buerger and M. Hagedorn (2010). "Morphologic characterization of osteosarcoma growth on the chick chorioallantoic membrane." BMC Res Notes **3**: 58.
Bayrak, O., I. Seckiner, S. Erturhan, A. Aydin and F. Yagci (2012). "Adult intrarenal neuroblastoma presenting as renal cell carcinoma." Can Urol Assoc J **6**(4): E144-146.
Berry, T., W. Luther, N. Bhatnagar, Y. Jamin, E. Poon, T. Sanda, D. Pei, B. Sharma, W. R. Vetharoy, A. Hallsworth, Z. Ahmad, K. Barker, L. Moreau, H. Webber, W. Wang, Q. Liu, A. Perez-Atayde, S. Rodig, N. K. Cheung, F. Raynaud, B. Hallberg, S. P. Robinson, N. S. Gray, A. D. Pearson, S. A. Eccles, L. Chesler and R. E. George (2012). "The ALK(F1174L) mutation potentiates the oncogenic activity of MYCN in neuroblastoma." Cancer Cell **22**(1): 117-130.
Bjornland, K., A. Bratland, E. Rugnes, S. Pettersen, H. T. Johansen, A. O. Aasen, O. Fodstad, A. H. Ree and G. M. Maelandsmo (2001). "Expression of matrix metalloproteinases and the

metastasis-associated gene S100A4 in human neuroblastoma and primitive neuroectodermal tumor cells." J Pediatr Surg **36**(7): 1040-1044.
Bourdeaut, F., D. Trochet, I. Janoueix-Lerosey, A. Ribeiro, A. Deville, C. Coz, J. F. Michiels, S. Lyonnet, J. Amiel and O. Delattre (2005). "Germline mutations of the paired-like homeobox 2B (PHOX2B) gene in neuroblastoma." Cancer Lett **228**(1-2): 51-58.
Brockmann, M., E. Poon, T. Berry, A. Carstensen, H. E. Deubzer, L. Rycak, Y. Jamin, K. Thway, S. P. Robinson, F. Roels, O. Witt, M. Fischer, L. Chesler and M. Eilers (2013). "Small Molecule Inhibitors of Aurora-A Induce Proteasomal Degradation of N-Myc in Childhood Neuroblastoma." Cancer Cell **24**(1): 75-89.
Brodeur, G. M., J. E. Minturn, R. Ho, A. M. Simpson, R. Iyer, C. R. Varela, J. E. Light, V. Kolla and A. E. Evans (2009). "Trk receptor expression and inhibition in neuroblastomas." Clin Cancer Res **15**(10): 3244-3250.
Brodeur, G. M., J. Pritchard, F. Berthold, N. L. Carlsen, V. Castel, R. P. Castelberry, B. De Bernardi, A. E. Evans, M. Favrot, F. Hedborg and et al. (1994). "Revisions of the international criteria for neuroblastoma diagnosis, staging and response to treatment." Prog Clin Biol Res **385**: 363-369.
Brodeur, G. M., R. C. Seeger, M. Schwab, H. E. Varmus and J. M. Bishop (1984). "Amplification of N-myc in untreated human neuroblastomas correlates with advanced disease stage." Science **224**(4653): 1121-1124.
Bronner, M. E. and N. M. LeDouarin (2012). "Development and evolution of the neural crest: an overview." Dev Biol **366**(1): 2-9.
Brose, K., K. S. Bland, K. H. Wang, D. Arnott, W. Henzel, C. S. Goodman, M. Tessier-Lavigne and T. Kidd (1999). "Slit proteins bind Robo receptors and have an evolutionarily conserved role in repulsive axon guidance." Cell **96**(6): 795-806.
Capecchi, M. R. (1989). "Altering the genome by homologous recombination." Science **244**(4910): 1288-1292.
Carachi, R. (2002). "Perspectives on neuroblastoma." Pediatr Surg Int **18**(5-6): 299-305.
Carpenter, E. L. and Y. P. Mossé (2012). "Targeting ALK in neuroblastoma-preclinical and clinical advancements." Nature Reviews Clinical Oncology **9**(7): 391-399.
Carrodeguas, J. A., A. Rodolosse, M. V. Garza, A. Sanz-Clemente, R. Perez-Pe, A. M. Lacosta, L. Dominguez, I. Monleon, R. Sanchez-Diaz, V. Sorribas and M. Sarasa (2005). "The chick embryo appears as a natural model for research in beta-amyloid precursor protein processing." Neuroscience **134**(4): 1285-1300.
Castel, V., V. Segura and P. Berlanga (2013). "Emerging drugs for neuroblastoma." Expert Opinion on Emerging Drugs **18**(2): 155-171.
Chanthery, Y. H., W. C. Gustafson, M. Itsara, A. Persson, C. S. Hackett, M. Grimmer, E. Charron, S. Yakovenko, G. Kim, K. K. Matthay, W. A. Weiss, Y. H. Chanthery, W. C. Gustafson, M. Itsara, A. Persson, C. S. Hackett, M. Grimmer, E. Charron, S. Yakovenko, G. Kim, K. K. Matthay and W. A. Weiss (2012). "Paracrine Signaling Through MYCN Enhances Tumor-Vascular Interactions in Neuroblastoma." Science Translational Medicine **4**(115): 115ra113.
Chesler, L., D. D. Goldenberg, R. Collins, M. Grimmer, G. E. Kim, T. Tihan, K. Nguyen, S. Yakovenko, K. K. Matthay and W. A. Weiss (2008). "Chemotherapy-induced apoptosis in a transgenic model of neuroblastoma proceeds through p53 induction." Neoplasia **10**(11): 1268-1274.
Chesler, L., D. D. Goldenberg, I. T. Seales, R. Satchi-Fainaro, M. Grimmer, R. Collins, C. Struett, K. N. Nguyen, G. Kim, T. Tihan, Y. Bao, R. A. Brekken, G. Bergers, J. Folkman and W.

A. Weiss (2007). "Malignant progression and blockade of angiogenesis in a murine transgenic model of neuroblastoma." Cancer Res **67**(19): 9435-9442.
Chesler, L. and W. A. Weiss (2011). "Genetically engineered murine models--contribution to our understanding of the genetics, molecular pathology and therapeutic targeting of neuroblastoma." Semin Cancer Biol **21**(4): 245-255.
Cheung, N. K. V. and M. A. Dyer (2013). "Neuroblastoma: Developmental biology, cancer genomics and immunotherapy." Nature Reviews Cancer **13**(6): 397-411.
Chiu, F. C., L. Feng, S. O. Chan, C. Padin and J. H. Federoff (1995). "Expression of neurofilament proteins during retinoic acid-induced differentiation of P19 embryonal carcinoma cells." Brain Res Mol Brain Res **30**(1): 77-86.
Choi, Y. P., J. H. Lee, M. Q. Gao, B. G. Kim, S. Kang, S. H. Kim and N. H. Cho (2014). "Cancer-associated fibroblast promote transmigration through endothelial brain cells in three-dimensional in vitro models." Int J Cancer.
Chu, P. W., W. M. Cheung and Y. L. Kwong (2003). "Differential effects of 9-cis, 13-cis and all-trans retinoic acids on the neuronal differentiation of human neuroblastoma cells." Neuroreport **14**(15): 1935-1939.
Claviez, A., M. Lakomek, J. Ritter, M. Suttorp, B. Kremens, R. Dickerhoff, D. Harms, F. Berthold and B. Hero (2004). "Low occurrence of familial neuroblastomas and ganglioneuromas in five consecutive GPOH neuroblastoma treatment studies." Eur J Cancer **40**(18): 2760-2765.
Corvi, R., L. C. Amler, L. Savelyeva, M. Gehring and M. Schwab (1994). "MYCN is retained in single copy at chromosome 2 band p23-24 during amplification in human neuroblastoma cells." Proc Natl Acad Sci U S A **91**(12): 5523-5527.
Cotterman, R. and P. S. Knoepfler (2009). "N-Myc regulates expression of pluripotency genes in neuroblastoma including lif, klf2, klf4, and lin28b." PLoS One **4**(6): e5799.
D'Orazio, J. A. (2010). "Inherited cancer syndromes in children and young adults." J Pediatr Hematol Oncol **32**(3): 195-228.
Davenport, K. P., F. C. Blanco and A. D. Sandler (2012). "Pediatric malignancies: neuroblastoma, Wilm's tumor, hepatoblastoma, rhabdomyosarcoma, and sacroccygeal teratoma." Surg Clin North Am **92**(3): 745-767, x.
De Preter, K., J. Vermeulen, B. Brors, O. Delattre, A. Eggert, M. Fischer, I. Janoueix-Lerosey, C. Lavarino, J. M. Maris, J. Mora, A. Nakagawara, A. Oberthuer, M. Ohira, G. Schleiermacher, A. Schramm, J. H. Schulte, Q. Wang, F. Westermann, F. Speleman and J. Vandesompele (2010). "Accurate outcome prediction in neuroblastoma across independent data sets using a multigene signature." Clin Cancer Res **16**(5): 1532-1541.
Deryugina, E. I. and J. P. Quigley (2008). "Chapter 2. Chick embryo chorioallantoic membrane models to quantify angiogenesis induced by inflammatory and tumor cells or purified effector molecules." Methods Enzymol **444**: 21-41.
Devine, C. A. and B. Key (2008). "Robo-Slit interactions regulate longitudinal axon pathfinding in the embryonic vertebrate brain." Dev Biol **313**(1): 371-383.
Domingo-Fernandez, R., K. Watters, O. Piskareva, R. L. Stallings and I. Bray (2013). "The role of genetic and epigenetic alterations in neuroblastoma disease pathogenesis." Pediatr Surg Int **29**(2): 101-119.
Du, W., N. Hozumi, M. Sakamoto, J. Hata and T. Yamada (2008). "Reconstitution of Schwannian stroma in neuroblastomas using human bone marrow stromal cells." Am J Pathol **173**(4): 1153-1164.

DuBois, S. G., Y. Kalika, J. N. Lukens, G. M. Brodeur, R. C. Seeger, J. B. Atkinson, G. M. Haase, C. T. Black, C. Perez, H. Shimada, R. Gerbing, D. O. Stram and K. K. Matthay (1999). "Metastatic sites in stage IV and IVS neuroblastoma correlate with age, tumor biology, and survival." J Pediatr Hematol Oncol **21**(3): 181-189.
EE, L. (1997). Tumors of the adrenal gland and extra-adrenal paraganglia. Washington DC, Armed Forces Institute of Pathology.
EE, L. (2007). Tumors of the autonomic nervous system (including paraganglia), Elsevier Limited.
EMA. "European Medicines Agency "Better medicines for children"." Retrieved 18th April, 2014, from http://www.ema.europa.eu/docs/en_GB/document_library/Other/2009/12/WC500026493.pdf.
Engler, S., C. Thiel, K. Forster, K. David, R. Bredehorst and H. Juhl (2001). "A novel metastatic animal model reflecting the clinical appearance of human neuroblastoma: growth arrest of orthotopic tumors by natural, cytotoxic human immunoglobulin M antibodies." Cancer Res **61**(7): 2968-2973.
Esiashvili, N., M. Goodman, K. Ward, R. B. Marcus, Jr. and P. A. Johnstone (2007). "Neuroblastoma in adults: Incidence and survival analysis based on SEER data." Pediatr Blood Cancer **49**(1): 41-46.
Faria, A. M. and M. Q. Almeida (2012). "Differences in the molecular mechanisms of adrenocortical tumorigenesis between children and adults." Mol Cell Endocrinol **351**(1): 52-57.
Fergelot, P., J. C. Bernhard, F. Soulet, W. W. Kilarski, C. Leon, N. Courtois, C. Deminiere, J. M. Herbert, P. Antczak, F. Falciani, N. Rioux-Leclercq, J. J. Patard, J. M. Ferriere, A. Ravaud, M. Hagedorn and A. Bikfalvi (2013). "The experimental renal cell carcinoma model in the chick embryo." Angiogenesis **16**(1): 181-194.
Fisher, J. P. and D. A. Tweddle (2012). "Neonatal neuroblastoma." Semin Fetal Neonatal Med **17**(4): 207-215.
Fishman, M. C. and J. A. Porter (2005). "Pharmaceuticals: a new grammar for drug discovery." Nature **437**(7058): 491-493.
Frese, K. K. and D. A. Tuveson (2007). "Maximizing mouse cancer models." Nat Rev Cancer **7**(9): 645-658.
Gabrielli, M. G. and D. Accili (2010). "The chick chorioallantoic membrane: a model of molecular, structural, and functional adaptation to transepithelial ion transport and barrier function during embryonic development." J Biomed Biotechnol **2010**: 940741.
Gadea, B. B., J. A. Joyce, B. B. Gadea and J. A. Joyce (2006). "Tumour–host interactions: implications for developing anti-cancer therapies." Expert Reviews in Molecular Medicine **8**(30): 1-32.
Gammill, L. S. and M. Bronner-Fraser (2003). "Neural crest specification: migrating into genomics." Nat Rev Neurosci **4**(10): 795-805.
George, R. E., T. Sanda, M. Hanna, S. Fröhling, W. Luther Ii, J. Zhang, Y. Ahn, W. Zhou, W. B. London, P. McGrady, L. Xue, S. Zozulya, V. E. Gregor, T. R. Webb, N. S. Gray, D. G. Gilliland, L. Diller, H. Greulich, S. W. Morris, M. Meyerson and A. T. Look (2008). "Activating mutations in ALK provide a therapeutic target in neuroblastoma." Nature **455**(7215): 975-978.
Gherardi, S., E. Valli, D. Erriquez and G. Perini (2013). "MYCN-mediated transcriptional repression in neuroblastoma: the other side of the coin." Front Oncol **3**: 42.

Gordon, J. W. and F. H. Ruddle (1981). "Integration and stable germ line transmission of genes injected into mouse pronuclei." Science **214**(4526): 1244-1246.
Grenningloh, G., S. Soehrman, P. Bondallaz, E. Ruchti and H. Cadas (2004). "Role of the microtubule destabilizing proteins SCG10 and stathmin in neuronal growth." J Neurobiol **58**(1): 60-69.
Guglielmi, L., C. Cinnella, M. Nardella, G. Maresca, A. Valentini, D. Mercanti, A. Felsani and I. D'Agnano (2014). "MYCN gene expression is required for the onset of the differentiation programme in neuroblastoma cells." Cell Death Dis **5**: e1081.
Gurcan, M. "Neuroblastoma." Retrieved 23rd April, 2014, from http://bmi.osu.edu/~gurcan/neuroblastoma.php.
Guthrie, S. (2004). "Axon guidance: mice and men need Rig and Robo." Curr Biol **14**(15): R632-634.
Hagedorn, M., S. Javerzat, D. Gilges, A. Meyre, B. de Lafarge, A. Eichmann and A. Bikfalvi (2005). "Accessing key steps of human tumor progression in vivo by using an avian embryo model." Proc Natl Acad Sci U S A **102**(5): 1643-1648.
Hagedorn, M., S. Javerzat, D. Gilges, A. Meyre, eacute, lie, B. de Lafarge, A. Eichmann, A. Bikfalvi, M. Hagedorn, S. Javerzat, D. Gilges, A. Meyre, B. de Lafarge, A. Eichmann and A. Bikfalvi (2005). "Accessing key steps of human tumor progression in vivo by using an avian embryo model." Proceedings of the National Academy of Sciences **102**(5): 1643-1648.
Hamburger, V. and H. L. Hamilton (1951). "A series of normal stages in the development of the chick embryo." J Morphol **88**(1): 49-92.
Health, U. S. N. I. o. (2014). "Study of MLN8237 in Combination With Irinotecan and Temozolomide." Retrieved 23rd April, 2014, from http://clinicaltrials.gov/ct2/show/NCT01601535.
Heck, J. E., B. Ritz, R. J. Hung, M. Hashibe and P. Boffetta (2009). "The epidemiology of neuroblastoma: a review." Paediatr Perinat Epidemiol **23**(2): 125-143.
Hildebrandt, T. and H. Traunecker (2005). "Neuroblastoma: A tumour with many faces." Current Paediatrics **15**(5): 412-420.
Hima Vangapandu, W. A. (2009). "Kruppel like factor 4 (KLF4): A transcription factor with diverse context-dependent functions." Gene therapy and molecular biology **13**(1): 194-203.
Hogarty, M. D., M. D. Norris, K. Davis, X. Liu, N. F. Evageliou, C. S. Hayes, B. Pawel, R. Guo, H. Zhao, E. Sekyere, J. Keating, W. Thomas, N. C. Cheng, J. Murray, J. Smith, R. Sutton, N. Venn, W. B. London, A. Buxton, S. K. Gilmour, G. M. Marshall and M. Haber (2008). "ODC1 is a critical determinant of MYCN oncogenesis and a therapeutic target in neuroblastoma." Cancer Res **68**(23): 9735-9745.
Houghton, P. J., C. L. Morton, C. Tucker, D. Payne, E. Favours, C. Cole, R. Gorlick, E. A. Kolb, W. Zhang, R. Lock, H. Carol, M. Tajbakhsh, C. P. Reynolds, J. M. Maris, J. Courtright, S. T. Keir, H. S. Friedman, C. Stopford, J. Zeidner, J. Wu, T. Liu, C. A. Billups, J. Khan, S. Ansher, J. Zhang and M. A. Smith (2007). "The pediatric preclinical testing program: description of models and early testing results." Pediatr Blood Cancer **49**(7): 928-940.
Huber, K., S. Combs, U. Ernsberger, C. Kalcheim and K. Unsicker (2002). "Generation of neuroendocrine chromaffin cells from sympathoadrenal progenitors: beyond the glucocorticoid hypothesis." Ann N Y Acad Sci **971**: 554-559.
Hughes, J. P., S. Rees, S. B. Kalindjian and K. L. Philpott (2011). "Principles of early drug discovery." Br J Pharmacol **162**(6): 1239-1249.
Ikeda, H., T. Iehara, Y. Tsuchida, M. Kaneko, J. Hata, H. Naito, M. Iwafuchi, N. Ohnuma, H. Mugishima, Y. Toyoda, M. Hamazaki, J. Mimaya, S. Kondo, K. Kawa, A. Okada, E. Hiyama, S.

Suita and H. Takamatsu (2002). "Experience with International Neuroblastoma Staging System and Pathology Classification." Br J Cancer **86**(7): 1110-1116.
Institute, N. C. (2014). "Neuroblastoma Staging." Retrieved 22nd July, 2014, from http://www.cancer.gov/cancertopics/pdq/treatment/neuroblastoma/HealthProfessional/page3.
ITCC. "Innovative Therapies for Children with Cancer (ITCC) European Consortium." from http://www.itcc-consortium.org.
Izbicki, T., J. Mazur and E. Izbicka (2003). "Epidemiology and etiology of neuroblastoma: an overview." Anticancer Res **23**(1B): 755-760.
Janoueix-Lerosey, I., G. Schleiermacher, E. Michels, V. Mosseri, A. Ribeiro, D. Lequin, J. Vermeulen, J. Couturier, M. Peuchmaur, A. Valent, D. Plantaz, H. Rubie, D. Valteau-Couanet, C. Thomas, V. Combaret, R. Rousseau, A. Eggert, J. Michon, F. Speleman and O. Delattre (2009). "Overall genomic pattern is a predictor of outcome in neuroblastoma." Journal of Clinical Oncology **27**(7): 1026-1033.
Jorge Mestre-Ferrandiz, J. S. a. A. T. (2012). "The R&D Cost of a New Medicine." London: Office of health economics.
Joshi, V. V. (2000). "Peripheral neuroblastic tumors: pathologic classification based on recommendations of international neuroblastoma pathology committee (Modification of shimada classification)." Pediatr Dev Pathol **3**(2): 184-199.
Kain, K. H., J. W. Miller, C. R. Jones-Paris, R. T. Thomason, J. D. Lewis, D. M. Bader, J. V. Barnett and A. Zijlstra (2014). "The chick embryo as an expanding experimental model for cancer and cardiovascular research." Dev Dyn **243**(2): 216-228.
Kallioniemi, A., O. P. Kallioniemi, J. Piper, M. Tanner, T. Stokke, L. Chen, H. S. Smith, D. Pinkel, J. W. Gray and F. M. Waldman (1994). "Detection and mapping of amplified DNA sequences in breast cancer by comparative genomic hybridization." Proc Natl Acad Sci U S A **91**(6): 2156-2160.
Kamijo, T. and A. Nakagawara (2012). "Molecular and genetic bases of neuroblastoma." Int J Clin Oncol **17**(3): 190-195.
Kaplan, D. R., K. Matsumoto, E. Lucarelli and C. J. Thiele (1993). "Induction of TrkB by retinoic acid mediates biologic responsiveness to BDNF and differentiation of human neuroblastoma cells. Eukaryotic Signal Transduction Group." Neuron **11**(2): 321-331.
Katz, L. H., Y. Li, J. S. Chen, N. M. Munoz, A. Majumdar, J. Chen and L. Mishra (2013). "Targeting TGF-beta signaling in cancer." Expert Opin Ther Targets **17**(7): 743-760.
Kearns, P. and B. Morland (2014). "New drug development in childhood cancer." Curr Opin Pediatr **26**(1): 37-42.
Kelland, L. R. (2004). "Of mice and men: values and liabilities of the athymic nude mouse model in anticancer drug development." Eur J Cancer **40**(6): 827-836.
Kelly, K. R., J. Ecsedy, D. Mahalingam, S. T. Nawrocki, S. Padmanabhan, F. J. Giles and J. S. Carew (2011). "Targeting aurora kinases in cancer treatment." Curr Drug Targets **12**(14): 2067-2078.
Khanna, C., J. J. Jaboin, E. Drakos, M. Tsokos and C. J. Thiele (2002). "Biologically relevant orthotopic neuroblastoma xenograft models: primary adrenal tumor growth and spontaneous distant metastasis." In Vivo **16**(2): 77-85.
Khleif SN, C. G. (2000). Animal Models in Developmental Therapeutics.
Kim, S. and D. H. Chung (2006). "Pediatric solid malignancies: neuroblastoma and Wilms' tumor." Surg Clin North Am **86**(2): 469-487, xi.

Klingenberg, M. (2014). "The chick chorioallantoic membrane as an in vivo xenograft model for Burkitt lymphoma." BMC Cancer: 339.
Kobayashi, T., K. Koshida, Y. Endo, T. Imao, T. Uchibayashi, T. Sasaki and M. Namiki (1998). "A chick embryo model for metastatic human prostate cancer." Eur Urol **34**(2): 154-160.
Korecka, J. A., R. E. van Kesteren, E. Blaas, S. O. Spitzer, J. H. Kamstra, A. B. Smit, D. F. Swaab, J. Verhaagen and K. Bossers (2013). "Phenotypic characterization of retinoic acid differentiated SH-SY5Y cells by transcriptional profiling." PLoS One **8**(5): e63862.
Korshunov, A., M. Remke, W. Werft, A. Benner, M. Ryzhova, H. Witt, D. Sturm, A. Wittmann, A. Schottler, J. Felsberg, G. Reifenberger, S. Rutkowski, W. Scheurlen, A. E. Kulozik, A. von Deimling, P. Lichter and S. M. Pfister (2010). "Adult and pediatric medulloblastomas are genetically distinct and require different algorithms for molecular risk stratification." J Clin Oncol **28**(18): 3054-3060.
Kruczynski, A., G. Delsol, C. Laurent, P. Brousset and L. Lamant (2012). "Anaplastic lymphoma kinase as a therapeutic target." Expert Opinion on Therapeutic Targets **16**(11): 1127-1138.
Kumar, H. R., X. Zhong, D. J. Hoelz, F. J. Rescorla, R. J. Hickey, L. H. Malkas and J. A. Sandoval (2008). "Three-dimensional neuroblastoma cell culture: Proteomic analysis between monolayer and multicellular tumor spheroids." Pediatric Surgery International **24**(11): 1229-1234.
Kumar, S., R. B. Mokhtari, H. Yeger and S. Baruchel (2012). "Preclinical models for pediatric solid tumor drug discovery: current trends, challenges and the scopes for improvement." Expert Opin Drug Discov **7**(11): 1093-1106.
Kurosawa, G., Y. Akahori, M. Morita, M. Sumitomo, N. Sato, C. Muramatsu, K. Eguchi, K. Matsuda, A. Takasaki, M. Tanaka, Y. Iba, S. Hamada-Tsutsumi, Y. Ukai, M. Shiraishi, K. Suzuki, M. Kurosawa, S. Fujiyama, N. Takahashi, R. Kato, Y. Mizoguchi, M. Shamoto, H. Tsuda, M. Sugiura, Y. Hattori, S. Miyakawa, R. Shiroki, K. Hoshinaga, N. Hayashi, A. Sugioka and Y. Kurosawa (2008). "Comprehensive screening for antigens overexpressed on carcinomas via isolation of human mAbs that may be therapeutic." Proc Natl Acad Sci U S A **105**(20): 7287-7292.
Laverdiere, C., Q. Liu, Y. Yasui, P. C. Nathan, J. G. Gurney, M. Stovall, L. R. Diller, N. K. Cheung, S. Wolden, L. L. Robison and C. A. Sklar (2009). "Long-term outcomes in survivors of neuroblastoma: a report from the Childhood Cancer Survivor Study." J Natl Cancer Inst **101**(16): 1131-1140.
Lin, J., Y. Chen, L. Wei, Z. Hong, T. J. Sferra and J. Peng (2013). "Ursolic acid inhibits colorectal cancer angiogenesis through suppression of multiple signaling pathways." Int J Oncol **43**(5): 1666-1674.
Lokman, N. A., A. S. Elder, C. Ricciardelli and M. K. Oehler (2012). "Chick Chorioallantoic Membrane (CAM) Assay as an In Vivo Model to Study the Effect of Newly Identified Molecules on Ovarian Cancer Invasion and Metastasis." Int J Mol Sci **13**(8): 9959-9970.
London, W. B., V. Castel, T. Monclair, P. F. Ambros, A. D. Pearson, S. L. Cohn, F. Berthold, A. Nakagawara, R. L. Ladenstein, T. Iehara and K. K. Matthay (2011). "Clinical and biologic features predictive of survival after relapse of neuroblastoma: a report from the International Neuroblastoma Risk Group project." J Clin Oncol **29**(24): 3286-3292.
Long, H., C. Sabatier, L. Ma, A. Plump, W. Yuan, D. M. Ornitz, A. Tamada, F. Murakami, C. S. Goodman and M. Tessier-Lavigne (2004). "Conserved roles for Slit and Robo proteins in midline commissural axon guidance." Neuron **42**(2): 213-223.

Lopez-Carballo, G., L. Moreno, S. Masia, P. Perez and D. Barettino (2002). "Activation of the phosphatidylinositol 3-kinase/Akt signaling pathway by retinoic acid is required for neural differentiation of SH-SY5Y human neuroblastoma cells." J Biol Chem **277**(28): 25297-25304.
Malakho, S. G., A. Korshunov, A. M. Stroganova and A. B. Poltaraus (2008). "Fast detection of MYCN copy number alterations in brain neuronal tumors by real-time PCR." J Clin Lab Anal **22**(2): 123-130.
Mangieri, D., B. Nico, A. M. Coluccia, A. Vacca, M. Ponzoni and D. Ribatti (2009). "An alternative in vivo system for testing angiogenic potential of human neuroblastoma cells." Cancer Lett **277**(2): 199-204.
Marill, J., N. Idres, C. C. Capron, E. Nguyen and G. G. Chabot (2003). "Retinoic acid metabolism and mechanism of action: a review." Curr Drug Metab **4**(1): 1-10.
Marimpietri, D., C. Brignole, B. Nico, F. Pastorino, A. Pezzolo, F. Piccardi, M. Cilli, D. Di Paolo, G. Pagnan, L. Longo, P. Perri, D. Ribatti and M. Ponzoni (2007). "Combined therapeutic effects of vinblastine and rapamycin on human neuroblastoma growth, apoptosis, and angiogenesis." Clin Cancer Res **13**(13): 3977-3988.
Maris, J. M., M. D. Hogarty, R. Bagatell and S. L. Cohn (2007). "Neuroblastoma." Lancet **369**(9579): 2106-2120.
Maris, J. M. and K. K. Matthay (1999). "Molecular biology of neuroblastoma." J Clin Oncol **17**(7): 2264-2279.
Mason, I. (2008). "The avian embryo: an overview." Methods Mol Biol **461**: 223-230.
Matthay, K. K., C. P. Reynolds, R. C. Seeger, H. Shimada, E. S. Adkins, D. Haas-Kogan, R. B. Gerbing, W. B. London and J. G. Villablanca (2009). "Long-term results for children with high-risk neuroblastoma treated on a randomized trial of myeloablative therapy followed by 13-cis-retinoic acid: a children's oncology group study." J Clin Oncol **27**(7): 1007-1013.
Matthay, K. K., J. G. Villablanca, R. C. Seeger, D. O. Stram, R. E. Harris, N. K. Ramsay, P. Swift, H. Shimada, C. T. Black, G. M. Brodeur, R. B. Gerbing and C. P. Reynolds (1999). "Treatment of high-risk neuroblastoma with intensive chemotherapy, radiotherapy, autologous bone marrow transplantation, and 13-cis-retinoic acid. Children's Cancer Group." N Engl J Med **341**(16): 1165-1173.
Mazur, K. A. (2010). "Neuroblastoma: What the nurse practitioner should know." J Am Acad Nurse Pract **22**(5): 236-245.
Mccartney, A. (2013). "From Amphibians to Amniotes." Retrieved 19th October, 2014, from http://annmccartneyblog.com/2013/01/23/from-amphibians-to-amniotes/.
Minchinton, A. I. and I. F. Tannock (2006). "Drug penetration in solid tumours." Nat Rev Cancer **6**(8): 583-592.
Miranda Soares, P. B., S. Quirino Filho, D. E. S. W. Pereira, P. R. Ferreti Bonan and H. Martelli-Junior (2010). "Neuroblastoma in an adult: case report." Rev Med Chil **138**(9): 1131-1134.
Molenaar, J. J., J. Koster, D. A. Zwijnenburg, P. Van Sluis, L. J. Valentijn, I. Van Der Ploeg, M. Hamdi, J. Van Nes, B. A. Westerman, J. Van Arkel, M. E. Ebus, F. Haneveld, A. Lakeman, L. Schild, P. Molenaar, P. Stroeken, M. M. Van Noesel, I. Øra, E. E. Santo, H. N. Caron, E. M. Westerhout and R. Versteeg (2012). "Sequencing of neuroblastoma identifies chromothripsis and defects in neuritogenesis genes." Nature **483**(7391): 589-593.
Monclair, T., G. M. Brodeur, P. F. Ambros, H. J. Brisse, G. Cecchetto, K. Holmes, M. Kaneko, W. B. London, K. K. Matthay, J. G. Nuchtern, D. von Schweinitz, T. Simon, S. L. Cohn, A. D. Pearson and I. T. Force (2009). "The International Neuroblastoma Risk Group (INRG) staging system: an INRG Task Force report." J Clin Oncol **27**(2): 298-303.

Moreno, L., L. Chesler, D. Hargrave, S. A. Eccles and A. D. Pearson (2011). "Preclinical drug development for childhood cancer." Expert Opin Drug Discov **6**(1): 49-64.
Morgenstern, D. A., S. Baruchel and M. S. Irwin (2013). "Current and future strategies for relapsed neuroblastoma: Challenges on the road to precision therapy." Journal of Pediatric Hematology/Oncology **35**(5): 337-347.
Mosse, Y. P., M. Laudenslager, D. Khazi, A. J. Carlisle, C. L. Winter, E. Rappaport and J. M. Maris (2004). "Germline PHOX2B mutation in hereditary neuroblastoma." Am J Hum Genet **75**(4): 727-730.
Mossé, Y. P., A. Wood and J. M. Maris (2009). "Inhibition of ALK signaling for cancer therapy." Clinical Cancer Research **15**(18): 5609-5614.
Mullassery, D., C. Dominici, E. C. Jesudason, H. P. McDowell and P. D. Losty (2009). "Neuroblastoma: contemporary management." Arch Dis Child Educ Pract Ed **94**(6): 177-185.
Murphy, J. B. (1916). "The Effect of Adult Chicken Organ Grafts on the Chick Embryo." J Exp Med **24**(1): 1-5.
Nakagawara, A. (2001). "Trk receptor tyrosine kinases: a bridge between cancer and neural development." Cancer Lett **169**(2): 107-114.
Nakagawara, A. (2004). "Neural crest development and neuroblastoma: the genetic and biological link." Prog Brain Res **146**: 233-242.
NCI. "Mouse Cancer Models." Retrieved 11th April, 2014, from http://emice.nci.nih.gov/aam/mouse.
NCI. "National Cancer Institute, Generating Models, Genetic Modifications." Retrieved 18th April, 2014, from http://emice.nci.nih.gov/generating-models/mouse-cancer-models-1/genetic-modifications.
NCI. "National Cancer Institute, Neuroblastoma." Retrieved 21st April, 2014, from http://www.cancer.gov/cancertopics/pdq/treatment/neuroblastoma/HealthProfessional#Reference1.46.
NCI. "Pediatric preclinical testin programme." Retrieved 18th June, 2014, from http://pptp.nchresearch.org/documents/PPTPOverview.pdf.
Noujaim, D., C. M. van Golen, K. L. van Golen, A. Grauman and E. L. Feldman (2002). "N-Myc and Bcl-2 coexpression induces MMP-2 secretion and activation in human neuroblastoma cells." Oncogene **21**(29): 4549-4557.
Ohtaki, Y., G. Ishii, T. Hasegawa and K. Nagai (2011). "Adult neuroblastoma arising in the superior mediastinum." Interact Cardiovasc Thorac Surg **13**(2): 220-222.
OLPA, U. S. O. o. L. P. a. A. "Pharmaceuticals for Children Act, Public Law 107-109." from http://olpa.od.nih.gov/legislation/107/publiclaws/1best.asp.
Otto, T., S. Horn, M. Brockmann, U. Eilers, L. Schuttrumpf, N. Popov, A. M. Kenney, J. H. Schulte, R. Beijersbergen, H. Christiansen, B. Berwanger and M. Eilers (2009). "Stabilization of N-Myc is a critical function of Aurora A in human neuroblastoma." Cancer Cell **15**(1): 67-78.
Ozcetin, A., A. Aigner and U. Bakowsky (2013). "A chorioallantoic membrane model for the determination of anti-angiogenic effects of imatinib." Eur J Pharm Biopharm **85**(3 Pt A): 711-715.
Palmer, T. D., J. Lewis and A. Zijlstra (2011). "Quantitative analysis of cancer metastasis using an avian embryo model." J Vis Exp(51).
Park, J. R., R. Bagatell, W. B. London, J. M. Maris, S. L. Cohn, K. M. Mattay and M. Hogarty (2013). "Children's Oncology Group's 2013 blueprint for research: Neuroblastoma." Pediatric Blood and Cancer **60**(6): 985-993.

Paugh, B. S., C. Qu, C. Jones, Z. Liu, M. Adamowicz-Brice, J. Zhang, D. A. Bax, B. Coyle, J. Barrow, D. Hargrave, J. Lowe, A. Gajjar, W. Zhao, A. Broniscer, D. W. Ellison, R. G. Grundy and S. J. Baker (2010). "Integrated molecular genetic profiling of pediatric high-grade gliomas reveals key differences with the adult disease." J Clin Oncol **28**(18): 3061-3068.
Paul, S. M., D. S. Mytelka, C. T. Dunwiddie, C. C. Persinger, B. H. Munos, S. R. Lindborg and A. L. Schacht (2010). "How to improve RD productivity: The pharmaceutical industry's grand challenge." Nature Reviews Drug Discovery **9**(3): 203-214.
Pei, D., W. Luther, W. Wang, B. H. Paw, R. A. Stewart and R. E. George (2013). "Distinct neuroblastoma-associated alterations of PHOX2B impair sympathetic neuronal differentiation in zebrafish models." PLoS Genet **9**(6): e1003533.
Peterson, J. K. and P. J. Houghton (2004). "Integrating pharmacology and in vivo cancer models in preclinical and clinical drug development." Eur J Cancer **40**(6): 837-844.
Puaux, A. L., L. C. Ong, Y. Jin, I. Teh, M. Hong, P. K. Chow, X. Golay and J. P. Abastado (2011). "A comparison of imaging techniques to monitor tumor growth and cancer progression in living animals." Int J Mol Imaging **2011**: 321538.
Reynolds, C. P., D. J. Kane, P. A. Einhorn, K. K. Matthay, V. L. Crouse, J. R. Wilbur, S. B. Shurin and R. C. Seeger (1991). "Response of neuroblastoma to retinoic acid in vitro and in vivo." Prog Clin Biol Res **366**: 203-211.
Ribatti, D., B. Nico, A. Vacca, L. Roncali, P. H. Burri and V. Djonov (2001). "Chorioallantoic membrane capillary bed: a useful target for studying angiogenesis and anti-angiogenesis in vivo." Anat Rec **264**(4): 317-324.
Ribatti, D., A. Vacca, L. Roncali and F. Dammacco (1996). "The chick embryo chorioallantoic membrane as a model for in vivo research on angiogenesis." Int J Dev Biol **40**(6): 1189-1197.
Rice, M. (2013). "The Roles of Hypoxia on Neuroblastoma Cell Migration and Invasion."
Richmond, A. and Y. Su (2008). "Mouse xenograft models vs GEM models for human cancer therapeutics." Dis Model Mech **1**(2-3): 78-82.
Roskoski Jr, R. (2013). "Anaplastic lymphoma kinase (ALK): Structure, oncogenic activation, and pharmacological inhibition." Pharmacological Research **68**(1): 68-94.
Rounbehler, R. J., W. Li, M. A. Hall, C. Yang, M. Fallahi and J. L. Cleveland (2009). "Targeting ornithine decarboxylase impairs development of MYCN-amplified neuroblastoma." Cancer Res **69**(2): 547-553.
Rubie, H., O. Hartmann, J. Michon, D. Frappaz, C. Coze, P. Chastagner, M. C. Baranzelli, D. Plantaz, H. Avet-Loiseau, J. Benard, O. Delattre, M. Favrot, M. C. Peyroulet, A. Thyss, Y. Perel, C. Bergeron, B. Courbon-Collet, J. P. Vannier, J. Lemerle and D. Sommelet (1997). "N-Myc gene amplification is a major prognostic factor in localized neuroblastoma: results of the French NBL 90 study. Neuroblastoma Study Group of the Societe Francaise d'Oncologie Pediatrique." J Clin Oncol **15**(3): 1171-1182.
Ruggeri, B. A., F. Camp and S. Miknyoczki (2014). "Animal models of disease: pre-clinical animal models of cancer and their applications and utility in drug discovery." Biochem Pharmacol **87**(1): 150-161.
Sandberg, D. I., M. H. Bilsky, B. H. Kushner, M. M. Souweidane, K. Kramer, M. P. Laquaglia, K. S. Panageas and N. K. Cheung (2003). "Treatment of spinal involvement in neuroblastoma patients." Pediatr Neurosurg **39**(6): 291-298.
Sasaki, T., K. Okuda, W. Zheng, J. Butrynski, M. Capelletti, L. Wang, N. S. Gray, K. Wilner, J. G. Christensen, G. Demetri, G. I. Shapiro, S. J. Rodig, M. J. Eck and P. A. Janne (2010). "The Neuroblastoma-Associated F1174L ALK Mutation Causes Resistance to an ALK Kinase Inhibitor in ALK-Translocated Cancers." Cancer Research **70**(24): 10038-10043.

Scala, S., K. Wosikowski, P. Giannakakou, P. Valle, J. L. Biedler, B. A. Spengler, E. Lucarelli, S. E. Bates and C. J. Thiele (1996). "Brain-derived neurotrophic factor protects neuroblastoma cells from vinblastine toxicity." Cancer Res **56**(16): 3737-3742.
Schilling, F. H., C. Spix, F. Berthold, R. Erttmann, N. Fehse, B. Hero, G. Klein, J. Sander, K. Schwarz, J. Treuner, U. Zorn and J. Michaelis (2002). "Neuroblastoma screening at one year of age." N Engl J Med **346**(14): 1047-1053.
Schlegel, J., G. Stumm, H. Scherthan, T. Bocker, H. Zirngibl, J. Ruschoff and F. Hofstadter (1995). "Comparative genomic in situ hybridization of colon carcinomas with replication error." Cancer Res **55**(24): 6002-6005.
Schönherr, C., K. Ruuth, S. Kamaraj, C. L. Wang, H. L. Yang, V. Combaret, A. Djos, T. Martinsson, J. G. Christensen, R. H. Palmer and B. Hallberg (2012). "Anaplastic Lymphoma Kinase (ALK) regulates initiation of transcription of MYCN in neuroblastoma cells." Oncogene **31**(50): 5193-5200.
Schreiber, R. D., L. J. Old, M. J. Smyth, R. D. Schreiber, L. J. Old and M. J. Smyth (2011). "Cancer Immunoediting: Integrating Immunity's Roles in Cancer Suppression and Promotion." Science **331**(6024): 1565-1570.
Shalinsky, D. R., E. D. Bischoff, M. L. Gregory, M. M. Gottardis, J. S. Hayes, W. W. Lamph, R. A. Heyman, M. A. Shirley, T. A. Cooke, P. J. Davies and et al. (1995). "Retinoid-induced suppression of squamous cell differentiation in human oral squamous cell carcinoma xenografts (line 1483) in athymic nude mice." Cancer Res **55**(14): 3183-3191.
Shang, X., S. M. Burlingame, M. F. Okcu, N. Ge, H. V. Russell, R. A. Egler, R. D. David, S. A. Vasudevan, J. Yang and J. G. Nuchtern (2009). "Aurora A is a negative prognostic factor and a new therapeutic target in human neuroblastoma." Mol Cancer Ther **8**(8): 2461-2469.
Shea, T. B., R. K. Sihag and R. A. Nixon (1988). "Neurofilament triplet proteins of NB2a/d1 neuroblastoma: posttranslational modification and incorporation into the cytoskeleton during differentiation." Brain Res **471**(1): 97-109.
Shimada, H., I. M. Ambros, L. P. Dehner, J. Hata, V. V. Joshi, B. Roald, D. O. Stram, R. B. Gerbing, J. N. Lukens, K. K. Matthay and R. P. Castleberry (1999). "The International Neuroblastoma Pathology Classification (the Shimada system)." Cancer **86**(2): 364-372.
Sidell, N. (1982). "Retinoic acid-induced growth inhibition and morphologic differentiation of human neuroblastoma cells in vitro." J Natl Cancer Inst **68**(4): 589-596.
Sidell, N., A. Altman, M. R. Haussler and R. C. Seeger (1983). "Effects of retinoic acid (RA) on the growth and phenotypic expression of several human neuroblastoma cell lines." Exp Cell Res **148**(1): 21-30.
Sigma. "Tripsin." Retrieved 30th May, 2014, from http://www.sigmaaldrich.com/life-science/metabolomics/enzyme-explorer/analytical-enzymes/trypsin.html.
Smith, L., S. Minter, P. O'Brien, J. M. Kraveka, A. M. Medina and J. Lazarchick (2013). "Neuroblastoma in an adult: case presentation and literature review." Ann Clin Lab Sci **43**(1): 81-84.
Sommers, S. C., B. A. Sullivan and S. Warren (1952). "Heterotransplantation of human cancer. III. Chorioallantoic membranes of embryonated eggs." Cancer Res **12**(12): 915-917.
Sridhar, S., B. Al-Moallem, H. Kamal, M. Terrile and R. L. Stallings (2013). "New insights into the genetics of neuroblastoma: Implications for diagnosis and therapy." Molecular Diagnosis and Therapy **17**(2): 63-69.
Stephanie Li Mei Tay, P. W. S. H. a. L. W. C. (2011). "An investigation of the chick chorioallantoic membrane as an alternative model to various biological tissues for permeation studies." Journal of Pharmacy and Pharmacology (63:): 1283-1289.

Stetler-Stevenson, W. G., S. Aznavoorian and L. A. Liotta (1993). "Tumor cell interactions with the extracellular matrix during invasion and metastasis." Annu Rev Cell Biol **9**: 541-573.
Strojnik, T., R. Kavalar, T. A. Barone and R. J. Plunkett (2010). "Experimental model and immunohistochemical comparison of U87 human glioblastoma cell xenografts on the chicken chorioallantoic membrane and in rat brains." Anticancer Res **30**(12): 4851-4860.
Subauste, M. C., T. A. Kupriyanova, E. M. Conn, V. C. Ardi, J. P. Quigley and E. I. Deryugina (2009). "Evaluation of metastatic and angiogenic potentials of human colon carcinoma cells in chick embryo model systems." Clin Exp Metastasis **26**(8): 1033-1047.
Sugiura, Y., H. Shimada, R. C. Seeger, W. E. Laug and Y. A. DeClerck (1998). "Matrix metalloproteinases-2 and -9 are expressed in human neuroblastoma: contribution of stromal cells to their production and correlation with metastasis." Cancer Res **58**(10): 2209-2216.
Sultan, I., I. Qaddoumi, S. Yaser, C. Rodriguez-Galindo and A. Ferrari (2009). "Comparing adult and pediatric rhabdomyosarcoma in the surveillance, epidemiology and end results program, 1973 to 2005: an analysis of 2,600 patients." J Clin Oncol **27**(20): 3391-3397.
Sung, P. J., N. Boulos, M. J. Tilby, W. D. Andrews, R. F. Newbold, D. A. Tweddle and J. Lunec (2013). "Identification and characterisation of STMN4 and ROBO2 gene involvement in neuroblastoma cell differentiation." Cancer Lett **328**(1): 168-175.
Sys, G., M. Van Bockstal, R. Forsyth, M. Balke, B. Poffyn, D. Uyttendaele, M. Bracke and O. De Wever (2012). "Tumor grafts derived from sarcoma patients retain tumor morphology, viability, and invasion potential and indicate disease outcomes in the chick chorioallantoic membrane model." Cancer Lett **326**(1): 69-78.
Sys, G. M. L., L. Lapeire, N. Stevens, H. Favoreel, R. Forsyth, M. Bracke and O. De Wever (2013). "The In ovo CAM-assay as a Xenograft Model for Sarcoma." (77): e50522.
Taizi, M., V. R. Deutsch, A. Leitner, A. Ohana and R. S. Goldstein (2006). "A novel and rapid in vivo system for testing therapeutics on human leukemias." Exp Hematol **34**(12): 1698-1708.
Teitz, T., M. Inoue, M. B. Valentine, K. Zhu, J. E. Rehg, W. Zhao, D. Finkelstein, Y. D. Wang, M. D. Johnson, C. Calabrese, M. Rubinstein, R. Hakem, W. A. Weiss and J. M. Lahti (2013). "Th-MYCN mice with caspase-8 deficiency develop advanced neuroblastoma with bone marrow metastasis." Cancer Res **73**(13): 4086-4097.
Teitz, T., J. J. Stanke, S. Federico, C. L. Bradley, R. Brennan, J. Zhang, M. D. Johnson, J. Sedlacik, M. Inoue, Z. M. Zhang, S. Frase, J. E. Rehg, C. M. Hillenbrand, D. Finkelstein, C. Calabrese, M. A. Dyer and J. M. Lahti (2011). "Preclinical models for neuroblastoma: establishing a baseline for treatment." PLoS One **6**(4): e19133.
Thiele, C. J., C. P. Reynolds and M. A. Israel (1985). "Decreased expression of N-myc precedes retinoic acid-induced morphological differentiation of human neuroblastoma." Nature **313**(6001): 404-406.
Thorner, P. S. (2014). "The molecular genetic profile of neuroblastoma." Diagnostic Histopathology **20**(2): 76-83.
TJL. "The Jackson Laboratory Mouse Phenome Database." Retrieved 14th April, 2014, from http://phenome.jax.org/.
TJL. "The Jackson Laboratory, Inbred mice." Retrieved 14th April, 2014, from http://research.jax.org/grs/type/inbred/.
Trochet, D., F. Bourdeaut, I. Janoueix-Lerosey, A. Deville, L. de Pontual, G. Schleiermacher, C. Coze, N. Philip, T. Frebourg, A. Munnich, S. Lyonnet, O. Delattre and J. Amiel (2004). "Germline mutations of the paired-like homeobox 2B (PHOX2B) gene in neuroblastoma." Am J Hum Genet **74**(4): 761-764.

Tsubono, Y. and S. Hisamichi (2004). "A halt to neuroblastoma screening in Japan." N Engl J Med **350**(19): 2010-2011.
Tuveson, D. A. and T. Jacks (2002). "Technologically advanced cancer modeling in mice." Curr Opin Genet Dev **12**(1): 105-110.
Vandesompele, J., M. Baudis, K. De Preter, N. Van Roy, P. Ambros, N. Bown, C. Brinkschmidt, H. Christiansen, V. Combaret, M. Lastowska, J. Nicholson, A. O'Meara, D. Plantaz, R. Stallings, B. Brichard, C. Van den Broecke, S. De Bie, A. De Paepe, G. Laureys and F. Speleman (2005). "Unequivocal delineation of clinicogenetic subgroups and development of a new model for improved outcome prediction in neuroblastoma." J Clin Oncol **23**(10): 2280-2299.
Vargas, A., M. Zeisser-Labouebe, N. Lange, R. Gurny and F. Delie (2007). "The chick embryo and its chorioallantoic membrane (CAM) for the in vivo evaluation of drug delivery systems." Adv Drug Deliv Rev **59**(11): 1162-1176.
Vergara, M. N. and M. V. Canto-Soler (2012). "Rediscovering the chick embryo as a model to study retinal development." Neural Dev **7**: 22.
Vermeulen, J., K. De Preter, A. Naranjo, L. Vercruysse, N. Van Roy, J. Hellemans, K. Swerts, S. Bravo, P. Scaruffi, G. P. Tonini, B. De Bernardi, R. Noguera, M. Piqueras, A. Canete, V. Castel, I. Janoueix-Lerosey, O. Delattre, G. Schleiermacher, J. Michon, V. Combaret, M. Fischer, A. Oberthuer, P. F. Ambros, K. Beiske, J. Benard, B. Marques, H. Rubie, J. Kohler, U. Potschger, R. Ladenstein, M. D. Hogarty, P. McGrady, W. B. London, G. Laureys, F. Speleman and J. Vandesompele (2009). "Predicting outcomes for children with neuroblastoma using a multigene-expression signature: a retrospective SIOPEN/COG/GPOH study." Lancet Oncol **10**(7): 663-671.
Wada, R. K., R. C. Seeger, C. P. Reynolds, T. Alloggiamento, J. M. Yamashiro, C. Ruland, A. C. Black and J. D. Rosenblatt (1992). "Cell type-specific expression and negative regulation by retinoic acid of the human N-myc promoter in neuroblastoma cells." Oncogene **7**(4): 711-717.
Waheed Roomi, M., T. Kalinovsky, N. W. Roomi, A. Niedzwiecki and M. Rath (2013). "Inhibition of the SK-N-MC human neuroblastoma cell line in vivo and in vitro by a novel nutrient mixture." Oncol Rep **29**(5): 1714-1720.
Wang, J., L. Wang, L. Cai, J. Wang, L. Wang and L. Cai (2009). "Establishment of a transplantation tumor model of human osteosarcoma in chick embryo." The Chinese-German Journal of Clinical Oncology **8**(9): 531-536.
Weiss, W. A., K. Aldape, G. Mohapatra, B. G. Feuerstein and J. M. Bishop (1997). "Targeted expression of MYCN causes neuroblastoma in transgenic mice." EMBO J **16**(11): 2985-2995.
Westermark, U. K., M. Wilhelm, A. Frenzel and M. A. Henriksson (2011). "The MYCN oncogene and differentiation in neuroblastoma." Semin Cancer Biol **21**(4): 256-266.
Westermark, U. K., M. Wilhelm, A. Frenzel and M. A. Henriksson (2011). "The MYCN oncogene and differentiation in neuroblastoma." Seminars in Cancer Biology **21**(4): 256-266.
Woods, W. G., R. N. Gao, J. J. Shuster, L. L. Robison, M. Bernstein, S. Weitzman, G. Bunin, I. Levy, J. Brossard, G. Dougherty, M. Tuchman and B. Lemieux (2002). "Screening of infants and mortality due to neuroblastoma." N Engl J Med **346**(14): 1041-1046.
Wu, G., Y. Fang, Z. H. Lu and R. W. Ledeen (1998). "Induction of axon-like and dendrite-like processes in neuroblastoma cells." J Neurocytol **27**(1): 1-14.
Yamamoto, K., R. Hanada, A. Kikuchi, M. Ichikawa, T. Aihara, E. Oguma, T. Moritani, Y. Shimanuki, M. Tanimura and Y. Hayashi (1998). "Spontaneous regression of localized neuroblastoma detected by mass screening." J Clin Oncol **16**(4): 1265-1269.

Yang, Q., Bai, Y.-X. , Yan, L.-Y. Wang, Q.-Y, Yang, G.-X. (2014). "Establishment of a transplantation tumor model of human anaplastic thyroid carcinoma in chick embryo and its biological characteristics." 西安交通大学学报 (医学版) = Journal of Xi'an Jiaotong University (Medical Sciences) **35**(2): 208-212.
Yang, Y., S. J. Adelstein and A. I. Kassis (2012). "Target discovery from data mining approaches." Drug Discov Today **17 Suppl**: S16-23.
Young, G., J. A. Toretsky, A. B. Campbell and A. E. Eskenazi (2000). "Recognition of common childhood malignancies." Am Fam Physician **61**(7): 2144-2154.
Young, M. R., L. V. Ileva, M. Bernardo, L. A. Riffle, Y. L. Jones, Y. S. Kim, N. H. Colburn and P. L. Choyke (2009). "Monitoring of tumor promotion and progression in a mouse model of inflammation-induced colon cancer with magnetic resonance colonography." Neoplasia **11**(3): 237-246, 231p following 246.
Zhou, H., J. Kuang, L. Zhong, W. L. Kuo, J. W. Gray, A. Sahin, B. R. Brinkley and S. Sen (1998). "Tumour amplified kinase STK15/BTAK induces centrosome amplification, aneuploidy and transformation." Nat Genet **20**(2): 189-193.
Zhou, Q., J. Facciponte, M. Jin, Q. Shen and Q. Lin (2014). "Humanized NOD-SCID IL2rg(-/-) mice as a preclinical model for cancer research and its potential use for individualized cancer therapies." Cancer Lett **344**(1): 13-19.
Zwaan, C. M., P. Kearns, H. Caron, A. Verschuur, R. Riccardi, J. Boos, F. Doz, B. Geoerger, B. Morland, G. Vassal and c. innovative therapies for children with cancer' European (2010). "The role of the 'innovative therapies for children with cancer' (ITCC) European consortium." Cancer Treat Rev **36**(4): 328-334.